CHARLES UNIVERSITY IN PRAGUE

Faculty of Science

Program of study: Biology

Field of study: Immunology

MUDr. Viktor Černý

UŽITÍ BIODEGRADABILNÍCH POLYMERNÍCH KONJUGÁTŮ S VYSOKOU MOLEKULOVOU HMOTNOSTÍ K ÚČINNÉMU DORUČENÍ CYTOSTATICKÝCH LÉČIV DO SOLIDNÍCH NÁDORŮ

BIODEGRADABLE HIGH MOLECULAR WEIGHT POLYMERIC CONJUGATES FOR EFFICIENT DELIVERY OF CYTOSTATIC DRUGS INTO SOLID TUMORS

Diploma thesis

Supervisor: RNDr. Marek Kovář, PhD.

Prague 2015

Prohlášení

Prohlašuji, že jsem závěrečnou práci zpracoval samostatně a že jsem uvedl všechny použité informační zdroje a literaturu. Tato práce ani její podstatná část nebyla předložena k získání jiného nebo stejného akademického titulu.

V Praze dne 12. 8. 2015 .....

podpis

Acknowledgments

I would like to thank my supervisor RNDr. Marek Kovář, PhD. for his exceptional patience. I would also like to thank all of my collaborators at the Laboratory of Tumor Immunology for their help, and in particular to RNDr. Milada Šírová, PhD. and MUDr. Miloslav Kverka, PhD. for valuable feedback and advice.

Further thanks go to the co-workers at IMC, CAS, especially Ing. Martin Studenovský, PhD. for all chemical work on MBZ derivatives and HPMA polymers and consultations regarding chemistry.
I would also like to thank MUDr. Pavel Rossmann, DrSc. for his work on and advice regarding the histological samples.

Last but not least, I would like to thank my family, friends and loved ones for their unrelenting faith and support, and to all the beings who ever enriched my life.

Abstract

Cancer remains one of the most pressing issues of contemporary science and medicine. Incidence of malignant diseases is rising worldwide and they represent a major problem for the society due to both economic and ethical issues they cause. Although the progress in cancer biology, therapy and immunology has led to the introduction of many novel therapeutic protocols, approaches and drugs with specificity defined on a molecular level into clinical practice, many malignancies retain their poor prognosis. Therefore, intense research into new ways to increase our therapeutic options is warranted.

Unfortunately, bringing a completely novel drug into clinical use takes extremely high amounts of time and money and entails a high risk of failure. Therefore, a promising approach has been recently adopted which lies in repurposing compounds already used in human medicine for cancer treatment. This form of research can advance through clinical trials for a new indication much easier, faster and cheaper than researching completely new drugs.

The aim of this study was to examine the anticancer potential of one such drug, mebendazole. An anthelminthic from the family of benzimidazoles, mebendazole has been in common clinical use from the 1970s and is marked by its low toxicity as well as its very low solubility. Due to this low solubility, mebendazole is only administered perorally and this application is marked by a low biological availability.

We tested the cytostatic effect of mebendazole and two of its derivatives in the model of several murine cancer cell lines with the aim of preparing HPMA copolymer-bound conjugate of mebendazole which would increase its solubility and enable parenteral application. Mebendazole and both derivatives were shown to possess cytostatic activity *in vitro* comparable to the cytostatic activity of doxorubicin.

We synthesized the HPMA copolymer-bound conjugate and tested its *in vivo* toxicity and therapeutic efficacy in the model of induced syngeneic tumors in mice. A pronounced increase in toxicity was observed and a suppression of erythropoiesis was described. Bone marrow suppression as well as acute liver toxicity were seen in histology, findings consistent with the rare reports of mebendazole toxicity from literature. The therapeutic experiments were unsuccessful due to this high toxicity; nevertheless, the experiments marked the first account of parenteral application of high molecular weight conjugate of mebendazole in mice.

Keywords: **Cancer, mebendazole, HPMA copolymer-bound drugs, drug repurposing, toxicity, mice, chemotherapy.**

Abstrakt

Nádorová onemocnění představují jeden z nejzávažnějších problémů současné vědy i medicíny. Incidence maligních nádorů je celosvětově na vzestupu a představují závažný celospolečenský problém jak z důvodů ekonomických, tak společenských. Ačkoli pokroky v nádorové biologii, výzkumu nádorové terapie i imunologii umožnily zavést do klinické praxe mnoha nových léčebných protokolů, modalit i léčiv s molekulárně definovanou specificitou, mnoho nádorových onemocnění má stále velmi nepříznivou prognózu. Je tedy nezbytně nutné pokračovat v intenzivním výzkumu nových způsobů, jak rozšířit dostupné léčebné možnosti.

Zavést do klinického užívání zcela nové léčivo je nicméně extrémně časově a finančně náročné a zahrnuje vysoké riziko neúspěchu. V posledních letech se z těchto důvodů objevil nový výzkumný trend, spočívající v pátrání po potenciálních látkách s protinádorovým účinkem mezi léčivy, která jsou nebo byla zavedena v lidské medicíně pro použití v nenádorových indikacích. Tento typ výzkumu může úspěšně zavést látku pro použití v nové indikaci podstatně snáze, rychleji a levněji než výzkum zcela nových terapeutik.

Cílem této práce bylo prozkoumat protinádorovou účinnost jednoho z léčiv odhalených tímto přístupem, benzimidazolového anthelmintika mebendazolu. Mebendazol je rutinně užíván v klinické praxi od 70. let 20. století a je známý pro svou nízkou toxicitu, stejně jako velmi nízkou rozpustnost ve vodných roztocích. Z tohoto důvodu je mebendazol podávaný výhradně perorálně a toto podání je charakteristické nízkou biologickou dostupností.

Prozkoumali jsme cytostatickou účinnost mebendazolu a jeho dvou derivátů na modelu několika myších nádorových linií s cílem připravit konjugát, obsahující mebendazol navázaný na HPMA kopolymerový nosič za účelem zvýšení jeho rozpustnosti, které by umožnilo parenterální aplikaci. Mebendazol a oba jeho deriváty se vyznačovaly cytostatickou aktivitou *in vitro* srovnatelnou s cytostatickou aktivitou doxorubicinu.

Dále jsme připravili konjugát mebendazolu na HPMA a otestovali jeho toxicitu a terapeutickou účinnost *in vivo* na modelu syngenních myších nádorů. Zaznamenali a popsali jsme výrazné zvýšení toxicity a útlum erytropoézy. Na histologii jsme pozorovali nález odpovídající útlumu kostní dřeně a projevům akutní hepatotoxicity; tyto nálezy odpovídají ojedinělým záznamům toxicity mebendazolu v dostupné literatuře. Léčebné experimenty byly z důvodu této toxicity neúspěšné, nicméně naše experimenty představovaly první popsané podání konjugátu mebendazolu s vysokou molekulovou hmotností na myším modelu.

Klíčová slova: **Nádor, mebendazol, léčiva vázaná na HPMA kopolymer, toxicita, zavádění léčiva v nové indikaci, myši, chemoterapie.**

List of Abbreviations

17-DMAG	Alvespimycin
ABC	ATP-binding cassette
ABT-737	specific BH3-mimetic
ALL	acute lymphocytic leukemia
APC	antigen presenting cell
ATCC	American Type Culture Collection
BCG	Bacillus Calmette-Guérin
BCR-ALB	breakpoint cluster region – Abelson tyrosine kinase
Carf	Carfilzomib
CD	cluster of Differentiation
CML	chronic myeloid leukemia
CTLA4	cytotoxic T-lymphocyte antigen 4
DC	dendritic cell
DMF	dimethylformamide
DMSO	dimethyl sulphoxide
DOX	doxorubicin
EC50	half-maximal effective concentration
EPR	enhanced permeability and retention
eq.	equivalent
FasL	Fas ligand
FCS	fetal calf serum
GIT	gastrointestinal tract
HMGB1	high-mobility group protein B1
HMW	high molecular weight
HPMA	*N*-(2-hydroxypropyl)methacrylamide
Hsp90	heat shock protein 90
IC50	half-maximal inhibitory concentration
ICD	immunogenic cell death
IFN-α	interferon α

IL	interleukin
IMC	Institute of Macromolecular Chemistry
LMW	low molecular weight
Mab	monoclonal antibody
MBZ	mebendazole
MDR	multidrug resistance
MDSC	myeloid-derived suppressor cell
MHC	major histocompatibility complex
MTD	maximum tolerated dose
MTT	3-(4,5-dimethylthiazol-2-yl)-2,5-diphenyltetrazolium bromide
NK	natural killer cell
PAMAM	polyamidoamine
PBS	phosphate buffered saline
PEG	polyethylene glycol
Pgp	P-glycoprotein
RT	radiation therapy
TAM	tumor-associated macrophage
TAN	tumor-associated neutrophil
TGF-β	transforming growth factor β
TIL	tumor infiltrating lymphocyte
TLR4	Toll-like receptor 4
TNM	cancer staging system
T_{reg}	regulatory T-cell
TSG	tumor suppressor gene
VEGF	vascular endothelial growth factor
VEGFR2	vascular endothelial growth factor receptor 2
WHO	World Health Organization

Contents

I. Introduction

Despite numerous significant advances in the field of cancer biology both in terms of understanding how various malignancies arise and function and in terms of making treatment more effective, cancer in its numerous forms and variations remains one of the most pressing issues of contemporary biological science. Cancer diseases represent the third most common cause of death worldwide and their incidence grows with increasing age. Incidence of many types of malignant diseases worldwide is on a rise and its often unfavorable prognosis and progressively debilitating effect on quality of life of patients represent a heavy burden not only from the medical, but also economic, social and ethical standpoint.

In the past decades, the traditional triad of therapeutic modalities available for cancer treatment, i.e. surgery, radiotherapy and chemotherapy, are being constantly improved and rationalized to keep pace with and better reflect the current state of understanding tumor biology in general and the pathophysiology of the respective clinical entity in particular. The conventional approaches have also in recent decades been supported by the advent of altogether novel therapeutic approaches based on latest advancements in the field of cancer biology, i.e. immunotherapy and a new vein within chemotherapy based on more selectively blocking the function of specifically defined biological targets, the so-called molecular target-specific therapy. These new approaches have revolutionized tumor treatment in some malignancies and in the ideal case offer highly specific treatment with few systemic side effects. This specificity however makes this kind of treatment generally suitable only for a narrow group of diseases which share a single vital characteristic, and in some cases only for one particular form of cancer or a single clinical unit.

Therefore, although the treatment efficiency of some tumor types has been greatly improved and some previously lethal malignancies can now be treated with a remarkable long-term success, progress is needed in other areas. Many malignancies retain their poor prognosis and continue to rely on highly aggressive treatment which is limited by severe systemic toxicity due to its non-specific nature. In frequent cases temporary success may be achieved only for the disease to relapse with increased aggressiveness and resistance to further therapy. Therefore, intense research to broaden our understanding of tumors and offer further options to improve this *status quo* and rationalize current approach to cancer treatment based on cutting-edge science is highly warranted.

I.1. The origin and biology of cancer

Cancer (i.e. malignant neoplastic disease) can be defined as a group of diseases, characterized by abnormal proliferation of a single cell and its clonal progeny with the potential to invade or spread to other parts of the body and eventually if untreated burden the organism and deplete its resources, leading to death. It has soon become apparent that induced or spontaneous mutations of particular types of proteins labelled proto-oncogenes or tumor-suppressor genes (TSG) play a crucial role in this deregulation [1], [2], [3], [4], [5], [6] and that a series of mutation events is required to compromise the control and feedback systems healthy cells utilize to keep their proliferation within physiologically regulated levels [2], [7], [8]. The advent of molecular biology and rapid advances in this and related fields of study in the second half of 20^{th} century brought about a breakthrough in our ability to discover, describe and interpret the molecular and subcellular mechanisms behind the causes and principles underlying this uncontrolled proliferation. The large amount of experimental data collected using the newly developed technologies and methods showed that while there exists a staggering number of variations among the particular mutations and abnormalities described in the model of different cancer cells, a set of characteristics which are true for most or all types of malignant diseases can nevertheless be formulated to combine these diverse data into categories by functional relevance. In a pivotal work published in 2000, Hanahan and Weinberg defined six of the most common overarching characteristics shared in different forms over a number of tumors into such categories, coining the term "hallmarks of cancer" [9]. This work established a conceptual framework which united the previously diverse findings into a comprehensive system and allowed the researchers to further elucidate the broader underlying mechanisms and concentrate on developing rational therapy tailor-suited to target the individual categories of tumor-enabling and tumor-promoting characteristics. Together with continually improving understanding of the principles of cell function and cell cycle regulation, a vast network of interconnected pathways is slowly being uncovered painting an increasingly clear picture of how complex and carefully regulated the physiological state is both in the context of an individual cell and in the context of its interactions with the surrounding environment and the system as a whole.

A noteworthy aspect of the development in the field of cancer biology in the past few decades is a shift of focus from the cancer cells as the sole population of interest to a broader view which recognizes the critical roles of other populations of cells (Fig I.1) [9]. Most important of these are the elements of the immune system and the stromal cells, which create

and maintain the tumor microenvironment required for support, growth and progression of the tumor as well as resistance against treatment. This shift from the reductionist to a broader point of view is both caused by and in turn further contributes to the advances in the study of tumor immunology and tumor microenvironment, both of which contribute in a major way to the leading edge in cancer biology research.

The concept of hallmarks was revised and updated in 2011 based on the progress in the field and in light of the emerging importance of elements of the immune system and tumor microenvironment in tumor formation and maintenance two additional emerging hallmarks as well as two "enabling characteristics" were introduced, leaving the total amount of these mechanistic categories at ten (Fig I.2) [10].

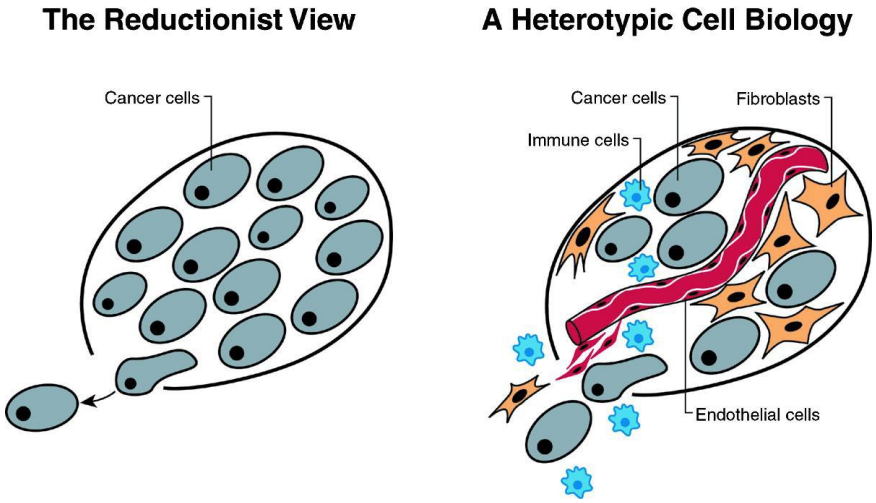

Fig I.1 Reductionist versus heterotypic view of tumor composition. Comparison of the reductionist view of cancer and the heterotypic model, stressing the importance of immune cells, stromal fibroblasts and angiogenesis in tumor homeostasis.
Taken from Hanahan and Weinberg [9].

The original hallmarks largely focused on the various aspects of deregulation of tumor cell proliferation and avoidance of control networks which limit or hamper the long term survival of normal proliferating cells. These hallmarks included sustained proliferative signaling, reflecting the importance of proto-oncogenes and signal cascades conveying the mitogenic stimuli from the environment [11], [12], enabling replicative immortality, which dealt with the way malignant cells overcome the Hayflick limit [13], as well as the evasion of growth suppressors and disruption of the proper function of TSG regulatory pathways [2], [14], [15], [16] therefore allowing tumor cells to proliferate regardless of the normal control mechanisms. Another important hallmark, resisting cell death, was described as a result of the increase in understanding of cell death and in particular apoptosis. The last two of the original

hallmarks were concerned to a greater extent with the direct contact or interaction of the tumor with surrounding tissue and the system as a whole, concentrating upon the importance and specific characteristics and mechanisms of angiogenesis in newly formed tumor tissue [17], [18] as well as the mechanisms governing the processes of invasion and metastasis. The emerging hallmarks described in 2011 [10] reflect the rising importance of studying tumor cell metabolism as a major contributing factor and, perhaps most importantly from the point of view of our study, include the hallmark of avoiding immune destruction as one of the universal defining characteristics of cancer, confirming and solidifying the role of tumor immunity.

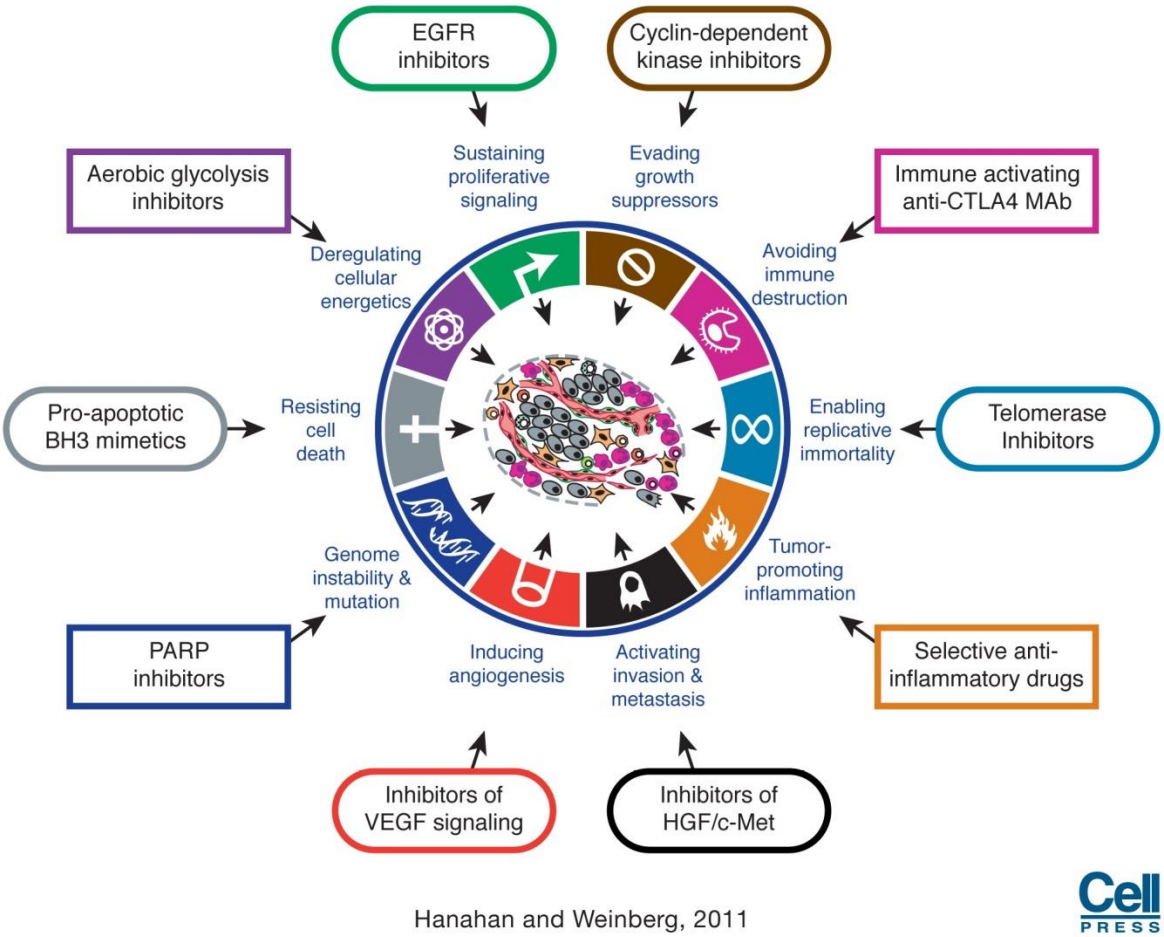

Fig I.2 The hallmarks and enabling characteristics of cancer. Updated version of the scheme showing the original six hallmarks of cancer as suggested in 2000 as well as the emerging hallmarks (deregulating cellular energetics and avoiding immune destruction) and the enabling characteristics of genome instability & mutation and tumor-promoting inflammation.
The boxes list illustrative examples of drugs under investigation which are designed to target the respective hallmarks/enabling characteristics.
Taken from Hanahan and Weinberg [10].

I.1.1. Cancer immunology

The capability of the immune system to recognize the arising tumor cells as aberrant and eliminate them or limit their spread was suggested as early as 1957 by Burnet [19], who postulated the concept of "immune surveillance". While great controversy marked this concept for the better part of the second half of 20th century, eventually it became clear that the immune system does indeed play a crucial role in tumor control as well as progression. A new concept, known as the process of immunoediting, has been therefore suggested [20]. The immune system is capable of recognizing the aberrant features of tumor cells, most commonly antigens, both tumor-specific (i.e. exclusively occurring in tumors) [21] and tumor-associated (i.e. those which occur physiologically in organism but are expressed in an aberrant temporal, spatial or quantitative pattern on cancer cells) [22]. Afterwards, components of the immune system – mainly T cells, natural killer (NK) cells and macrophages [23] – contribute to elimination and keeping the tumor in check. In the process of immunoediting, this represents the phase of elimination (Fig I.3, adapted from [24]) The tumor, however, represents a complex tissue composed of numerous clones and subclones derived from the original cancer cell due to its intrinsically high genome instability. Therefore, any given tumor may contain subpopulations of cells which successfully evade the immune system recognition and continue to survive despite the immune surveillance, a stage known as equilibrium (Fig I.3). During this phase, additional subpopulations are created in response to the continuous pressure exerted by the immune system, until the tumor progresses into a stage where it no longer can be contained by the immune systems. This is known as the escape phase (Fig I.3) and is often accompanied not only by the loss of immune system control, but also by the conscription of immune mechanisms to promote the tumor growth by actively suppressing any further anti-tumor immune response. The escape phase is then characterized by exponential growth and rapid progression of the tumor, which can then quickly spread and lead to serious clinical conditions.

There are numerous ways in which tumor cell subpopulations can escape the immune system. Among these number diverse effects which take place both within the tumor cells themselves and in the tumor microenvironment. Downregulation of major histocompatibility complex (MHC) class I molecules [25] and expression of proapoptotic ligands such as FasL (CD95L) occur on the tumor cell surface [26] while the tumor cells and stromal cells both can contribute towards the creation of a highly immunosuppressive environment within the tumor, producing factors such as TGF-β [25], [27] and upregulating the activity of enzymes such as Indoleamine 2,3-dioxygenase [28], [29] and arginase [25], [30], [31].

Among the most important subversive mechanisms tumors employ to circumvent the immune control is the suppressive activity of the recruited regulatory immune cell populations, predominantly regulatory T cells (T_{regs}) [23], [32], [33], [34] but also suppressive cells of other immune origin, including tumor-associated macrophages (TAMs), tumor-associated neutrophils (TANs) and myeloid-derived suppressor cells (MDSC) [30], [35]. These cells upon their recruitment into tumor confer immunoprotective effects both by directly eliminating and inhibiting anti-cancer immune cells and by further changing the tumor microenvironment milieu in favor of the immunosuppressive state, further facilitating the recruitment and suppressive activity of more elements in a vicious circle.

An important part of the problem is that since cancer cells most often arise from ordinary somatic cells and only differ in minor ways from healthy cells in the early stages of tumor progression (exceptions being e.g. tumors induced by oncogenic viruses [36]), there is generally a strong bias towards a tolerogenic response that the immune system has to overcome in order to effectively start the anti-tumor immune response. The induction of this response can be facilitated by appropriate forms of treatment of the patient, giving rise to an array of approaches which collectively form immune therapy (see chapter I.2.3.)

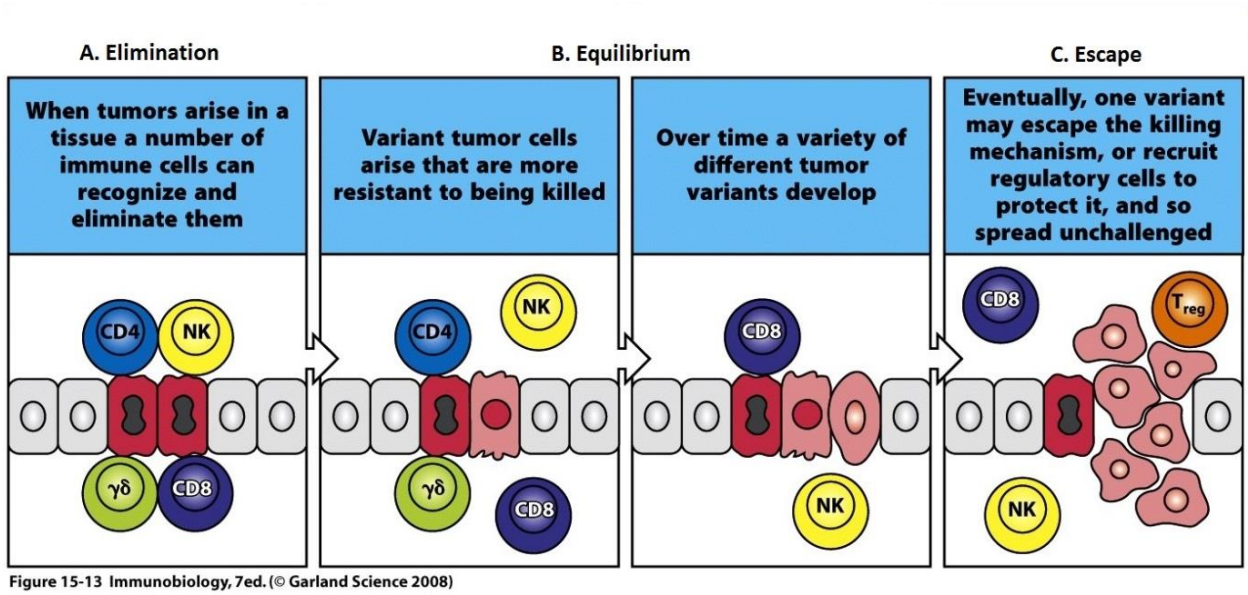

Fig I.3 The three phases of immunoediting. Adapted from Janeway *et al.* [24].

I.1.1.1. Immunogenic cell death

A breakthrough in our understanding of tumor immunity and our ability to fully exploit its potential came with the realization that under specific conditions, some therapeutic modalities (e.g. doxorubicin) previously thought to be immunosuppressive not only do not have this detrimental property, but in fact elicit effective antitumor immune response [37]. It has soon been proven that this occurs when the tumor cells are killed in a specific fashion, dubbed immunogenic apoptosis or immunogenic cell death (ICD) [38], [39], which stimulates dendritic cells (DCs) to mature and become effective antigen presenting cells (APCs), priming the further effectors of the immune response. The functional basis for this lies in exposition on membrane and/or release of certain factors functioning as alarmins and eat-me signals by the dying cells, which then effectively attract phagocytes and stimulate the immune response. The key molecules implicated in this effect are calreticulin [38], HMGB1 [39] and Hsp90 [40], molecules typically functioning via stimulation of receptors including scavenger receptors and Toll-like receptor 4 (TLR4) [39] on cells of innate immune system such as DCs, leading to effective stimulation.

A noteworthy fact is that this effect is not solely limited to chemotherapy by agents such as doxorubicin [37], [41], [42] but also occurs when cells die after exposition to X-rays [39] and even specific physical stress such as high hydrostatic pressure [43].

This discovery is proving to be of extremely high significance, as it allows for identification, research and improvement of those chemotherapeutic agents and treatment modalities/regimens which offer the optimal immunostimulatory effect and may serve as the basis for novel therapeutic protocols maximizing the benefit of combining chemotherapy or radiotherapy with immunotherapeutic approaches.

I.1.2. Angiogenesis

Another hallmark described earlier is the dependence of the tumor on angiogenesis. It has been proven that while very small primary and metastatic clusters of tumor cells are sufficiently supplied with oxygen and nutrients through diffusion from vessels located in surrounding tissue, in order to progress past certain size (less than 2 mm) [18], the tumor needs to elicit growth of a system of novel blood vessels, otherwise growth is offset by death of cells in the center of the tumor caused by the insufficient nutrient and oxygen supply [9], [44], [45]. This is known as the tumor neoangiogenesis or neovasculogenesis and is characterized by the process of sprouting of new capillaries from the preexisting blood vessels in the vicinity of the tumor [46], [17] and formation of capillary loops which finally give rise

to a complete blood vessel network within the tumor [17]. This complex process, which is initiated at a particular stage of the tumor progression and likely is a prerequisite to the exponential growth phase which results in the appearance of a macroscopically detectable tumor [9], [46], [17], is orchestrated by a balance of upregulating the proangiogenic stimuli produced by the tumor cells and/or stroma and downregulating the antiangiogenic regulatory mechanisms [17].

Arguably the most important proangiogenic factor is the vascular endothelial growth factor (VEGF) [47], [48], [49]. Its role in tumor neo-angiogenesis has been confirmed by the findings that inhibition of its function led to tumor growth prevention in *in vivo* conditions [50], [51] and subsequently its therapeutic potential has become the subject of intensive research. This ultimately resulted in the introduction of bevacizumab, an anti-VEGF recombinant humanized monoclonal antibody (Mab), into clinical practice as the first antiangiogenic biological agent in the history [52], [53].

An important facet of the newly created vasculature in solid tumors is its highly abnormal morphology and its dysfunction. The vasculature network is denser and far less organized than in healthy tissues and the blood vessels are improperly formed [54]. They were also described to lack a contiguous layer of pericytes [55] and to be formed of defective endothelial cells with numerous openings in between them [56]. Together with the effective absence of lymphatic drainage [57] this creates a highly specific environment within a tumor tissue. The leakiness of the aberrant tumor vasculature allows for passage of high molecular weight (HMW) compounds into the tumor, whereas in the ordinary tissues, this is prevented by the barrier function of the intact epithelium. Moreover, the dysfunctional lymphatic drainage of tumor tissue ensures far longer half time of efflux of HMW compounds from tumor tissue than would be the case in a tissue with properly functional lymphatic drainage. Together, this means that tumor tissues accumulate HMW substances with far greater efficiency than healthy tissues, and any such compounds therefore show high selectivity for tumor tissue unlike ordinary, low molecular weight compounds such as most conventional chemotherapeutics (Fig I.4). This mechanism was described in 1986 and the term enhanced permeability and retention (EPR) effect was coined [58]. Subsequently, EPR effect has been widely exploited as a rationale and basis for design of systems for passive targeting of therapeutics into tumor, effectively forming a foundation of an entire new branch of cancer therapy research. The resulting vast quantity of research data and works furthering the understanding of this phenomenon and exploiting it for design of novel therapeutic agents has recently been comprehensively reviewed in [59] and [60].

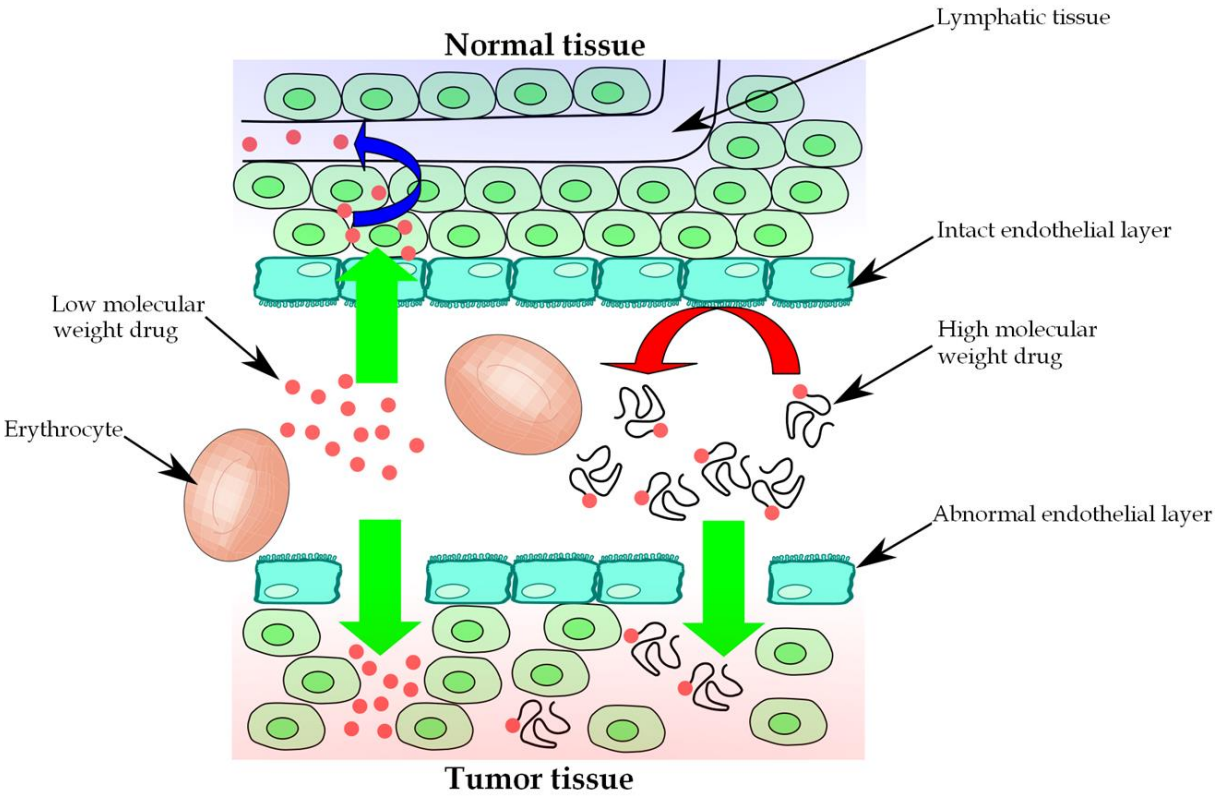

Fig I.4 The EPR effect. Figure shows the different blood vessel permeability for high molecular weight compounds in tumor and intact tissue as described in the text.

I.2. Cancer therapy

Traditionally, tumor therapy has relied on three basic treatment modalities, i.e. surgery, radiotherapy and conventional (also called cytotoxic) chemotherapy, often combined into complex treatment regimens depending on the disease type and the accessibility of its location. In the past few decades, this battery of options has been expanded to include immunotherapy and molecular target-specific therapy which brought many novel and promising avenues of research and revolutionized therapy of some tumor types. The three traditional treatment modalities however still represent the most common and in many cases only possibilities to stop or mitigate malignant disease progression. As a result, massive effort is continuously expended to improve their efficacy, to alter and optimize treatment regimens, often tailor-made to address the particular cancer subtype and individual patient's needs, to

uncover novel avenues within these established treatment modalities and to counter the specific issues limiting their full potential.

I.2.1. Surgery

Historically, surgical excision has been the first treatment option available for tumor patients and it remained the only treatment until the advent of radiotherapy in the 1920s. It retained its prominent role as the most effective method to reduce tumor volume and decrease the burden on the patients. Surgery has over the last century been subject to vast improvement in terms of standardly available operating tools and conditions, development of novel surgical protocols to better incorporate the understanding of tumor biology and the consideration of the particular surgical needs arising from the biological characteristics of the tumor in question and its relations to the surrounding of the tissue and the system as a whole. Perhaps most importantly, surgery is constantly being pushed to make full use of the possibilities offered by innovations in radiotherapy and chemotherapy, as well as immune therapy and biological therapy since their appearance in the last decades.

This includes the fact that in the current stage of malignant disease treatment, surgery is almost always employed as a part of a combination scheme. In a neoadjuvant regimen, the patient is first subjected to a round of treatment with a different modality (usually radio or chemotherapy) before surgery in order to decrease the tumor volume or stabilize the tumor to increase the likelihood of successful surgery and decrease the risks of intra- and postoperative complications. In the case of an adjuvant treatment scheme, the tumor is first surgically removed, and then the patient is subjected to further treatment with a different modality according to the particular protocol in order to remove the residual and circulating tumor cells and treat the potential metastasis. Surgery plays a critical role in this not only in reducing the tumor volume, but above all in providing important diagnostic tool in pathological analysis and scoring of the removed tumor. This is universally expressed in the form of a standardized classification (known as the AJCC/UICC-TNM classification) and serves to evaluate the aggressiveness of the disease in order to choose the optimal postoperative treatment regimen from the available scale [61]. This is done according to the finding in the primary tumor site (T), findings in the draining lymph nodes (N) and signs of systemic metastases (M). An important initiative is also currently underway worldwide to update these staging guidelines to also include immune score, based on the observation that immune infiltration in the tumor site and systemic parameters of immune system in many cases provide better

predictive effectiveness of prognosis than the currently used TNM classification [61], [62], [63],[64].

The limitations of surgical treatment include the often unfavorable location of the tumor which renders surgery difficult or outright impossible, the often high burden surgery and general anesthesia impose upon patients, who are usually old and in poor overall condition, and above all the inability to causally treat tumors which progress past the strictly local stage into locally invasive or metastatic stages. Surgery is however often used even in the cases when complete cure is no longer possible as a palliative measure to relieve pain and improve the quality of the remainder of the patient's life.

I.2.2. Radiotherapy

Radiation therapy (RT) became available following the discovery of X-rays by Röntgen in 1895 and came into use as a mode of cancer treatment in the early 20^{th} century. It is commonly combined into treatment regimens including the other forms of cancer treatment according to the properties of the particular type of cancer. It can also be used as a palliative measure to reduce the tumor volume and relieve the symptoms if this is not achievable surgically for some reason.

Its efficiency is derived from a direct or indirect effect of the ionizing radiation on DNA of the cells and it therefore mainly affects tissues characterized by a high level of proliferation, accounting for the anticancer efficacy as well as the common adverse side effects.

Due to this fact, radiotherapy exhibits different levels of effectiveness on different types of cancer, with malignancies of hematopoietic origin (leukemias and lymphomas) and germ-line tumors being the most radiosensitive. An important indication of highly aggressive radiotherapy is the use of RT in myeloablation, a technique of complete destruction of patient's own hemopoietic elements in preparation for subsequent bone marrow transplantation, procedures which revolutionized the treatment of some forms of leukemia and other malignancies of hemopoietic origin and continue to be used till today [65].

Radiotherapy can be categorized according to the type of ionizing radiation used or according to the way of administering the radiation dose into internal radiotherapy, which is characterized by the direct application of a radioactive substance into a patient's body, and external beam radiotherapy, in which external sources of radiation beams are used.

The considerable side effects of radiotherapy include its damaging effects on healthy tissues with high proliferation rate, most importantly bone marrow and gastrointestinal tract

(GIT) as well as hair follicles. Possibly the most serious adverse effect is the risk of secondary malignancies, which may arise years or decades after radiation treatment especially in the cases treated with high doses of radiation. Research and improvement of both the technology used and therapeutic protocols continually strive to curtail these unwanted side effects while maintaining therapeutic efficacy. In the case of internal radiotherapy, this can be achieved by conjugating the radiotherapeutic agent with a targeting moiety such as an antibody [66], a polypeptidic targeting moiety [67] or even just exploiting the natural affinity of the radiotherapeutic to the target tissue, as is commonly used in the treatment of some forms of thyroid cancer using ^{131}I thyroid ablation. In the case of external beam RT, contemporary methods allow for using of highly coherent radiation beams of lower individual radiation burden which intersect at the precise location of the tumor and combine to expose it to a higher dose needed for effective therapy. The ultimate precision can be achieved in this way in the so-called stereotactic radiosurgery, when highly focused and precisely applied radiation beams are used *in lieu* of conventional surgery for tumors localized to places inaccessible to conventional surgery, such as intracranially [68].

I.2.3. Immunotherapy

The rising awareness of the importance of tumor immunity naturally led to the various attempts to support or induce immune response against tumors which collectively form immune therapy. With the refinement of available methods and progress in understanding the components and functions, multiple forms of cancer immunotherapy have already been introduced into clinical use and more are in the phase of clinical trials.

The first forms of immune therapy used were non-specific, i.e. aimed at indiscriminately supporting and activating the immune elements already present at the time of treatment. This included the use of adjuvant-like substances such as intravesical application of Bacillus Calmette-Guerin (BCG) to treat superficial forms of urinary bladder malignancies [69]. This treatment proved high long-term benefit [70], but the toxicity resulting from the live attenuated mycobacteria warrants further research [71]. Another approach of passive immunotherapy is using cytokines. The most commonly used cytokine in cancer therapy is IL-2, which is in clinical use against several forms of cancer, most notably renal cell carcinoma [72] and metastatic melanoma [73]. Systemic administration of high-dose IL-2 is however significantly burdened with toxicity; hence, substantial effort is made to improve its tolerability without sacrificing the therapeutic effect [74]. Another cytokine commonly used in cancer immunotherapy is IFN-α, functioning via a number of biological effects, including

antiproliferative, proapoptotic and antiangiogenic. IFN-α is used in clinical practice in the treatment of hematological malignancies, angiomas and metastatic malignant melanoma [75], [76], [77].

A more selective approach is the induction of a specific antitumor response, i.e. vaccination or immunization in the strict sense. This can be done passively, i.e. by administering immune cells extracted from the patient and activated *ex vivo* for efficient anti-tumor function, such as lymphokine-activated killers (LAKs; i.e. lymphocytes isolated from peripheral blood and activated under laboratory conditions with IL-2 [78]) or tumor infiltrating lymphocytes (TILs; autologous leukocytes isolated from the tumor, activated and cultured into high numbers before being adoptively administered back into the patient) [79]. Another approach is active anti-tumor vaccination, an area that holds much promise. The possibilities include tumor cell based vaccines, relying on administration of tumor cells killed via the pathway of ICD [80], DNA-based tumor vaccines which attempt to induce anti-tumor response by presenting the immune system with tumor antigens in a manner which elicits effective response [81], and perhaps most importantly, dendritic cell based vaccination. This approach was made possible by improving the technology of DC generation and maintenance in culture, enabling their efficient maturation into effective APCs and arming with relevant tumor antigens, which then upon administration into the patient elicit potent anti-tumor response. The first DC vaccine against castration-resistant prostate cancer was based on prostatic acid phosphatase tumor-specific antigen and was clinically approved in 2010 [82]. Further clinical studies of DC-based vaccines as well as their inclusion into combinatory therapeutic protocols e.g. with chemotherapy are underway [83], [84].

Last but not least, spanning the border between immunotherapy and the molecular target-specific therapy is the use of monoclonal antibodies (MAbs) or their fragments in cancer therapy. This highly versatile class of molecules combines multiple benefits both for cancer therapy and in other fields, such as anti-inflammatory biological therapy of autoimmune diseases. Their advanced and well characterized manner of synthesis allows efficient creation of well-tolerated humanized or fully human MAbs. Their high molecular weight and ability to specifically target tumor environment can improve unfavorable pharmacokinetics of other therapeutic agents, such as in conjugates of MAbs and cytokines labelled immunocytokines, e.g. L19-IL2 [85], [86], [87]. Their capability to selectively target any antigen is used in cancer treatment in a variety of ways and by a number of clinically approved MAbs. Modes of function include activating antigen-dependent cellular cytotoxicity and complement-dependent cytotoxicity via their Fc fragments (e.g. rituximab, anti-CD20

[88]), direct inhibitory effect of various biological pathways implicated in the hallmarks of cancer, such as angiogenesis (e.g. bevacizumab, anti-VEGF [52], [53]) or sustained proliferative signaling (e.g. trastuzumab, anti-HER2/neu [89]), counteracting suppressive pathways employed by regulatory immune cells in the tumor (known as immune checkpoint inhibitors, e.g. ipilimumab, anti-CTLA4 [86], [90], [91]) and finally, serving as a targeting entity to deliver chemotherapeutic agents [92] or radionuclides [66], [93] directly into tumors.

I.2.4. Chemotherapy

Chemotherapy represents the final modality of the conventional triad of cancer treatment options, and the first one to offer an effect encompassing the whole organism, including the circulating cancer cells and metastases. As a discipline, chemotherapy was established with the describing of the first conventional chemotherapeutical agents in the 1940s and by 1960s had achieved practically universal importance as the number of available cancer chemotherapeutics rapidly grew due to intensive research. Chemotherapy is still used to complement both radiotherapeutic and surgical protocols in the complex treatment regimens of almost all types of cancer and countless chemotherapeutical protocols have been devised and implemented to tailor-suit the myriad clinical forms of cancer with the most effective possible treatment schemes. Despite this, the prognosis in many cases remains poor.

The most commonly used categories of conventional chemotherapeutic drugs still being used in clinical practice include: antimetabolites (i.e. metabolite analogues which either inhibit crucial enzymes mostly in the metabolism of nucleic acids or induce irreparable damage upon integration into DNA; e.g. methotrexate, fludarabin, cytarabin, 5-fluorouracil); alkylating agents (i.e. compounds which covalently modify DNA, leading to failure of replication and cell death, e.g. mitomycin C, cyclophosphamide, cisplatin and its derivatives); intercalating agents (i.e. compounds which work by non-covalently intercalating into the DNA spiral and consequently render transcription and replication impossible, e.g. anthracyclin antibiotics such as doxorubicin, actinomycin D, mitoxantrone); topoisomerase inhibitors (i.e. substances hampering replication via inhibiting topoisomerases, e.g. irinotecan, topotecan); and antimitotic agents, i.e. chemotherapeutics which induce mitotic catastrophe by disrupting the microtubule dynamic instability and therefore function either by inhibiting microtubule polymerization (e.g. colchicine and vinblastine, working via different binding sites) or inhibiting microtubule depolymerization (signature activity of taxanes, e.g. docetaxel and paclitaxel).

All of the categories mentioned above differ greatly in all of their important characteristics, including their origins, modes of function, toxicity profiles, pharmacokinetic and chemical properties, portfolios of effectiveness in various cancer types etc. Despite this, all conventional chemotherapeutic agents share certain attributes as well as certain issues these attributes bring. Generally speaking, the conventional cytostatic drugs are all small, low molecular weight (LMW) compounds. When viewed along the perspective of the cancer hallmarks as presented in [10], it is noteworthy that virtually all the conventional chemotherapeutics practically exclusively act via the two of them which manifest in rapid proliferation (i.e. sustaining proliferative signaling and evading tumor suppressors) while affecting the other hallmarks with random collateral damage at best and actively abetting some of the hallmarks and enabling characteristics at worst (e.g. the mutagenesis inherent in the mode of function of some of the groups; immunosuppressive effect of many of these drugs). This effectively limits their effect to rapidly proliferating tissues which means that they are not only nonspecific, but also show only limited effectiveness in the types of tumors or populations of tumor cells which proliferate less aggressively.

I.2.4.1. Issues limiting the conventional chemotherapy

From the common properties mentioned previously arise several surprisingly universal pitfalls which limit the effectiveness of tumor chemotherapy by conventional chemotherapeutics and need to be overcome or circumvented if cancer treatment is to be further improved.

The LMW nature (molecular weight usually less than 1500 [58]) of the conventional chemotherapeutics limits their half-life in the blood circulation and also accounts for the fact that they are generally distributed according to the relative perfusion of a given organ and the characteristics of the drug in question. Coupled with the unspecific nature of mechanism of these drugs, this unfavorable biodistribution leads to high systemic toxicity and commonly severe organ-specific side effects. The first category are universal side effects which result from the effect of all LMW drugs on rapidly proliferating cells, such as gastrointestinal toxicity, hair loss and importantly, bone marrow toxicity resulting in immunosuppression and anemia. Individual classes of conventional cytostatic drugs may also have other systemic or organ-specific side effects, e.g. the typical cardiotoxicity of anthracyclins including doxorubicin [94], [95]. The high toxicity is usually the most important dose-limiting factor of conventional chemotherapy. The short circulatory half-life also necessitates using unfavorable

treatment schemes to keep the concentration of the drug in the tumor on the effective level. Usually, this means either administration of high bolus doses which are followed by correspondingly high systemic side effects, or administering the drug in the form of a continual infusion, which necessitates hospitalization of the patient at least for a short time. Both of these increase the costs incurred and decrease the quality of life of the patient, which is an extremely important medical aspect as it reduces the patients' compliance and the probability of treatment success.

The threshold on dosage created by the high toxicity leads to the fact that often the drug cannot efficiently reach the concentration in the tumor needed to elicit the full therapeutic effect. Solid tumors are usually somewhat harder to treat with chemotherapy due to the highly dysfunctional nature of tumor vasculature, which limits the biological availability of both nutrients and other compounds including drugs. The tumor stroma, which contains tumor cells, fibroblasts, immune cells and extracellular matrix in a highly disorganized pattern, typically has higher interstitial pressure than healthy tissues, further complicating the diffusion of LMW drugs into solid tumors [96]. This is further compounded by the phenomenon of intrinsic or more importantly acquired drug resistance. Intrinsic resistance may be caused by the specific biological properties of the tumor cells, which render different types of tumor more responsive to some classes of therapeutics and less to others. Generally, some tumor types show particularly low sensitivity to conventional chemotherapy, often reflecting low overall proliferative activity. Furthermore, as each tumor is in fact a complex population of many subclones derived from the original cell [20], some of these populations may also become more resistant to therapy than others due to acquired biological differences, effectively evolving to evade the therapeutic pressure. This is an example of acquired resistance, likewise a crucial factor limiting therapeutic efficacy. The induced resistance may be caused by a single specific change in a subpopulation of cancer cells, like the loss of dependence on a particular enzyme or a point mutation in the drug target (e.g. tubulin molecule in case of antimicrotubule drugs), in which case the tumor becomes resistant to a particular drug or class of drugs but retains sensitivity to others. A different situation occurs in the phenomenon known as the multi drug resistance (MDR), where the tumor cells become resistant to a wide range of structurally and functionally diverse therapeutics [97]. This is most commonly caused by the expression of a specific type of ATP-dependent efflux pumps known as ATP-binding cassette or ABC transporters [98], which are a conserved family of proteins used by many types of cells to transport a variety of diverse, usually foreign

compounds out of the cytoplasm [99]. The most important of ABC transporters is known as the P-glycoprotein (Pgp) [100].

Taken together, these factors contribute to the common scenario in which tumor seemingly responds well to the therapy, only to relapse after some time with the same or increased aggressiveness. This may to some degree also be caused by the presence of a population of slowly proliferating, highly chemoresistant cells with full tumorigenic potential known as cancer stem cells [101]. These cells may effectively weather the treatment regimen and afterwards repopulate the tumor under more favorable conditions.

Last but not least, due to its unspecific nature, conventional chemotherapy also often has a devastating effect on the patient's immune system, hampering its effectiveness against the residual populations of tumor cells after treatment.

Numerous avenues of research have been explored in order to circumvent these pitfalls. Dose-limiting adverse effects may be mitigated by adhering to a more rational treatment schedule and changing the way of application. Combination regimens of drugs with complementary effect and non-overlapping toxicities allow the potentiation of the therapeutic effect while lowering the doses of the individual therapeutics and limiting the overall toxicity [102]. An entire area of research is devoted to studying and preventing or inhibiting MDR [103], [104]. Treatment protocols are improved based on better understanding of tumor biology and immunology, favoring the compounds and regimens which not only leave immunological system intact, but effectively stimulate it to recognize and eliminate remaining tumor cells [41], [40], [80]. Among the most important implications, however, is the impetus the issues accompanying conventional chemotherapy gave to the research and implementation into clinical practice of novel ways to increase selectivity by passively or actively targeting tumors. There are two main facets of this focus on more selective treatment. The first is the design of high molecular weight (HMW) drug delivery systems which allow specific transport of drugs into tumors and the accumulation of drugs in them (i.e., tumor targeted therapy); and the second is the development of novel compounds which work selectively on specific targets within the tumor cells, based on better understanding the particular abnormalities and pathways of cancer biology (i.e., the molecular target-specific therapy).

I.2.4.2. HMW drug delivery systems

Various HMW systems are currently under research and development to improve the unfavorable pharmacokinetic profile and biodistribution of LMW chemotherapeutics, mainly

prolonging their time of activity at the target site and achieving preferential delivery into tumor tissue while keeping drug away from sites of potential damage. Many of the LMW drugs are hydrophobic compounds and the use of HMW delivery systems improves their water solubility and bioavailability [105]. Another important aspect of the HMW carrier research is the design of ways for controlled release of the drug from the carrier under tumor specific conditions, further improving the selectivity of the effect and decreasing toxicity.

The specific delivery and accumulation into tumors can be achieved either passively via taking advantage of the biochemical and pathophysiological characteristics of the tumor such as the EPR effect [58], or actively, i.e. by ligand targeting. This is based on the specific affinity of a ligand (e.g. antibodies, saccharide moieties etc.) bound to the HMW carrier with a specific partner in the target tissue (e.g. tumor antigens or surface lectins, respectively) and combined with the passive accumulation inherent to HMW systems greatly improves the preferential biodistribution into the tumor and therapeutic effect [106].

Controlled release of the drugs from HMW delivery systems may occur in the tumor tissue or within the tumor cells themselves after intake of the HMW carrier via endocytosis (note that this may offer the added benefit of partially circumventing the MDR efflux pumps which are present on the cell membrane [107]). The mechanism of controlled release depends on the design of the linker which forms the bond between the carrier and the drug and may be either enzyme-dependent or pH dependent. Enzyme dependent release employs some of the various proteases, glucuronidases or esterases expressed within or released by tumor cells, whereas the pH dependent release takes advantage of the characteristically low pH in the microenvironment of solid tumors.

Numerous HMW delivery systems have been designed so far. This includes nanosized carriers and water soluble polymer based drug delivery systems. Among the nanosized entities as comprehensively reviewed in [108], [109] are liposomes (i.e. lipid bilayer vesicles surrounding a core of aqueous solution), micelles (i.e. vesicles formed of a hydrophilic external layer surrounding a lipid core used for loading with hydrophobic drugs), emulsions and lipid nanospheres (similar to liposomes but possessing hydrophobic oil- or solid lipid-based cores, respectively), dendrimers (i.e. tree-like macromolecules possessing a highly branched but well-defined architecture, allowing for good control of their molecular weight and properties during synthesis, e.g. polyamidoamine [PAMAM] dendrimer [110]) and lastly, polymer nanoparticles (e.g. albumin-based nanosized particles for drug delivery) [111].

Water soluble polymer-based delivery systems include several of the best studied and most commonly used in clinical practice. In particular, synthetic polymers are widely used for

surface modification of proteins (e.g. to decrease their immunogenicity and increase their biological half-life [112]) or implants, construction of nanoparticle-based drug delivery systems and finally as the basis of HMW drug carriers, all due to the biologically inert nature of the majority of these compounds. The most important and well-studied examples of such polymers are polyethyleneglycol (PEG) [112] and *N*-2-hydroxypropyl)methacrylamide (HPMA) [113].

HPMA copolymer-based drug delivery systems in particular offer numerous well documented benefits for cancer treatment. The HPMA polymers have been first synthesized in the 1970s by Kopecek and co-workers and both the homo- and the copolymers were subsequently described to be non-toxic, biologically inert and non-immunogenic [114]. They are not metabolized and do not form deposits but instead are eliminated unchanged via renal excretion unless they exceed the renal excretion limit of approx. 45 kDa [115]. HPMA is also water-soluble and its conjugation commonly improves the solubility of even highly hydrophobic drugs [105].

The presence of multiple active sites on the HPMA monomer side chain allows for the binding of various types of cargo to the HPMA copolymer backbone such as anticancer drugs, moieties for active targeting, peptides and other biologically active agents via defined linkers, (Fig I.5). It has been proven that conjugation with HPMA copolymer significantly decreases immunogenicity of proteins [116] and toxicity of drugs such as LMW chemotherapeutics [117] while prolonging the biological half-life and allowing for prolonged and specific accumulation in the tumor owing to the EPR effect [118]. Directed synthesis can also allow for combining of HPMA monomers carrying multiple substituents into a single polymer, ensuring the effective delivery of a combination of drugs and/or biologically active substances into tumor at exactly the same time, allowing for very effective combination treatment [103], [119].

The exact pharmacokinetic parameters of an individual HPMA-drug conjugate and the effectivity of accumulation into tumors mainly depend on its hydrodynamic diameter, largely corresponding to the molecular weight [120]. This led to the design of various types of HMW HPMA copolymer-based carriers with higher molecular weight based on linking individual HPMA copolymer chains into a branched network or attaching them onto a dendrimer core formed e.g. by a defined PAMAM dendrimer [120]. The elimination can be then ensured by the inclusion biodegradable bonds between individual HPMA chains and to the dendrimer core, with the chemical properties of these bonds governing the kinetics of elimination [121].

The release of the drug from HPMA copolymer is controlled by the presence of a defined linker between the drug and the backbone. The release can be either enzymatic or pH-dependent, and its kinetics critically influence therapeutic effect as well as toxicity [122], [123]. While in some cases the drug retains its therapeutic efficacy while still bound to the HPMA copolymer backbone [124], generally, release from the carrier is necessary for the drug to reach its molecular target and achieve full function [125].

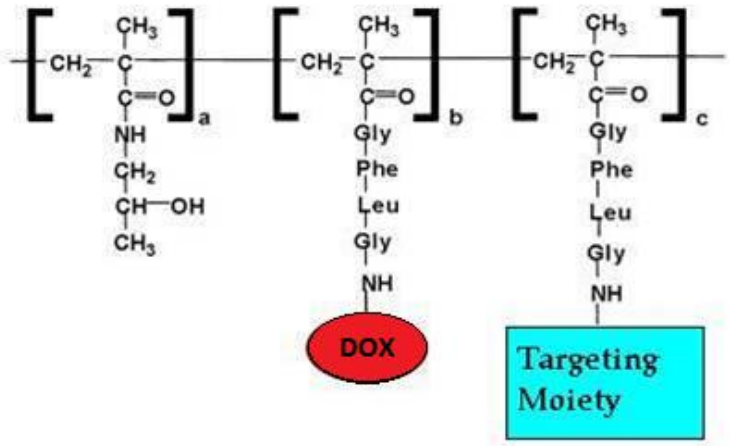

Fig I.5 Schematic draw of HPMA copolymer. Figure shows HPMA subunit without any substituents (a), a subunit with a drug bound via the amidic GFLG linker (b) and a subunit with a targeting moiety bound via the amidic GFLG linker.

A well-described and commonly used category of HPMA copolymers are HPMA copolymer-bound conjugates of doxorubicin (DOX; Adriamycin, Adriblastina). Belonging to the anthracyclin antibiotic family and acting via DNA intercalation and topoisomerase II inhibition, DOX is a widely used conventional LMW chemotherapeutic and a part of many chemotherapeutic treatment schemes [126]. It has recently been shown to induce the ICD in treated cells [37], [41]. An important limiting factor is its serious systemic toxicity, with myelosuppression and severe cardiotoxicity being the most serious adverse effects [95]. It is also subject to MDR.

The first described conjugate of DOX with HPMA was introduced in 1985 as DOX^{AM}-PHPMA (FCE 28068, also known as PK1), with DOX bound to the HPMA backbone via an enzymatically cleaved amidic linker composed of GFLG oligopeptide. PK1 showed improved half-life and decreased toxicity of DOX, and proved effective in preclinical

conditions [127] as well as in clinical trials [128]. More recent research established a line of DOX-HPMA conjugates with a pH sensitive hydrazone bond [129], which possess comparable or improved preclinical properties [130], as well as additional advantages such as retaining the ICD-inducing nature of DOX [41], which is lost in the copolymers with the amidic linker [42]. A highly significant characteristic of HPMA-bound conjugates DOX is the efficient induction of effective antitumor response [131].

I.2.4.3.Molecular target-specific therapy

The advances in understanding the molecular constituents and pathways of both physiological and cancer cells allowed the introduction of a novel class of LMW chemotherapeutic agents with improved specificity, the so called molecular target-specific therapy. This category of therapeutics is specifically engineered to selectively block the function of a very small number of molecules which represent the crucial components of the pathways which provide the tumor with one or more of its hallmark characteristics. The selective blockade of these tumor-specific aberrant pathways exerts a far more narrow effect, in the optimal case effectively treating the tumor while exerting very side toxicity.

The molecular targets of the novel LMW inhibitors include components of subcellular pathways which mediate parameters such as the cell cycle and proliferation control, signal reception and transduction, regulation of apoptosis, regulation of telomerase activity, protein metabolism and regulation of responses to cellular stress. Common examples of the targets are various kinases, anti-apoptotic proteins of the Bcl-2 family, telomerase or chaperones such as Hsp90 and related heat-shock proteins or the proteasome complex.

The first example and prototypic drug of this group is imatinib (imatinib mesylate; Glivec or Gleevec, Novartis Pharma), an inhibitor of activity of several targets, predominantly tyrosine kinases. The most important of these targets is a fusion protein BCR-ABL which plays the critical role in the pathogenesis of chronic myeloid leukemia (CML) and is also found in a subset of cases of acute lymphoblastic leukemia (ALL). BCR-ABL is a constitutively active tyrosine kinase which arises from the fusion of the *BCR* and *ABL* genes during the reciprocal chromosome translocation t(9; 22). This so called Philadelphia chromosome is created during CML pathogenesis in hematopoietic cells and the resulting constitutive activity of BCR-ABL represents the crucial step in CML pathogenesis. Therefore, the selective competitive inhibition of BCR-ABL kinase activity by imatinib revolutionized the treatment of CML [132]. Since the introduction of imatinib, second generation of BCR-

ABL inhibitors has been introduced with improved effectivity (e.g. dasatinib [133]) as well as numerous other molecularly specific kinase inhibitors.

Other promising classes of molecular target-specific drugs include for instance proteasome inhibitors such as bortezomib [40] and its next generation successor carfilzomib [134], [135] which found use in the treatment of multiple myeloma and other types of cancer; inhibitors of heat shock proteins such as geldanamycin and its derivative alvespimycin (17-dimethylaminoethylamino-17-demethoxygeldanamycin; 17-DMAG) [136]; and inhibitors of antiapoptotic proteins from the Bcl-2 family, such as the first BH3-specific mimetic ABT-737 [137].

Despite the marked safety and effectiveness of this approach, it nevertheless has its disadvantages. Cancer diseases are intrinsically characterized by high redundancy of the employed pathways as well as high variability between the cell populations within a single tumor and even much higher between different patients or tumor types [9]. In fact, very few cancer types are as highly reliant on a single molecular mechanism as in the case of CML and BCR-ABL. Therefore, in clinical practice, many of the drugs in this category find optimal use in combinatorial rather than single therapy protocols [89], [133], [138]. This cumulative effect could conceivably be further improved by the cotemporal delivery of multiple drugs that make up the combination via the controlled release from a HMW drug delivery system such as an HPMA copolymer, as has already been described [103].

I.2.4.4. Novel drugs and drug repurposing

In light of all that has been said above, despite the progress, there is still a pressing need to discover and implement novel chemotherapeutic compounds to further improve the options available in tumor treatment and offer new possibilities to effectively treat those malignancies which are largely unaffected by the current options. Unfortunately, bringing a completely new drug into clinical practice takes exceedingly high amounts of time and money and often encounters many pitfalls [139]. Therefore, a promising approach lies in repurposing compounds already registered for use in human medicine for cancer treatment. Such research can draw on readily available data and advance through clinical trials for a new indication much easier, faster and cheaper than researching completely new drugs [140], [141].

This approach is usually based either on *in silico* analyses and screening of already established drugs in terms of transcriptomic, genomic or side effects-related data for

characteristics potentially implying promise for cancer treatment [140], [142], or laboratory screening large libraries of rationally chosen compounds (e.g. anti-microbial drugs or kinase inhibitors) for *in vitro* effect in cancer cell lines [141]. Among the examples of drugs already repurposed or currently in the process of being investigated for anti-cancer potential in this way are such diverse compounds as quinacrine [143], metformin [144] or benzimidazole anthelminthic drugs including mebendazole [141].

I.2.4.5.Mebendazole

One example of a repurposed drug is mebendazole (MBZ; Fig I.6), an anthelminthic from the family of the heterocyclic benzimidazoles along with related drugs albendazole and fenbendazole. MBZ has been widely and consistently used in human and veterinary medicine since early 1970s [145] and is still marketed worldwide as Vermox or Mebendazole.

Main indications of MBZ include peroral (p.o.) treatment of both gastrointestinal and systemic forms of helminthiases, i.e. worm infections caused by the worms of Nematoda or Platyhelminthes phyla. Due to its low toxicity and high cure rates [146], MBZ is the drug of choice in the hydatid disease or echinococcosis, a systemic form of *Echinococcus multilocularis* infection [147], [148], [149]; trichuriasis (also known as whipworm infection), a gut helminthiasis caused by *Trichuris trichiura* [150]; ascariasis, a predominantly gastrointestinal helminthiasis caused by *Ascaris lumbricoides* [146]; and the so called hookworm infections caused by flatworms of the *Ancylostoma* and *Necator* genus, which represent a major cause of anemia and maternal and child morbidity in the developing countries [151], [152].

Fig I.6 The structure of mebendazole (MBZ).

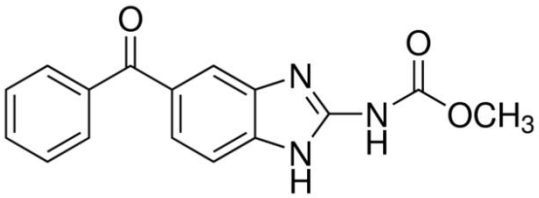

A striking attribute of MBZ is its negligible toxicity in humans as well as most studied animals [153], which is low enough for its application to be considered even in antenatal period with the exception of first trimester [152]. This is mainly due to its low bioavailability which is caused by extremely poor solubility [154] as well as its high vulnerability to the first pass effect [155], further decreasing its systemic availability. Nevertheless, the small quantity

of MBZ which does reach the systemic circulation is high enough to effectively both treat systemic helminthiases [155] and exert an anti-cancer effect in humans [156], [157]. The metabolism of MBZ occurs mainly in the liver and it is excreted mostly via urine and bile, with a substantial contribution of enterohepatic recycling [149]. The blood levels and biological half-life were found to vary significantly between patients and the bioavailability seemed higher in patients suffering from more severe helminthiases [153]. It was also noted that MBZ and its metabolites bind highly to serum proteins in circulation [149].

In the cases where toxicity was described, the most common forms were gastrointestinal such as abdominal pain or dyspepsia. There were only sporadic reports of serious toxicity; this included a case report of hepatitis suggestive of direct hepatotoxic effect of MBZ [158] and importantly also alopecia and granulocytopenia in a human patient [159] as well as severe and rapid bone-marrow aplasia followed by lethal septicemia observed in an experiment on red-legged pademelons (*Thylogale stigmatica*), an Australian marsupial of the family *Macropodidae* [160].

The antiparasitic effect of MBZ is mediated by blocking microtubule polymerization via the colchicine binding site on microtubules in the intestine of helminths [161], although the drug binds to mammalian tubulin with similar efficiency [162]. The different availability likely is the key factor in the selective anthelmithic effect.

The anticancer effect of MBZ was first described in 2002 in the model of human non-small-cell lung cancer [163], [164] and currently, there are reports of antitumor activity against numerous human cancer cell types, notably malignant melanoma [165], [166], mammary adenocarcinoma [167], CNS malignancies including medulloblastoma [168] and glioblastoma multiforme [169] and recently also colorectal carcinoma [170]. Similarly, anticancer activity has been observed in flubendazole, a sister drug from the benzimidazole family, in preclinical models of leukemia and myeloma [171]. Strikingly, MBZ has also been reported to elicit long-term disease control in two case reports [156], [157].

The reported anticancer effects of MBZ are just as varied. The disruption of microtubule system in favor of depolymerization similar to the effect in nematodes has been described [164], [169], [165]. The microtubule destabilization is also described as the basis of an inhibitory effect on the Hedgehog signaling cascade [172]. Another significant area of effect of MBZ lies in the facilitation of apoptosis via the inactivation of proteins from Bcl-2 family [163], [164], [165], as well as the downregulation of the X-linked inhibitor of apoptosis [166]. Furthermore, MBZ was also proven to be an effective inhibitor of a number of kinases with key roles in cancer biology, such as BRAF and BCR-ABL [170] and

VEGFR2 [168], accounting for the observed antiangiogenic effect of MBZ treatment in mice [163].

II. Aims

The subject of our work was mebendazole (MBZ), an anthelminthic from the family of benzimidazoles. It is an example of a drug repurposed for chemotherapy of malignant diseases. In this work, we focused to characterize its newly described anticancer effect *in vitro* in various murine tumor cell lines. We also designed and tested a novel HPMA copolymer-bound conjugate in order to allow the otherwise extremely poorly soluble MBZ to be administered parenterally. This allowed us to observe its toxicity *in vivo* and its potential therapeutic effect in syngeneic murine tumors.

The aims of our study were:

1. To determine the *in vitro* anticancer effect of MBZ in a panel of murine tumor cell lines of different tissue origins.
    a. To compare the cytostatic activity of MBZ in murine tumor cell lines with other drugs including doxorubicin.
    b. To compare the cytotoxic activity of MBZ in murine tumor cell lines with doxorubicin.
    c. To determine whether MBZ is subject to Pgp mediated MDR by comparing its activity in sensitive P388 and resistant P388/MDR cell lines.
2. To design and synthesize HPMA copolymer-bound MBZ conjugate which would improve the solubility of MBZ in aqueous environments and allow for its release under physiologic conditions.
    a. To synthesize derivatives of MBZ in order to enable the binding of the drug to HPMA copolymer and compare their *in vitro* cytostatic activity.
    b. To synthesize HPMA copolymer-bound MBZ conjugate based on the better performing of the two derivatives.
3. To determine *in vitro* anticancer effect of such conjugate and MBZ derivatives.
    a. To evaluate the solubility of HPMA copolymer-bound MBZ derivative and compare its *in vitro* anticancer activity with that of free MBZ.
    b. To compare the individual batches of HPMA copolymer-bound MBZ conjugate in terms of *in vitro* activity, stability under laboratory conditions and solubility.

4. To characterize the *in vivo* toxicity of the conjugate and its potential therapeutic effect in various syngeneic murine tumors.
    a. To confirm the possibility of parenteral administration of HPMA copolymer-bound MBZ and to determine its maximum tolerated dose (MTD) in mice.
    b. To evaluate therapeutic efficacy of parenterally administered HPMA copolymer-bound MBZ in syngeneic murine tumors.
    c. To determine the most prominent toxicities of parenterally administered HPMA copolymer-bound MBZ in mice by preparing histological samples of selected organs from mice treated with HPMA copolymer-bound MBZ and searching for signs of acute toxic injury in various tissues as well as using less invasive methods.

III. Materials

III.1. Solutions

Phosphate buffered saline (PBS)

Deionized H_2O

0.9% NaCl

0.14% $Na_2HPO_4.12H_2O$

0.12% $Na_2HPO_4.2H_2O$

pH adjusted for 7.2-7.4 (4M NaOH)

Kept at 4°C in dark.

Dulbecco's modified Eagle's minimal essential medium (D-MEM)

Obtained from Institute of Molecular Genetics, CAS, v.v.i., Prague, Czech Republic.

Kept at 4°C in dark.

Roswell Park Memorial Institute medium 1640 (RPMI)

Purchased from Gibco/Life Technologies, Czech Republic.

Kept at 4°C in dark.

Dimethyl sulfoxide (DMSO)

Purchased from Sigma-Aldrich, Czech Republic.

Kept at room temperature in dark.

Retic-Count (Thiazole orange) Reagent

Purchased from BD Biosciences, USA.

Kept at 4°C in dark.

III.2. Cell lines

All cell lines were purchased from ATCC except for P388 and P388/MDR cells which were kindly provided by Prof. I. Lefkovits (Basel Institute for Immunology, Basel, Switzerland).

LL2 murine Lewis lung carcinoma line (ATCC CRL-1642) was established as a clone of Lewis lung carcinoma cells adapted to cell culture [173]. The line is a non-small-cell lung carcinoma derived from C57BL/6 mice. *In vitro* LL2 cells are grown in D-MEM medium supplemented with 10% heat inactivated fetal calf serum (FCS, Invitrogen), L-glutamine (2 mM, Sigma-Aldrich), antibiotics (100 U penicillin + 0.1 mg streptomycin/ml, Sigma-Aldrich), HEPES (0.01M), glucose (4.5 g/l) and $NaHCO_3$ (0.15%). Cells grow in culture in a mixed pattern, partly loosely adherent, partly as a suspension. They induce tumors when subcutaneously injected into C57BL/6 mice.

EL4 murine T-cell lymphoma line (ATCC TIB-39) was derived from a T-cell lymphoma induced with 9,10-dimethyl-1,2-benzanthracen in C57BL/6 mice [174]. *In vitro* EL4 cells are grown in RPMI medium supplemented with 10% heat inactivated FCS, L-glutamine (4mM), antibiotics, glucose and sodium pyruvate (1 mM). Cells grow in culture as a suspension and induce tumors when subcutaneously injected into C57BL/6 mice.

EL4.IL2 subline (ATCC TIB-181) was defined as a subtype which produces IL-2 when stimulated with phorbol 12-myristate 13-acetate (PMA) [175]. This subline was used for *in vitro* assays since the original cell line does not incorporate [^{3}H]-thymidine at a sufficient quantity.

B16F10 murine melanoma line (ATCC CRL-6475) was derived from C57BL/6 mice [176]. *In vitro* B16F10 cells are grown in D-MEM medium supplemented with 10% heat inactivated FCS, L-glutamine, antibiotics, HEPES, glucose and $NaHCO_3$. They grow in culture in an adherent fashion and induce tumors when subcutaneously injected into C57BL/6 mice.

CT26 murine colorectal carcinoma line (ATCC CRL-2638) was induced with *N*-nitroso-*N*-methylurethane in BALB/c mice [177]. *In vitro* CT26 cells are grown in RPMI medium supplemented with 10% heat inactivated FCS, L-glutamine, antibiotics, HEPES,

glucose and sodium pyruvate. They grow in culture in an adherent fashion and induce tumors when subcutaneously injected into BALB/c mice.

BCL1 murine B-cell leukemia line (ATCC TIB-197) was derived from BALB/c mice [178]. *In vitro* BCL1 cells are grown in RPMI medium supplemented with 10% heat inactivated FCS, L-glutamine, antibiotics, HEPES, Na-pyruvate, and 2-mercaptoethanol (0.5 mM). They grow in culture as a suspension and grow in peritoneal cavity as tumor ascites as well as colonizing spleen and peripheral lymph nodes when intraperitoneally (i.p.) injected into BALB/c mice.

P388 murine monocytic leukemia line (ATCC CCL-46) was derived from DBA/2 mice where it was originally induced by painting the skin with methylcholanthrene [103]. *In vitro* P388 cells are grown in RPMI medium supplemented with 10% heat inactivated FCS, L-glutamine, antibiotics, sodium pyruvate and non-essential amino acids (5 ml; Sigma-Aldrich). They grow in culture in an adherent fashion.
P388/MDR cells represent a doxorubicin-resistant subline of P388 [103]. They are grown under the same conditions in culture, however unlike P388 cells they grow as a suspension.
Both P388 and P388/MDR lines were obtained from Prof. I. Lefkovits (Basel Institute for Immunology, Basel, Switzerland).

III.3. Mice

C57BL/6 mice and BALB/c mice were obtained from the breeding colony at the Institute of Physiology of CAS, v.v.i. All mice were kept in the animal facility of Institute of Microbiology of CAS, v.v.i in accordance with approved guidelines and provided food and water *ad libitum*. Mice were used for experimentation between the age of 9 and 15 weeks. The Animal Welfare Committee of the Institute of Microbiology, CAS, v.v.i approved all experiments.

III.4. Chemotherapeutics

Mebendazole (MBZ) was purchased in dry form from Sigma-Aldrich and kept at room temperature in the dark. The same stock which was used for preparing derivatives B-956 and B-957 was also used for *in vitro* experiments. For use in these experiments, MBZ was dissolved in DMSO at defined concentration and the solution was stored in aliquots at -20°C. When applied to cells, MBZ solution was diluted in culture medium to ensure that the end concentration of DMSO in all wells was lower than 1/100. All cell lines we used were tested to ensure that such low concentrations of DMSO have no effect on cell proliferation and metabolism.

Doxorubicin (DOX) was purchased in the form of Adriblastina solution (2 mg/ml) from Pfizer and kept at 4°C in the dark. For use in *in vitro* experiments, DOX was diluted with dH_2O and the solution stored in aliquots at -20°C. When applied to cells, DOX was diluted in culture medium.

Carfilzomib (Carf) was purchased in dry form from ChemieTek (USA), diluted in DMSO and the solution stored in aliquots at -80°C. When applied to cells, Carf solution was diluted in culture medium to ensure that the end concentration of DMSO in all wells was lower than 1/100.

Alvespimycin (17-DMAG) was purchased in dry form from Selleckchem (USA), diluted in DMSO and the solution stored in aliquots at -80°C. When applied to cells, 17-DMAG solution was diluted in culture medium to ensure that the end concentration of DMSO in all wells was lower than 1/100.

ABT-737 was purchased in dry form from Selleckchem (USA), diluted in DMSO and the solution stored in aliquots at -80°C. When applied to cells, ABT-737 solution was diluted in culture medium to ensure that the end concentration of DMSO in all wells was lower than 1/100.

III.5. Synthetic derivatives and HPMA copolymer conjugates

III.5.1. Synthetic derivatives of MBZ

Following low-molecular weight derivatives of MBZ were synthetized and characterized at Institute of Macromolecular Chemistry of CAS, v.v.i. (IMC).

B-956 (*N*-ethoxycarbonyl mebendazole)

This model compound (Fig III.1) was synthesized by reaction of sodium salt of MBZ (previously prepared by action of equimolar amount of sodium hydride to MBZ) with excess of ethyl chloroformate (Sigma-Aldrich) in dimethylformamide (DMF). The product was purified by repeated crystallization and characterized by HPLC (high-performance liquid chromatography) and NMR.

B-957 (*N*-(4-nitrobenzyloxy)carbonyl mebendazole)

This model compound (Fig III.1) was synthesized by reaction of sodium salt of MBZ (previously prepared by action of equimolar amount of sodium hydride to MBZ) with excess of 4-nitrobenzyl chloroformate in DMF. The product was purified by column chromatography on silica gel and characterized by HPLC and NMR.

III.5.2. HPMA copolymer-bound drugs

Following HPMA (*N*-(2-hydroxypropyl)methacrylamide) copolymer-bound conjugates of MBZ and DOX were synthetized and characterized at Institute of Macromolecular Chemistry of CAS, v.v.i.

B-967 (linear PHPMA conjugate of MBZ)

The linear HPMA-based copolymer bearing 3-azidopropyloxycarbonil derivative of MBZ linked by click reaction (Fig III.1) was synthesized by two-step synthetic procedure. First step consisted in preparation of *N*-(3-azidopropyloxy)carbonyl MBZ by reaction of sodium salt of MBZ (previously prepared by action of equimolar amount of sodium hydride to MBZ) with excess of 3-azidopropyl chloroformate in DMF. The intermediate product was purified by column chromatography on silica gel, characterized by HPLC and NMR. The second step involved a copper-free click reaction between this reactive derivative of MBZ and previously prepared HPMA-based copolymer bearing dibenzocyclooctyne groups (PHPMA/DBCO). The conjugate was then purified by repeated precipitation into diethyl ether and characterized by

GPC. The content of conjugated MBZ was determined by HPLC after hydrolysis in buffer pH 12.

The following four individual batches were used:

B-967/1
Mw = 51000; PDI = 1.35
7.2 wt% of MBZ

B-967/2
Mw = 150000; PDI = 1.8
10 wt% of MBZ

B-967/3
Mw = 46000; PDI = 1.85
5 wt% of MBZ

B-967/4
Mw = 88000; PDI = 3.6
6 wt% of MBZ

B-732 (linear PHPMA conjugate of DOX)
(P-Ahx-NH-N=DOX)
HPMA copolymer conjugate bearing doxorubicin via degradable hydrazone bond.
Mw = 27 000; PDI = 1.80
9.8 wt% of DOX

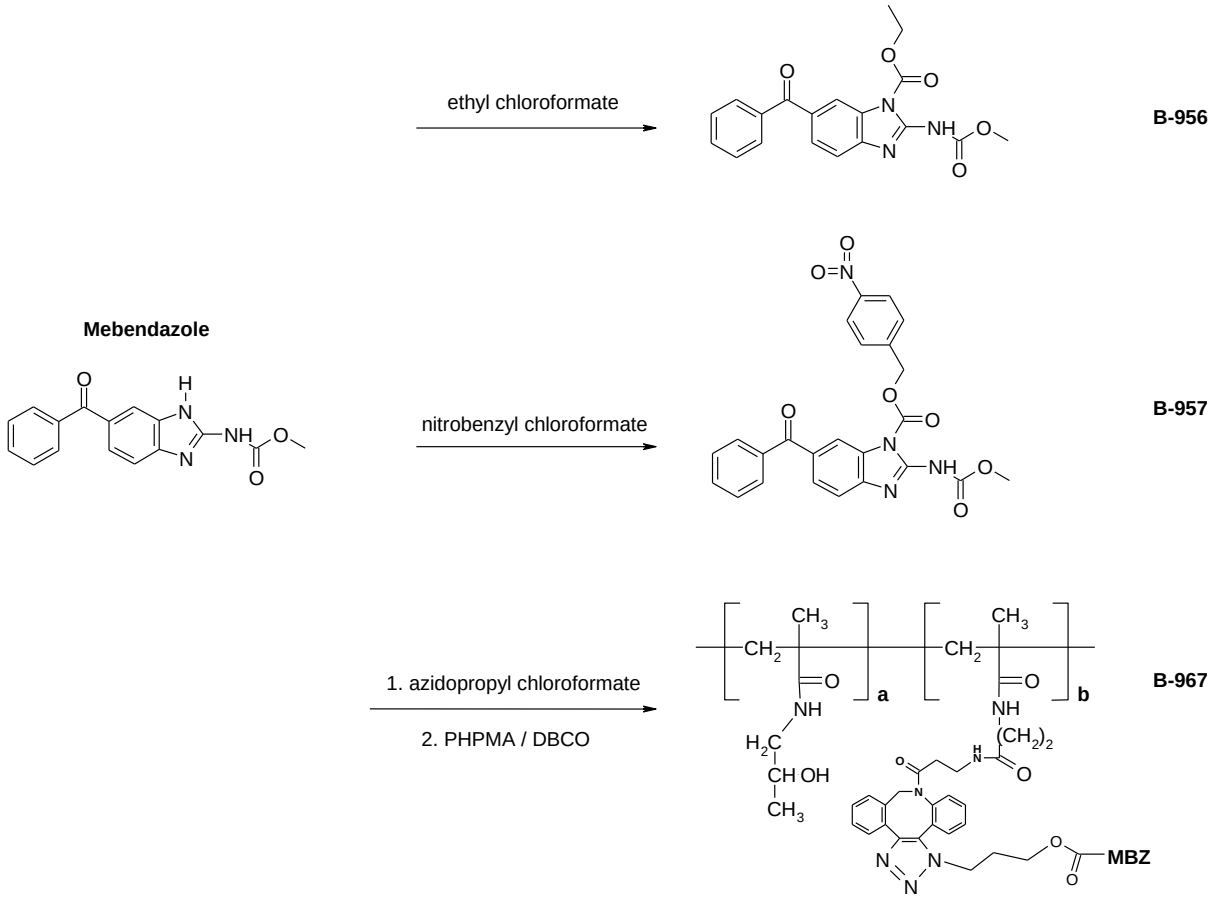

Fig III.1 Synthesis of MBZ derivatives and PHPMA conjugate of MBZ. Simplified schematic of synthesis of derivatives B-956 (top), and B-957 (middle) and PHPMA conjugate of MBZ B-967 (bottom). Scheme was obtained from IMC.

IV. Methods

IV.1. Cell line propagation

The murine cancer cell lines were obtained from ATCC with the exception of P388 and P388/MDR cells which were obtained from Prof. I. Lefkovits (Basel Institute for Immunology, Basel, Switzerland). All lines were propagated in culture cell media as described in chapter III.2. at 37 °C in a 5% CO_2 atmosphere in cell culture flasks (Nunclon, Denmark). The cell lines were regularly tested for mycoplasma infection (MycoAlert Mycoplasma Detection kit, Lonza, Switzerland).

The P388/MDR cells were continuously grown in the presence of 750 ng/ml doxorubicin to maintain the MDR-phenotype. One day before each experiment, the cells were grown in doxorubicin-free culture medium.

Cells were passaged and/or used for *in vitro* or *in vivo* experiments at the height of the log phase of growth. All adherent cell types were removed from the surface of the flask after incubating with a solution of trypsin for several minutes. Viability of cells used for *in vitro* experiments was always higher than 85%. Cell numbers and viability were determined based on trypan blue staining using a Countess automatic cell counter (Life technologies, Czech Republic).

IV.2. [^{3}H]-thymidine incorporation assay

To test the cytostatic effect of anticancer drugs, cell growth inhibition was determined using the [^{3}H]-thymidine incorporation assay. The cells of a tested line (0.5×10^4 in the case of LL2, EL4, BCL1 and CT26 lines; 1.0×10^4 in the case of B16F10, P388 and P388/MDR lines) were seeded onto a 96-well flat-bottomed tissue culture plate (Nunc, Denmark). A range of concentrations of the tested compound was created by diluting storage solution in the respective culture medium and added to the wells to reach final volume of 250 μl/well. Control cells were cultured with the same volume of medium alone. The samples of those drugs which were dissolved in DMSO (MBZ, Carf, 17-DMAG and ABT-737) were diluted so that the final concentration of DMSO in the wells was always lower than 1/100. All used cell lines were tested to confirm that at such low concentrations, DMSO had no effect on cell proliferation or mitochondrial metabolism. Quartet of wells was used for each test condition. Plates were incubated at 37 °C in a 5% CO_2 atmosphere for 72 hours. For the last 6 hours of

incubation, each well was pulsed with 1 μCi (37 kBq) of [^{3}H]-thymidine (PerkinElmer, USA) added in 50 μl. The cells from each well were then collected using a cell harvester (Tomtec, USA) and the radioactivity of each well was measured with a scintillation counter (1450 MicroBeta TriLux, Wallac, Finland). The inhibition of tumor cell growth was expressed as the half-inhibitory concentration (IC50), i.e. the concentration of the tested compound inhibiting the cell proliferation compared to control cells by 50%. Data obtained in this way were analyzed using Prism software (GraphPad Software). All IC50 values shown in this work represent a mean of at least three independent experiments.

IV.3. MTT assay

As an alternative measure of *in vitro* anticancer drug efficiency, mitochondrial activity inhibition was determined using the MTT (3-[4,5-dimethylthiazol-2-yl]-2,5 diphenyl tetrazolium bromide) assay. The cells of a tested line (0.5×10^4 in the case of LL2, EL4 and CT26 lines; 1.0×10^4 in the case of B16F10 lines) were seeded onto a 96-well flat-bottomed tissue culture plate (Nunc, Denmark) along with a range of concentrations of tested substances and incubated as described in IV.2. After the 72h incubation, the plates were centrifuged at 1200 rpm for 5 minutes at 4°C using a Rotanta 460R (Hettich, Germany) centrifuge and supernatant was removed. 100 μl of culture medium were added to each well along with 20 μl of MTT (Sigma-Aldrich) and cells were allowed to metabolize at 37 °C in a 5% CO_2 atmosphere for ~1 hour. Formazan crystals were then dissolved in DMSO and absorbance was measured using Tecan Infinite 200 (Tecan, Germany) at 540 nm using reference value of 690 nm. Half maximal effective concentration (EC50) was calculated as the concentration of the tested compound inhibiting the mitochondrial metabolism compared to control cells by 50%. Data obtained in this way were analyzed using Prism software. All EC50 values shown in this work represent a mean of at least two independent experiments unless otherwise noted.

IV.4. MTD determination

HPMA copolymer-bound MBZ polymers B-967/1–B-967/3 were tested *in vivo* in C57BL/6 mice to determine the maximum tolerated dose (MTD). MTD was defined as the highest dose which causes none of the following: 1) relative loss of 15% or more of starting weight; 2) observable signs of severe toxicity, such as abnormal behavior and motion patterns

suggestive of neurologic toxicity or other marks of distress including visible cachexia, stiff posture or ruffled fur; or 3) death of any animals in the tested group.

B-967 conjugate was dissolved in sterile PBS to appropriate concentration and injected intravenously (i.v.) into tail veins in the case of B-967/1 and 2 or intraperitoneally (i.p.) in the case of B-967/3. Injected volumes varied from 250 to 500 μl for i.v. application and up to 1 ml for i.p. application, depending on the batch and the dose applied. Control mice were injected in the same way and with equal volume of sterile PBS.

Mice weight was recorded before application and mice were periodically observed for toxicity and weight changes and death of animals were recorded.

IV.5. Determination of anti-tumor activity

Anti-tumor activity of B-967/2 conjugate was measured in the models of LL2, EL4 (C57BL/6 mice) and BCL1 (BALB/c) tumors. Growth of LL2 and EL4 tumors was induced by subcutaneously (s.c.) injecting 10^6 (LL2) or 10^5 (EL4) cells into a shaved area on the lower back of the mice. The resulting tumors were therefore accessible for periodic measurement with calipers and visual control to assess tumor progression. Growth of BCL cells was induced by i.p. injecting 5×10^5 BCL1 cells, the tumor growth therefore occurred within peritoneal cavity and tumor progression was assessed mainly via determination of mouse body weight. All tumor cells were applied in 100 μl of serum-free medium, cell numbers and viability were determined using Countess automated cell counter. Viability of applied cells was always >90%.

Tumors were observed after transplantation and upon reaching certain size (~5-8 mm in diameter) the mice were randomly divided into groups for treatment. As mice bearing BCL1 leukemia do not develop visible signs of tumor growth until later phases of disease progression, the mice in this experiment were treated on a fixed day according to standard practice in our laboratory. B-967/2 conjugate was dissolved in sterile PBS to appropriate dosing and injected i.v. into the tail vein. Injected volume varied from 250 to 500 μl depending on the dose applied. Control mice were i.v. injected with equal volume of sterile PBS.

Tumor size at the time of treatment was recorded before application and mice were periodically observed afterwards. Tumor progression measured by tumor growth (LL2, EL4) and mouse weight (BCL1) as well as the death of animals were recorded.

IV.6. Determination of reticulocyte % using flow cytometry

The percentage of reticulocytes in the erythrocyte population was determined by FACS analysis of peripheral blood samples in order to test the bone marrow toxicity [179] of the HPMA copolymer-bound MBZ polymer B-967/3. On day 0, C57BL/6 mice were i.p. treated with B-967/3 at a range of doses chosen in order to span the range from the expected MTD to a much lower dose with lower expected toxicity. B-967/3 was dissolved in sterile PBS and applied intraperitoneally in the volume of 1 ml; control mice were treated with the same volume of sterile PBS.

We also considered the possibility that mouse erythropoiesis might be stimulated by feedback loops started by the blood loss caused by collection of even a small amount of peripheral blood if it was repeated within days. To ensure that the possible effect of different scheme of blood collection between the treated groups of mice was properly accounted for, we established two control groups to test the effect of repeated blood collection from the tail vein in different regimens. Control 1 group consisted of three mice, with two of them subjected to bleeding for samples and the third resting at the given time point. Control 2 group contained four mice, with two being bled and two resting at each time point. The mice in each group were individually marked by puncturing their earlobes, which allowed for tracking the individual reticulocyte percent values over the consecutive time points.

Peripheral blood samples were collected on days 1, 2, 3, 4, 6, 8, 10 and 13 after application by gently incising the tail with a hypodermic needle tip to cause bleeding, then collecting the needed amount (~15µl) with a Gilson micropipette with tip lightly coated with heparin. Until day 8, only a subset of mice was subjected to sample collection on every time point (see also Figs V.17 – 19). These were chosen in accordance with the scheme described for control mice in the previous paragraph. From day 10 onward, all mice were bled for samples at each time point.

2.5 µl of blood from each sample were then stained with 250 µl of thiazol orange Retic-Count reagent [180]. Unstained samples were prepared by incubating 2.5 µl of blood with 250 µl of PBS. All samples were left to incubate at room temperature in dark for 30 minutes before measurement. Samples were analyzed on LSR II flow cytometer (BD Biosciences) within 3 hours after blood collection. Erythrocytes were identified and gated based on forward scatter and side scatter and the percentage of thiazol orange positive reticulocytes in the erythrocyte population was measured. A total of 50000 erythrocytes were analyzed in each sample. Data were evaluated in FlowJo software (Tree Star).

IV.7. Preparation and analysis of histology samples

A representative C57BL/6 mouse from a group treated with B-967/3 as described in chapter IV.6. was euthanized on day 3 by cervical dislocation. The mouse was then autopsied and liver, kidney, lung, heart, brain and femur were gently removed and allowed to fixate in 4% formaldehyde (Sigma-Aldrich) for at least 24 hours at room temperature. Tissue sections were prepared and stained with haematoxylin and eosin (P-lab, Czech Republic) according to the standard protocol. Specimens were afterwards analyzed for signs of acute tissue toxicity. Section preparation, decalcifying of the femur samples, staining and all analyses were performed at the Institute of Microbiology, CAS, v.v.i., Prague by MUDr. Pavel Rossmann, DrSc.

V. Results

V.1. Effect of mebendazole *in vitro*

V.1.1. Screening for cytostatic efficacy of several drugs in murine cancer cell lines

We performed a screening of cytostatic activity of a small panel of novel and/or repositioned therapeutics. This screening was done by testing each drug in two murine cancer cell lines, LL2 Lewis lung carcinoma and EL4.IL2 T-cell lymphoma, using [^{3}H]-thymidine incorporation assay (Fig V.1). The obtained values of IC50 for several of the tested substances (Table V.1) showed inhibition of proliferation comparable with that of doxorubicin (DOX), a commonly used anticancer agent we used as the benchmark.

Carfilzomib (Carf) and alvespimycin (17-DMAG), as well as mebendazole (MBZ), showed IC50 values comparable to DOX in LL2 cells. In the case of EL4.IL2 cell line, IC50 of 17-DMAG and MBZ were approximately half an order of magnitude higher than IC50 of DOX while Carf was slightly more effective in suppressing proliferation than DOX. ABT-737 was only poorly effective in both cell lines, with IC50 two orders of magnitude higher than DOX.

Thus, simple anthelminthic drug mebendazole, freely available in other indications, possesses cytostatic activity *in vitro* comparable to DOX, a potent and widely used anticancer drug. This suprising and highly interesting finding led us to focus on MBZ and investigate its potential anticancer activity.

Table V.1 Mean IC50 values for Carfilzomib, Alvespimycin, Mebendazole, ABT-737 and Doxorubicin in LL2 and EL4.IL2 cell lines.*

Drug	**LL2**	**EL4.IL2**
Carfilzomib	25±11	5±0.7
Alvespimycin	57±12	75±25
Mebendazole	67±11	60±7
ABT-737	4499±1884	1244±328
Doxorubicin	60±18	11±3

*LL2 and EL4.IL2 cells were seeded onto 96-well plates and incubated with a range of concentrations of each drug for 72h. [^{3}H]-thymidine was added for the last 6 hours of incubation. Cells were harvested and radioactivity measured. The activity of control cells was always higher than 25 000 cpm/well. IC50 values (ng/ml) were calculated as the concentration of drug which inhibited the incorporation of tracer to 50% of control cells; mean IC50 values ± standard deviations presented in this table were obtained from at least three independent experiments.

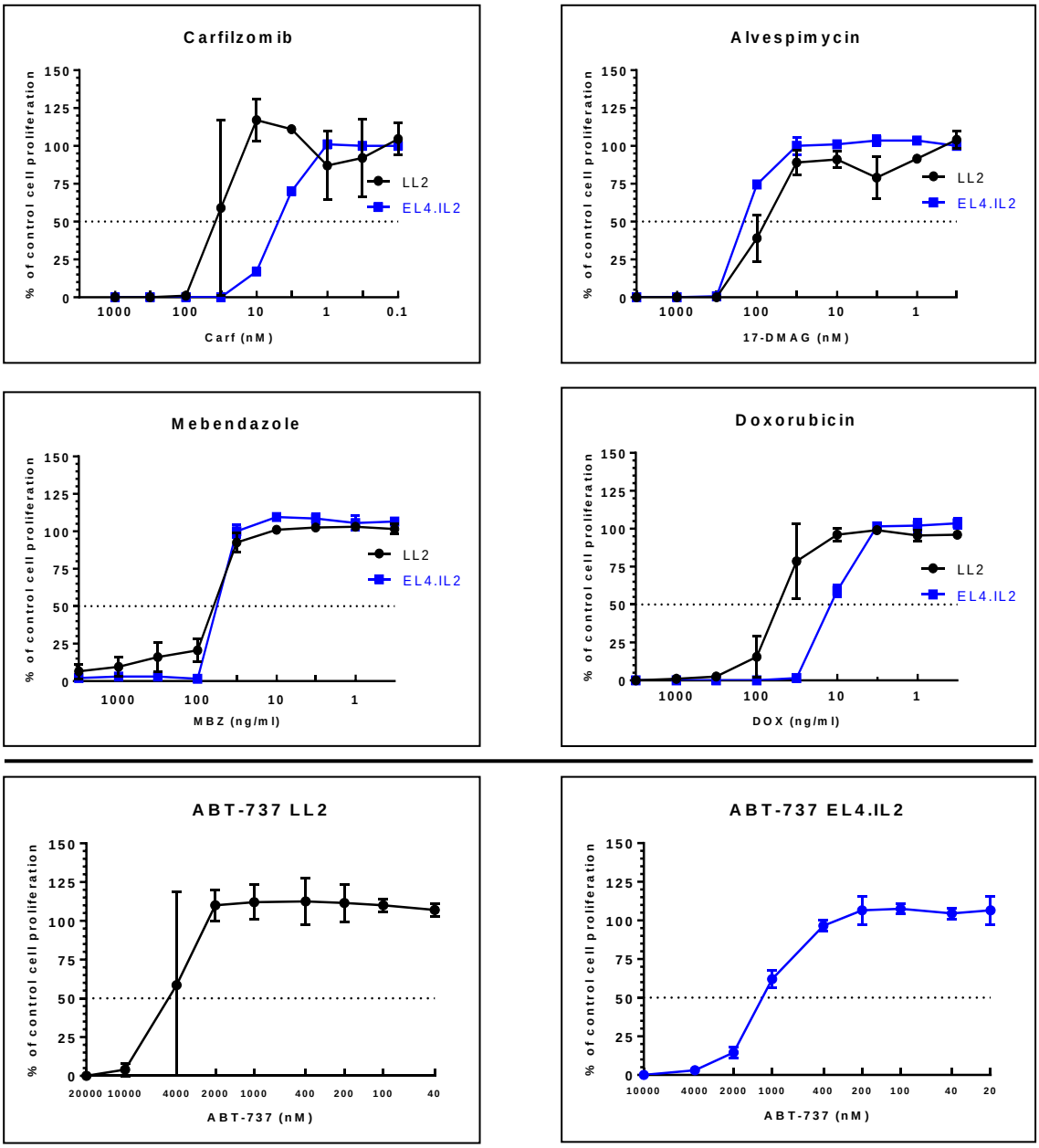

Figure V.1 Representative curves of [^{3}H]-thymidine incorporation assay for Carfilzomib, Alvespimycin, Mebendazole, ABT-737 and Doxorubicin in LL2 and EL4.IL2 cell lines. LL2 (black lines) and EL4.IL2 cells (blue lines) were seeded onto 96-well plates and incubated with a range of concentration of each drug for 72h under standard culture conditions. [^{3}H]-thymidine was added for the last 6 hours of incubation. Cells were harvested and radioactivity measured. The results are shown as the inhibition of the proliferation of the exposed cells relative to the controls (cells incubated with medium alone). The activity of control cells was always higher than 25 000 cpm/well. Results shown in this figure were obtained from at least three independent experiments.
Note that the significantly lower cytostatic activity of ABT-737 necessitated using much higher concentrations of the drug.

V.1.2. Cytostatic activity of mebendazole in a panel of murine cancer cell lines

MBZ has extremely low solubility in aqueous environments, thus the synthesis of HPMA copolymer-bound MBZ derivative could be a promising approach to exploit anti-cancer activity of MBZ. As an added benefit, MBZ is a repurposed drug, its safety for human use already well established in its original indication as an anthelmintic agent.

We proceeded to test the anti-proliferative effect of MBZ in several cell lines *in vitro*. In addition to LL2 and EL4.IL2 cells, both syngeneic with C57BL/6 mice, the tested panel included B16F10, CT26 and BCL1.

The results (Fig V.2) show that MBZ is highly effective against a diverse range of tumor cell lines, including lines of haematopoietic, epithelial and other origins, and cells derived from both C57BL/6 and BALB/c background. Comparison of IC50 values (Table V.2) shows that relative to DOX, MBZ is almost as effective in LL2 cells, by approximately half an order of magnitude less effective in EL4.IL2, B16F10 and CT26 lines and by one order of magnitude less effective in the case of BCL1 cells.

Table V.2 Mean IC50 values for Mebendazole and Doxorubicin in LL2, EL4.IL2, B16F10, BCL1 and CT26 cell lines.*

Cell line	**MBZ**	**DOX**
LL2	67±11	60±18
EL4.IL2	60±7	11±3
B16F10	81±5	19±6
BCL1	39±9	3±2
CT26	68±2	24±3

*LL2, EL4.IL2, B16F10, BCL1 and CT26 cells were seeded onto 96-well plates and incubated with a range of concentrations of MBZ or DOX for 72h. [^{3}H]-thymidine was added for the last 6 hours of incubation. Cells were harvested and radioactivity measured. IC50 values (ng/ml) were calculated as the concentration of drug which inhibited the incorporation of tracer to 50% of control cells. The activity of control cells was always higher than 25 000 cpm/well. Mean IC50 values ± standard deviations presented in this table were obtained from at least three independent experiments.

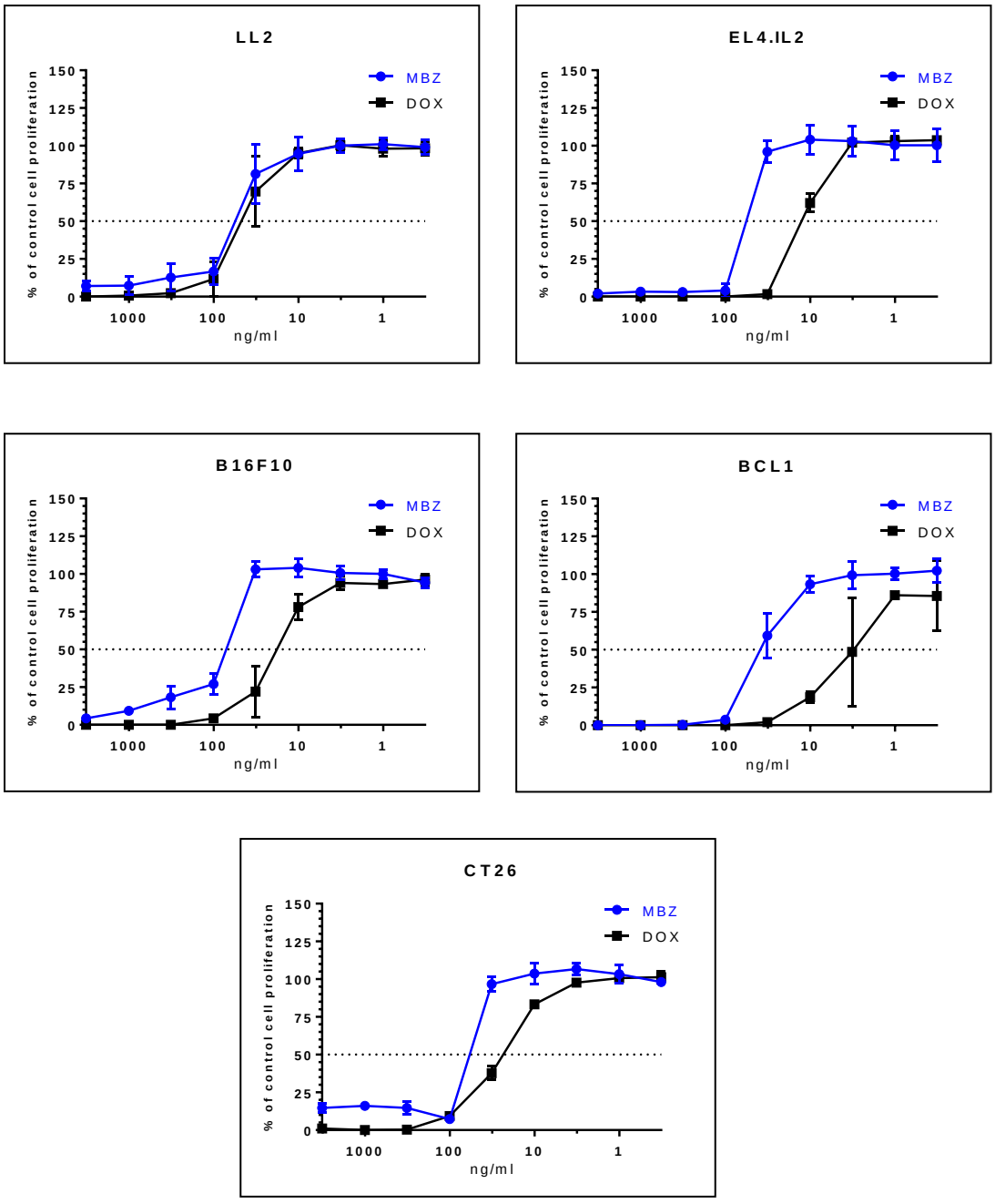

Figure V.2 Representative curves of [^{3}H]-thymidine incorporation assay for Mebendazole and Doxorubicin in LL2, EL4.IL2, B16F10, BCL1 and CT26 cell lines. LL2, EL4.IL2, B16F10, BCL1 and CT26 cells were seeded onto 96-well plates and incubated with a range of concentrations of MBZ (blue lines) or DOX (black lines) for 72h under standard culture conditions. [^{3}H]-thymidine was added for the last 6 hours of incubation. Cells were harvested and radioactivity measured. The results are shown as the inhibition of the proliferation of the exposed cells relative to the controls (cells incubated with medium alone). The activity of control cells was always higher than 25 000 cpm/well. Results shown in this figure were obtained from at least three independent experiments.

V.1.3. Cytotoxic activity of mebendazole in murine cancer cell lines

To further confirm the antitumor effect of mebendazole, we measured mitochondrial metabolism and evaluated cytotoxic efficacy of mebendazole *in vitro* using the MTT assay. A panel of cancer cell lines was used, including LL2, EL4.IL2, CT26 and B16F10 cells, and DOX was used for comparison. Fig V.3 and Table V.3 show that MBZ exhibits virtually identical effect as DOX in LL2 and CT26 cells, while for EL4.IL2 cells the result is analogous to the difference between the cytostatic activity as described in V.1.2 and V.1.1. In B16F10 cells, EC50 of MBZ was markedly higher than that of DOX, possibly suggesting that MBZ is slightly more effective in suppressing the proliferative capacity of this cell line than directly killing the cells.

In most cell lines, cytostatic activity of MBZ measured via [^{3}H]-thymidine incorporation assay corresponded well to the cytotoxic activity measured via MTT assay. Therefore, considering the higher sensitivity of [^{3}H]-thymidine incorporation assay, we continued to rely on measuring cytostatic activity to assess and compare the effectiveness of newly synthesized derivatives and HPMA conjugates.

Table V.3 Mean EC50 values for Mebendazole and Doxorubicin in LL2, EL4.IL2, B16F10 and CT26 cell lines.*

Cell line	**MBZ**	**DOX**
LL2	57±14	58±27
EL4.IL2	53±4	12±4
B16F10	199	46±25
CT26	77±3	67

*LL2, EL4.IL2, B16F10 and CT26 cells were seeded onto 96-well plates and incubated with a range of concentrations of MBZ or DOX for 72h. After incubation, plates were centrifuged and supernatant removed. 20µl of MTT were added and the cells were allowed to metabolize for approx. 1 hour before formazan crystals were dissolved in DMSO and absorbance was measured. EC50 values (ng/ml) were obtained; mean EC50 values ± standard deviation presented in this table were obtained from at least three independent experiments except for EC50 of MBZ in B16F10 and DOX in CT26 cell lines which are representative values.

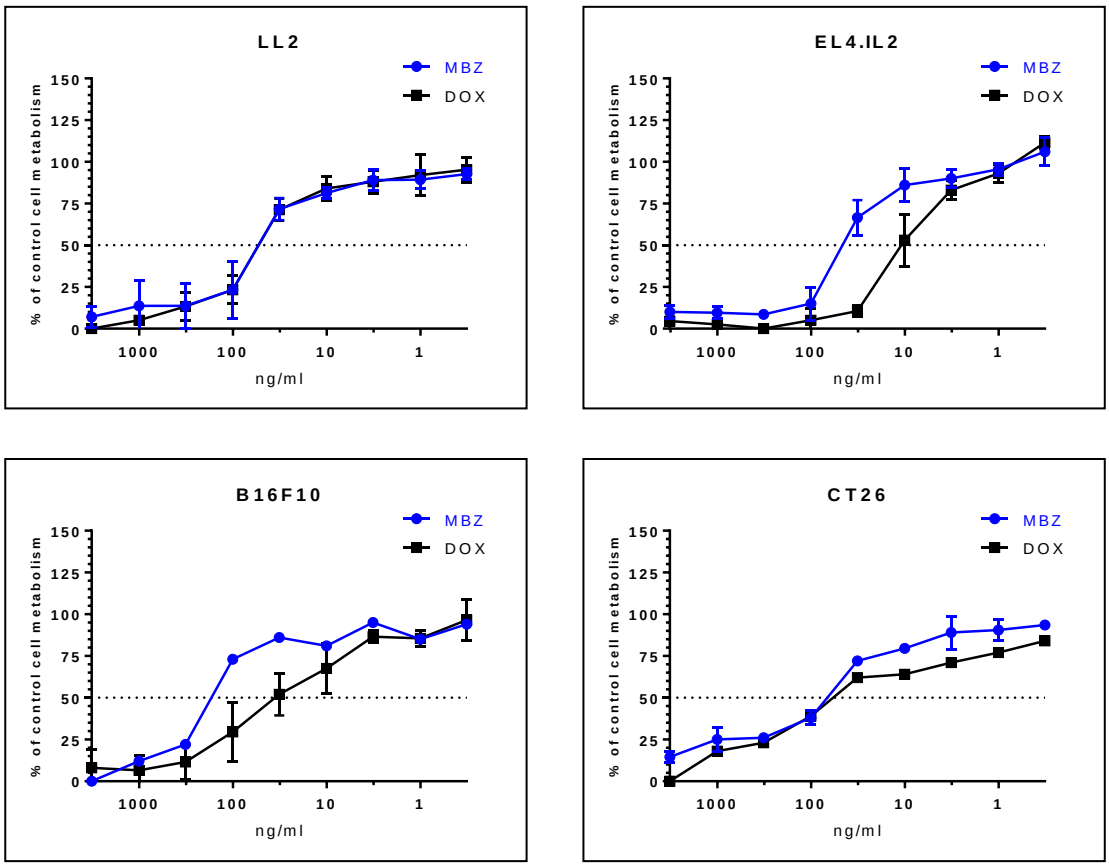

Figure V.3 Representative curves of MTT assay for Mebendazole and Doxorubicin in LL2, EL4.IL2, B16F10 and CT26 cell lines. LL2, EL4.IL2, B16F10 and CT26 cells were seeded onto 96-well plates and incubated with a range of concentrations of MBZ (blue lines) or DOX (black lines) for 72h. After incubation, plates were centrifuged and supernatant removed. 20µl of MTT were added and cells were allowed to metabolize for approx. 1 hour before formazan crystals were dissolved in DMSO and absorbance was measured. The results are shown as the inhibition of the metabolic activity of the exposed cells relative to the controls (cells incubated with medium alone). Data shown represent mean values ± standard deviations derived from three separate experiments.

5.1.4. Sensitivity of mebendazole to Pgp-mediated multidrug resistance

Considering the fact that the phenomenon of multiple drug resistance (MDR) is a crucial factor contributing to unfavourable prognosis and treatment failure in many cancer types, we tested cytostatic efficacy of MBZ in sensitive P388 and resistant P388/MDR cell lines to establish if it is subject to transport via Pgp (Fig V.4, Table V.4). The obtained results clearly show that while DOX was highly effective in P388 cells but several orders of magnitude less effective in the resistant P388/MDR line, MBZ showed the same level of effectiveness in both the sensitive and the resistant cell lines. This suggests that MBZ is not subject to MDR mediated by expression of Pgp in the P388/MDR cell line, further increasing its potential.

Table V.4 Mean IC50 values for Mebendazole and Doxorubicin in P388 and P388/MDR cell lines.*

Cell line	**MBZ**	**DOX**
P388	36±24	15±4
P388/MDR	66±20	6495±1954

*P388 and P388/MDR cells were seeded onto 96-well plates and incubated with a range of concentrations of MBZ or DOX for 72h. [^{3}H]-thymidine was added for the last 6 hours of incubation. Cells were harvested and radioactivity measured. IC50 values (ng/ml) were calculated as the concentration of drug which inhibited the incorporation of tracer to 50% of control cells. The activity of control cells was always higher than 25 000 cpm/well except in case of P388 cells, in which they were always higher than 10 000. Mean IC50 values ± standard deviations presented in this table were obtained from at least three independent experiments.

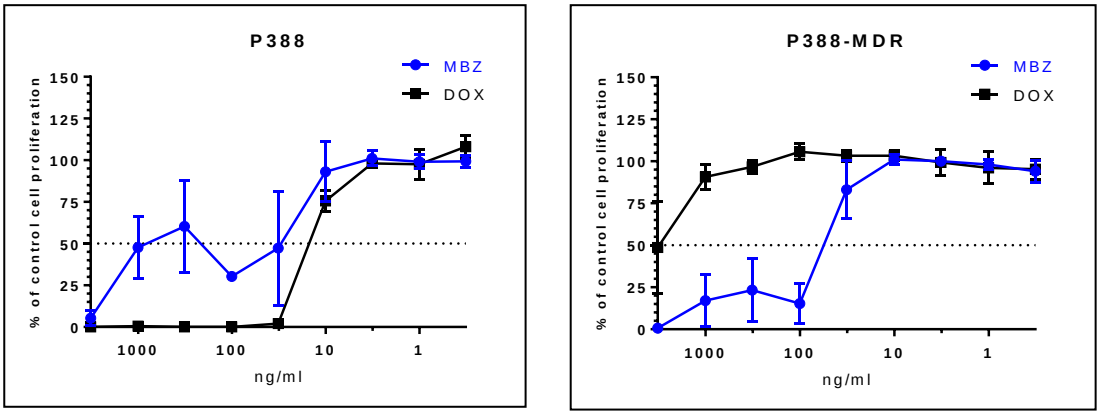

Figure V.4 Representative curves of [^{3}H]-thymidine incorporation assay for Mebendazole and Doxorubicin in P388 and P388/MDR cell lines. P388 and P388/MDR cells were seeded onto 96-well plates and incubated with a range of concentrations of MBZ (blue lines) or DOX (black lines) for 72h under standard culture conditions. [^{3}H]-thymidine was added for the last 6 hours of incubation. Cells were harvested and radioactivity measured. The results are shown as the inhibition of the proliferation of the exposed cells relative to the controls (cells incubated with medium alone). The activity of control cells was always higher than 25 000 cpm/well except in case of P388 cells, in which it was always higher than 10 000. Results shown in this figure were obtained from at least three independent experiments.

V.1.5. Testing the cytostatic activity of synthesised mebendazole derivatives B-956 and B-957

Two derivatives, labelled B-956 and B-957 (see Materials), were synthesized by a collaborating laboratory at the Institute of Macromolecular Chemistry (IMC) with the aim to enable binding MBZ to HPMA copolymer backbone. These compounds were then tested in LL2 and EL4.IL2 cell lines (Fig V.5, Table V.5) in order to evaluate the effect the bond used

in each derivative had on their anti-proliferative effect. This was done to choose the more promising chemical approach for conjugation with HPMA. Results showed that the derivative B-956 was more effective in both LL2 and EL4.IL2 cell lines, retaining the level of effectiveness of MBZ (compare Figs V.1 and V.2). Coupled with the fact that B-956 showed slightly better solubility, the bond chosen for use in conjugating MBZ to HPMA copolymer was based on B-956.

Table V.5 Mean IC50 values for B-956 and B-957 in LL2 and EL4.IL2 cell lines.*

Cell line	**B-956**	**B-957**
LL2	68±14	104±24
EL4.IL2	61±15	115±18

*LL2 and EL4.IL2 cells were seeded onto 96-well plates and incubated with a range of concentrations of B-956 or B-957 for 72h. [^{3}H]-thymidine was added for the last 6 hours of incubation. Cells were harvested and radioactivity measured. IC50 values (ng/ml) were calculated as the concentration of drug which inhibited the incorporation of tracer to 50% of control cells. The activity of control cells was always higher than 25 000 cpm/well. Mean IC50 values ± standard deviations presented in this table were obtained from at least three independent experiments.

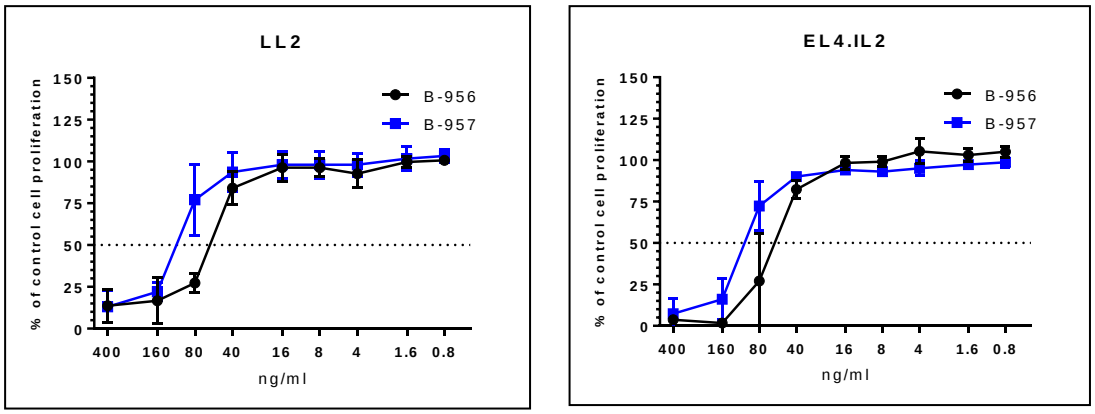

Figure V.5 Representative curves of [^{3}H]-thymidine assay for B-956 and B-957 in LL2 and EL4.IL2 cell lines. LL2 and EL4.IL2 cells were seeded onto 96-well plates and incubated with a range of concentrations of B-956 (black lines) or B-957 (blue lines) for 72h under standard culture conditions. [^{3}H]-thymidine was added for the last 6 hours of incubation. Cells were harvested and radioactivity measured. The results are shown as the inhibition of the proliferation of the exposed cells relative to the controls (cells incubated with medium alone). The activity of control cells was always higher than 25 000 cpm/well. Results shown in this figure were obtained from at least three independent experiments.

V.1.6. Testing the cytostatic activity of HPMA copolymer-bound derivative of mebendazole, B-967/1

The first batch of compound labelled B-967 (B-967/1; see Materials) with MBZ bound to HPMA copolymer backbone with a carbamate bond based on the B-956 derivative, was prepared by the collaborators at IMC. This conjugate was then tested for its *in vitro* anticancer effect in LL2, EL4.IL2 and BCL1 cell lines using [^{3}H]-thymidine incorporation assay. These cell lines were planned to be used in following therapeutic experiments *in vivo*. Fig V.6 and Table V.6 show that upon binding to HPMA, *in vitro* cytostatic effectiveness compared with that of free MBZ and B-956 slightly decreased; this is a commonly seen phenomenon. B-967/1 nonetheless possessed acceptable effectiveness in all three tested lines.

Table V.6 Mean IC50 values for B-967/1 and MBZ in LL2, EL4.IL2 and BCL1 cell lines.*

Cell line	**B-967/1**	**MBZ**
LL2	134±38	67±11
EL4.IL2	138±18	60±7
BCL1	70±24	39±9

*LL2, EL4.IL2 and BCL1 cells were seeded onto 96-well plates and incubated with a range of concentrations of B-967/1 or MBZ for 72h. [^{3}H]-thymidine was added for the last 6 hours of incubation. Cells were harvested and radioactivity measured. IC50 values (ng/ml MBZ eq.) were calculated as the concentration of drug which inhibited the incorporation of tracer to 50% of control cells. The activity of control cells was always higher than 25 000 cpm/well. Mean IC50 values ± standard deviations presented in this table were obtained from at least three independent experiments.

Due to the unique properties of the bond used in B-967 to bind B-956 to the HPMA copolymer backbone (see chapters III.5.2 and VI), exposition of B-967 conjugate to *in vitro* or *in vivo* experimental conditions would result in release (with $t_{½}$ of several hours) of free MBZ and not the MBZ derivative used for binding to the backbone. Therefore, in any subsequent *in vitro* testing, B-967 sample concentrations would be compared directly with the equivalent concentrations of MBZ to evaluate the variations of *in vitro* activity, e.g. between the batches of B-967 (see chapter V.2.5 and V.2.7).

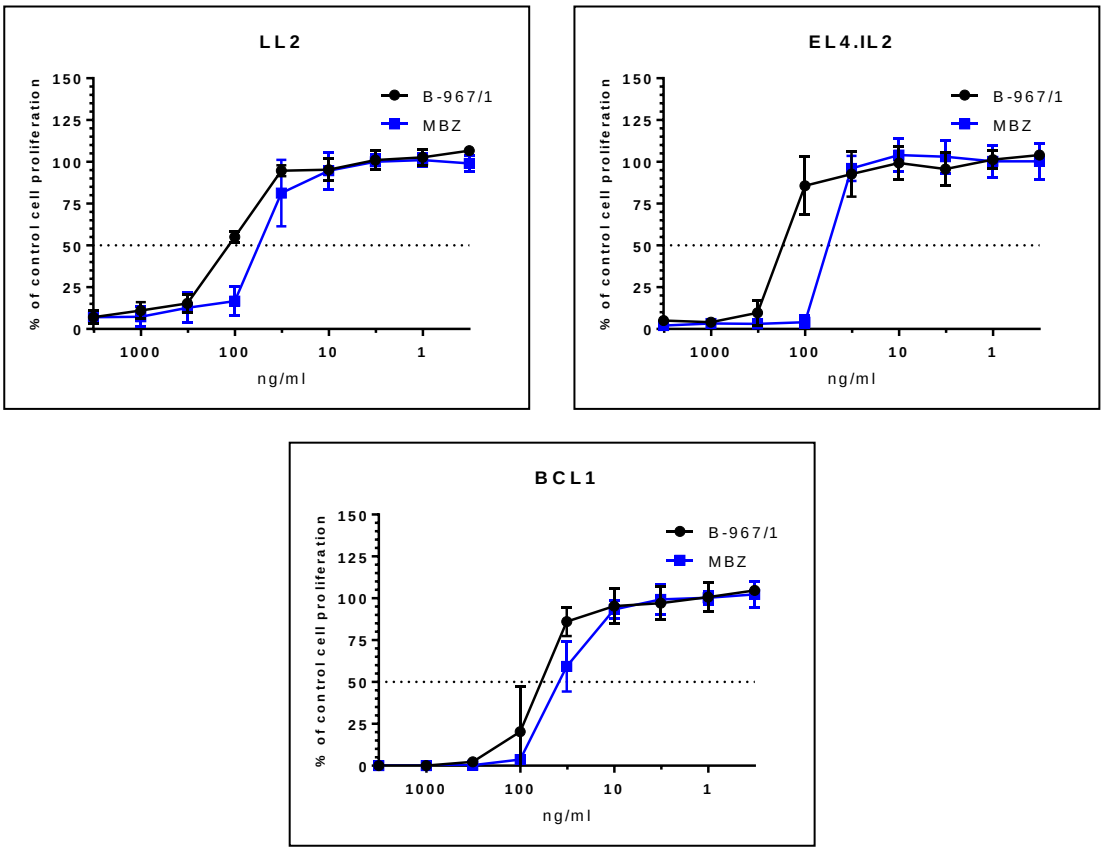

Figure V.6 Representative curves of [^{3}H]-thymidine incorporation assay for B-967/1 and Mebendazole in LL2, EL4.IL2 and BCL1 cell lines. LL2, EL4.IL2 and BCL1 cells were seeded onto 96-well plates and incubated with a range of concentrations of B-967/1 (black lines) or MBZ (blue lines) for 72h under standard culture conditions. [^{3}H]-thymidine was added for the last 6 hours of incubation. Cells were harvested and radioactivity measured. The results are shown as the inhibition of the proliferation of the exposed cells relative to the controls (cells incubated with medium alone). The activity of control cells was always higher than 25 000 cpm/well. Results shown in this figure were obtained from at least three independent experiments.

Minor problem arising from the aforementioned unique character of the bond in B-967 samples is that the release of MBZ from the conjugate occurs in aqueous environment somewhat faster than the usual kinetics of DOX release from DOX containing conjugates (see chapter VI).

Antitumor effectiveness of B-967/1 observed *in vitro* coupled with its greatly improved solubility in aqueous environments allowed us to proceed to *in vivo* application and testing of toxicity and therapeutic activity.

V.2. Toxicity and antitumor activity of mebendazole *in vivo*

As a first step after moving to *in vivo* conditions, we determined the maximum tolerated dose (MTD; see Methods) of B-967/1 in order to plan the treatment regimen and dosage for subsequent therapeutic experiments. These would be performed on mice bearing syngeneic murine tumors induced by subcutaneous injection of defined number of cells from tumor cell lines used to test MBZ, B-956 and B-967 *in vitro*.

Since the doses used in *in vivo* experiments required administration of large quantities of B-967 sample and the synthesis was both laborious and time consuming, it was impossible to use the available amount of B-967/1 to both determine MTD and perform the therapeutic experiments. The plan was that first, MTD would be determined with B-967/1, and later batches, beginning with B-967/2, would then be used to treat tumor-bearing mice. The reasoning behind this line of thought was that with the synthesis process being identical between batches, the resulting product would likewise retain very similar level of toxicity, with only minor alterations due to the unavoidable slight differences in molecular weight, polydispersity and weight percentage of MBZ bound to HPMA backbone in the given batch.

V.2.1.Toxicity of B-967/1

C57BL/6 mice were intravenously (i.v.) injected with B-967/1 dissolved in sterile PBS and administered in doses equivalent to 80 mg/kg and 120 mg/kg MBZ, respectively. Mice were observed for general signs of toxicity and their weight was recorded. Resulting data (Fig V.7) shows that the MTD for B-967/1 was determined to be higher than 120 mg/kg, as mice in neither group underwent a drop in body weight of 15% or more and no signs of overt toxicity were observed.

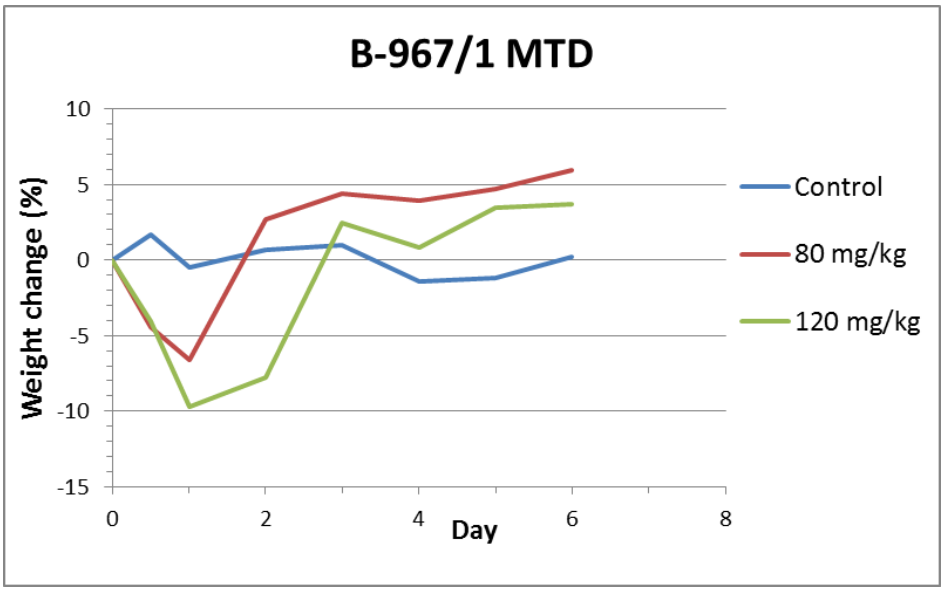

Figure V.7 Determination of MTD of conjugate B-967/1. Mice (n=2) were i.v. administered B-967/1 dissolved in sterile PBS in doses of 80 (red) resp. 120 (green) mg/kg of MBZ eq. Control mice (blue) were i.v. treated with sterile PBS. Mice were then observed for signs of toxicity and their body weight changes (shown in %) were recorded.

V.2.2. Toxicity of B-967/2

Next, we were supplied with the second batch of B-967 (B-967/2) from the laboratory at IMC. We i.v. administered B-967/2 at 140 mg/kg and 160 mg/kg MBZ equivalent in order to evaluate the actual MTD value. It needs to be mentioned that at such high dosage, the concentration of the conjugate seemed to markedly affect its solubility. Despite the visibly increased viscosity of the applied solution, the mice were however successfully administered the stated doses and subsequently were observed for signs of toxicity and their weight was recorded.

The weight of the mice in the groups treated with B-967/2 started dropping rapidly after administration of either dose of B-967/2 (Fig V.8). The treated mice exhibited signs of severe toxicity and distress, such as a drop in body temperature, trembling, uncharacteristically stiff posture and/or unusual patterns of motion and ruffled fur. Following these symptoms, mice started dying within a day after administration of B-967/2, and all mice from both treated groups were dead by 6th day after administration of the drug.

Therefore, combined with the previous results, we concluded that the MTD of the conjugate was between 120 and 130 mg/kg MBZ eq.

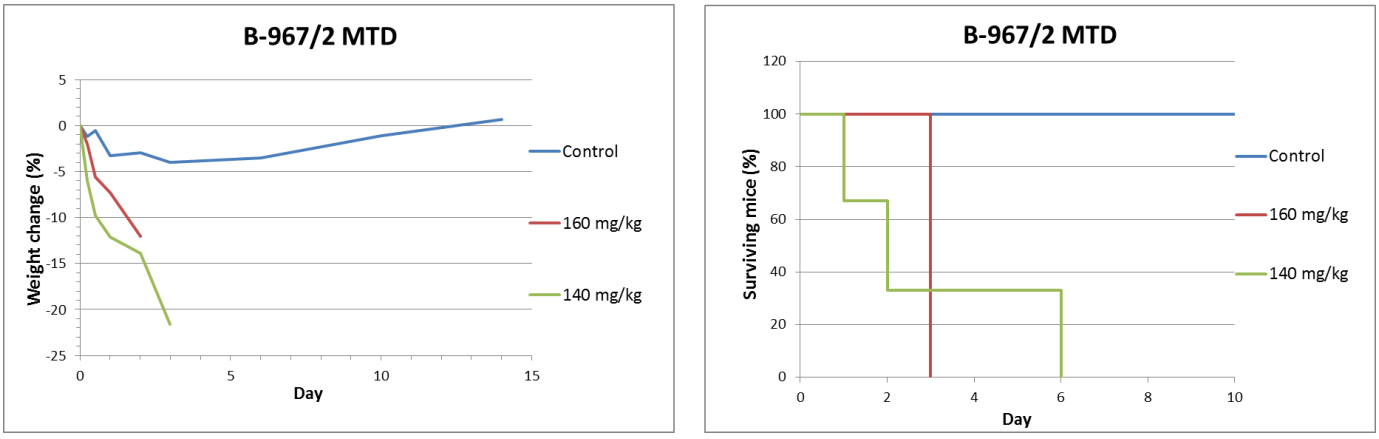

Figure V.8 Determination of MTD of conjugate B-967/2. C57BL/6 mice (n=3) were i.v. administered B-967/2 dissolved in sterile PBS in doses of 140 (green) resp. 160 (red) mg/kg of MBZ eq. Control mice (blue) were i.v. treated with sterile PBS. Mice were then observed for signs of toxicity and their weight changes (left; shown in %) and survival (right; shown as % of surviving mice) were recorded.

V.2.3. Antitumor efficacy of HPMA copolymer-bound mebendazole conjugate *in vivo*

We decided to test the antitumor efficacy of the conjugate, first in LL2 lung carcinoma bearing mice. C57BL/6 mice were s.c. injected with LL2 cells on day 0 and on day 6 treated i.v. with a single bolus dose of 110 mg/kg MBZ eq. of B-967/2. Linear HPMA copolymer-bound DOX conjugate B-732 (see chapter III.5.2) dosed at 82 mg/kg DOX eq. (i.e. MTD) was used for comparison of antitumor effect.

Results (Fig V.9) show that mice treated with B-967/2 at 110 mg/kg, a dose previously believed to be well below MTD, exhibited signs of severe toxicity as described in V.2.2 and all died within 5 days after application. Mice treated with B-732, on the other hand, showed slightly slower tumor growth and prolonging of survival.

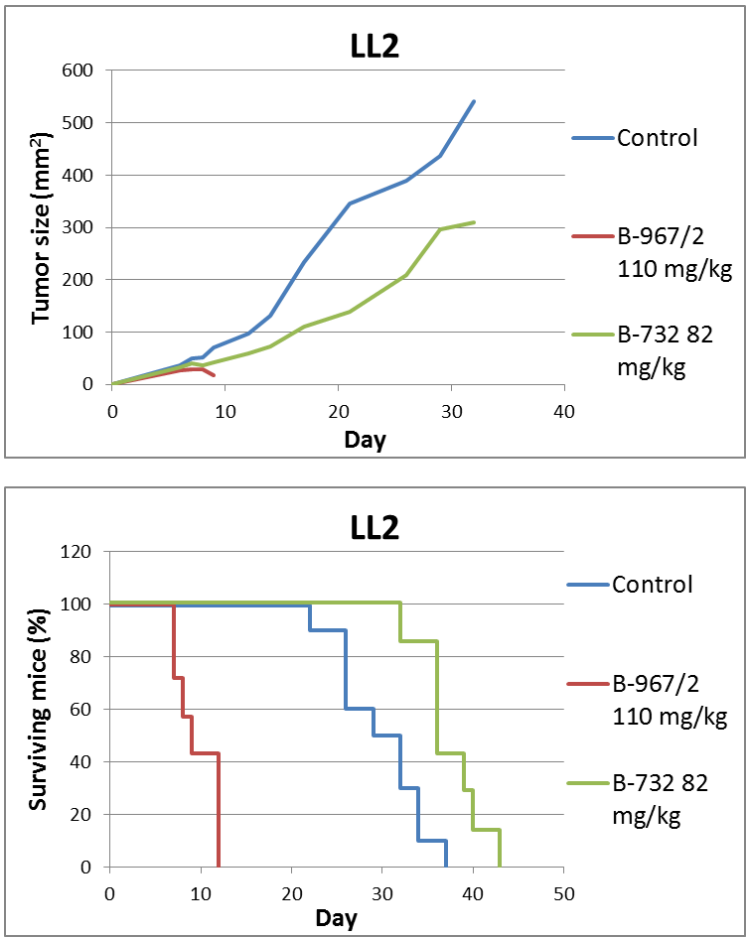

Figure V.9 Therapeutic activity of B-967/2 and B-732 conjugates in the model of LL2 murine non-small-cell lung carcinoma. C57BL/6 mice (n=7) were s.c. injected with 10^6 LL2 cells to elicit tumor growth on day 0. On day 6, mice were i.v. treated with B-967/2 (red) at a dose of 110 mg/kg MBZ eq., resp. with B-732 (green) at a dose of 82 mg/kg DOX eq. Control mice (blue) were i.v. treated with sterile PBS. Tumor size was measured (top; shown in mm^2) and survival (bottom; shown as % of surviving mice) recorded until day 43.

Thus, we decreased the dose of B-967/2 in the next therapeutic experiment. C57BL/6 mice were s.c. injected with EL4 cells on day 0 and treated with a bolus of 80 mg/kg MBZ eq. of B-967/2 on day 9. Results (Fig V.10) show that this dose still caused the mice to exhibit signs of toxicity; approximately half of the mice died within 5 days after application while the other half fully recovered. The mice that survived the application showed slower tumor growth and slight prolonging of survival in comparison with the control group.

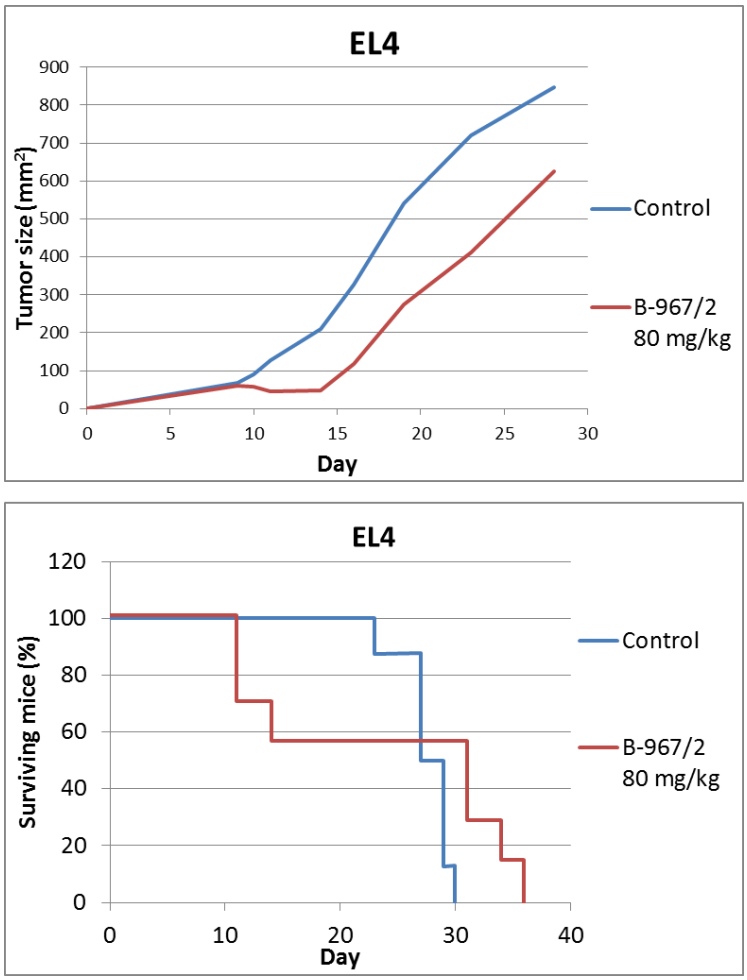

Figure V.10 Therapeutic activity of B-967/2 conjugate in the model of EL4 murine T-cell lymphoma. C57BL/6 mice (n=7) were s.c. injected with 10^5 EL4 cells to elicit tumor growth on day 0. On day 9, mice were i.v. treated with B-967/2 (red) at a dose of 80 mg/kg MBZ eq. Control mice (blue) were i.v. treated with sterile PBS. Tumor size (top, shown in mm^2) was measured and survival (bottom, shown as % of surviving mice) recorded until day 36.

Since the mice still exhibited signs of severe toxicity when treated with 80 mg/kg MBZ eq. of B-967/2, we decided to further decrease the dosing for the next experiment and introduce another group, in which mice would be treated with three injections of higher cumulative dose administered over three consecutive days.

Therefore, BALB/c mice were i.p. injected with BCL1 cells on day 0, then i.v. treated with a single bolus dose of 60 mg/kg MBZ eq. of B-967/2 on day 12 or sequentially with three doses of 30 mg/kg MBZ eq. of B-967/2 on days 12, 13 and 14. Results (Fig V.11) showed that the mice were not exhibiting any major signs of toxicity. The group treated with the bolus of 60 mg/kg MBZ eq. of B-967/2 showed just a very minor and short weight drop of no long term significance. Unfortunately, as evidenced with data showing weight and survival of BCL1 leukemia bearing mice, neither treatment scheme proved effective in this tumor model.

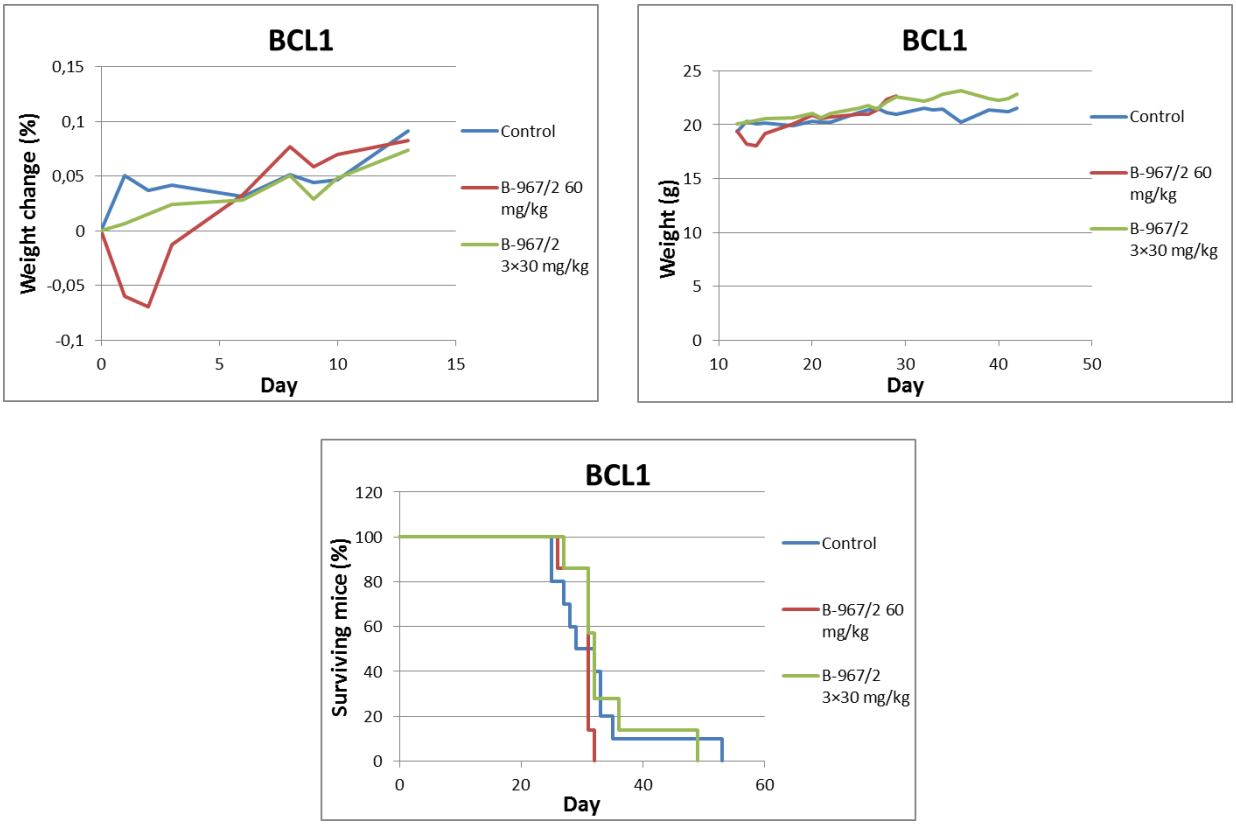

Figure V.11 Therapeutic activity of B-967/2 conjugate in the model of BCL1 murine B-cell leukemia. BALB/c mice (n=7) were i.p. injected with 5×10^5 BCL1 cells to elicit tumor growth on day 0. On day 12, mice from the bolus treated group (red) were i.v. treated with B-967/2 at a dose of 60 mg/kg MBZ eq. Mice from the sequentially treated group (green) were administered B-967/2 at a dose of 30 mg/kg MBZ eq. on days 12, 13 and 14. Control mice (blue) were i.v. treated with sterile PBS in the same scheme. Mouse weight was measured (top left, detail of weight changes at time of application, shown in %; top right, weight over longer period, shown in g) and survival (bottom, shown as % of surviving mice) recorded until day 53.

V.2.4. Elucidating the toxicity of B-967/2

After the failure of batch 967/2 in *in vivo* experiments, we strived to determine the reason of its unexpectedly high toxicity. Data collected *in vitro* showed no difference of the cytostatic effect between B-967/1 and B-967/2 (Table V.7). This led us to hypothesise that either the effect was caused by an increased sensitivity of tumor bearing mice towards MBZ-induced

toxicity compared to tumor-free mice, or else B-967/2 was a somewhat faulty batch. The latter hypothesis was corroborated by the observation that B-967/2 showed slightly worse solubility in PBS than B-967/1, with the resulting solution being more viscous.

Table V.7 Mean IC50 values for B-967/1, B-967/2 and MBZ in LL2 and EL4.IL2 cell lines.*

Cell line	**B-967/1**	**B-967/2**	**MBZ**
LL2	134±38	149±38	67±11
EL4.IL2	138±18	124±3	60±7

*LL2 and EL4.IL2 cells were seeded onto 96-well plates and incubated with a range of concentrations of B-967/1, B-967/2 or MBZ for 72h. [^{3}H]-thymidine was added for the last 6 hours of incubation. Cells were harvested and radioactivity measured. IC50 values (ng/ml MBZ eq.) were calculated as the concentration of drug which inhibited the incorporation of tracer to 50% of control cells. The activity of control cells was always higher than 25 000 cpm/well. Mean IC50 values ± standard deviations presented in this table were obtained from at least three independent experiments.

First, we ruled out the former hypothesis by i.v. administering the same dose of 110 mg/kg MBZ eq. to both LL2 tumor-bearing and tumor-free mice. Mice in both groups exhibited the signs of toxicity as described earlier (Table V.8) and all died within 3 days after application, regardless of the tumor burden (Fig V.12).

Table V.8 Signs of toxicity in LL2 tumor-bearing and tumor-free C57BL/6 mice.*

	Weight (g)				Rectal temperature (°C)			
Day	Tumor-free		LL2		Tumor-free			LL2
D1 (T+0)	25,6	26,9	25,1	23,7	physiological			
D1 (T+6h)	24,3	26,1	24,6	22,4	31,7	30,6	33,5	31,6
D2	22,8	24,9	23,6	21,2	29,3	EX	28,4	28,1
D3	EX							

*C57BL/6 mice were randomly divided into two groups (n=2) and one group was s.c. injected with 10^6 LL2 cells on day 0. On day 7, both LL2 tumor-bearing and control tumor-free mice were i.v. treated with B-967/2 at a dose of 110 mg/kg MBZ eq. Mice were then observed for signs of toxicity, their weight and rectal temperature were measured and survival was recorded. Table shows collected data on weight and rectal temperature of the individual mice. Death of mice is marked with "EX".

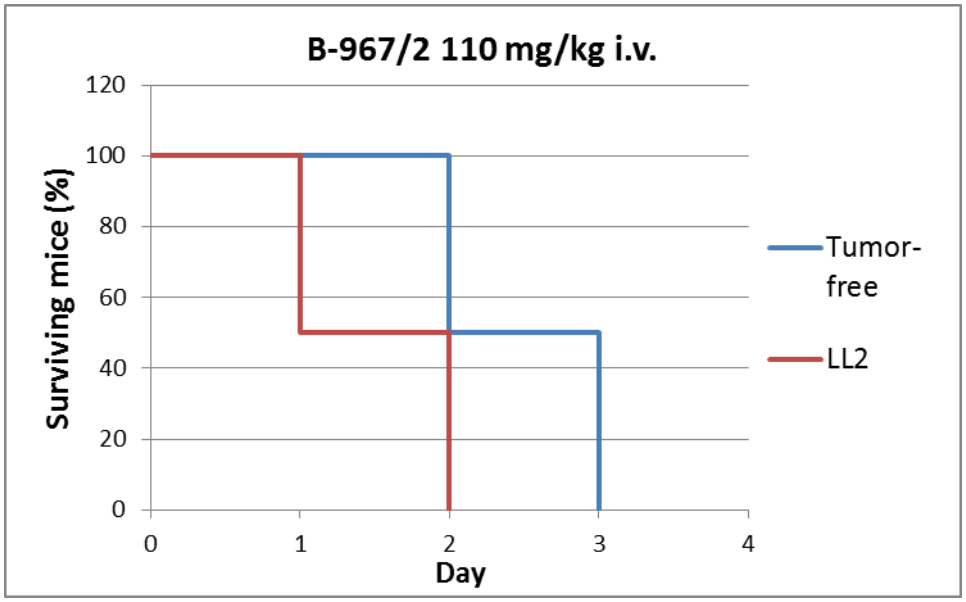

Figure V.12 Comparison of toxicity between LL2 tumor-bearing and tumor-free mice. C57BL/6 mice were randomly divided into two groups (n=2) and one group was s.c. injected with 10^6 LL2 cells on day 0. On day 7, both LL2 tumor-bearing (red) and control tumor-free (blue) mice were i.v. treated with B-967/2 at a dose of 110 mg/kg MBZ eq. Mice were then observed for signs of toxicity, their weight and rectal temperature were measured and survival was recorded. (Data shows % of surviving mice.)

Afterwards, additional testing of B-967/2 at the IMC laboratory proved that molecular weight of B-967/2 was significantly higher than was originally reported based on approximation from the value for B-967/1 (Table V.9), likely due to unwanted cross-linking of the polymer, which accounted for the worse solubility of the batch. The resulting increase in viscosity proved to be fatal for mice in higher doses, most likely by mechanism of embolism by the viscous and poorly soluble substance at the time of application, which possibly contributed to and potentiated the toxicity of MBZ itself.

Table V.9 B-967/2 molecular weight*

Batch	**B-967/2 (reported)**	**B-967/2 (actual)**	**B-967/1**
Molecular weight	~50000	150000	51000

*The molecular weight of B-967/2 as originally reported in comparison with the value actually measured and the previously known value for B-967/1.

V.2.5. *In vitro* and *in vivo* testing of B-967/3

We administered B-967/3 in doses of 140 mg/kg and 160 mg/kg MBZ eq. delivered via a single bolus as well as in four sequential doses of 25 mg/kg and 40 mg/kg MBZ eq. delivered over four consecutive days. Another change was that from this time onward, we performed the administration not intravenously but intraperitoneally (i.p.), reasoning that while being comparable from the pharmacokinetic standpoint [181], this mode of application should limit the potential adverse effects derived from high viscosity of the conjugates and should eliminate the risk of massive embolism we observed with B-967/2.

Results (Fig V.13) once again showed marked toxicity and we saw quick death of animals in all i.p. treated groups except the group which received 4×25 mg/kg MBZ eq. The application itself was once again complicated by poor solubility of B-967/3 in high concentrations required for administering high single bolus dose. This poor solubility might account for the single survivor in the 160 mg/kg treated group, which showed relatively little marks of toxicity. In the peritoneal cavity of this mouse, B-967/3 likely created a deposit which released the drug only slowly into circulation. Results led us to conclude that the MTD for this batch was lower than 140 mg/kg MBZ eq. for single bolus and ~4×25 mg/kg MBZ eq. for sequential administration over four consecutive days.

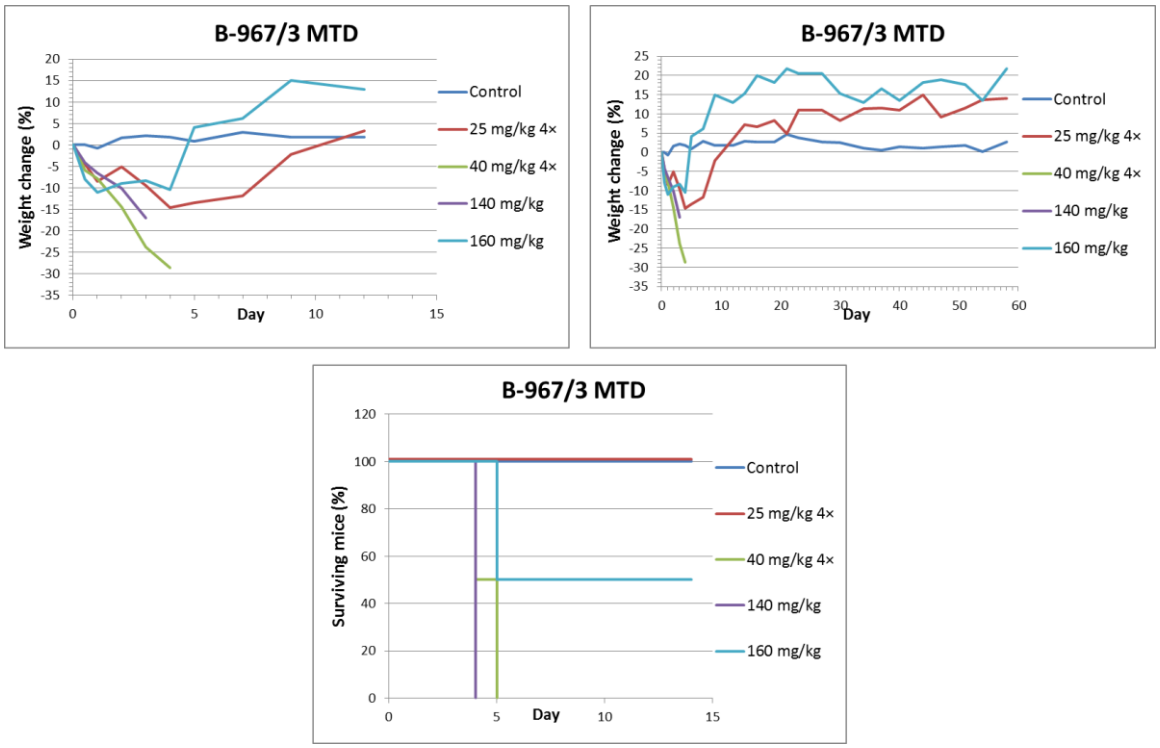

Fig V.13 Determination of MTD of conjugate B-967/3. C57BL/6 mice (n=2) were i.p. administered B-967/3 dissolved in sterile PBS in bolus doses of 140 (purple) resp. 160 (light blue) mg/kg of MBZ eq. or in doses of 25 (red) resp. 40 (green) mg/kg MBZ eq. injected i.p. four times on four consecutive days. Control mice (dark blue) were i.p. treated with an equivalent amount of sterile PBS. Mice were then observed for signs of toxicity and their weight (top right, detail top left; shown in %) and survival (bottom, shown as % of surviving mice) were recorded.

Testing B-967/3 *in vitro* revealed that batch B-967/3 possessed remarkably higher cytostatic activity than B-967/1 (Fig V.14 and Table V.10) in both LL2 and EL4.IL2 cells. In fact, the cytostatic effect of B-967/3 was comparable with that of free MBZ and B-967/3 thus did not show the reduction of *in vitro* activity seen in B-967/1 and B-967/2 (see also Figs V.6 and V.23). This could be explained by presence of a higher content of unbound MBZ in B-967/3 or by a markedly faster process of MBZ release from the conjugate. Nevertheless B-967/3 still possessed dramatically improved solubility in PBS in comparison with the free drug, which allowed the i.p. application and further testing of toxicity.

Table V.10 Mean IC50 values for B-967/1, B-967/2, B-967/3 and MBZ in LL2 and EL4.IL2 cell lines.*

Cell line	**B-967/1**	**B-967/2**	**B-967/3**	**MBZ**
LL2	134±38	149±38	77±7	67±11
EL4.IL2	138±18	124±3	57±5	60±7

*LL2 and EL4.IL2 cells were seeded onto 96-well plates and incubated with a range of concentrations of B-967/1, B-967/2, B-967/3 or MBZ for 72h. [^{3}H]-thymidine was added for the last 6 hours of incubation. Cells were harvested and radioactivity measured. IC50 values (ng/ml MBZ eq.) were calculated as the concentration of drug which inhibited the incorporation of tracer to 50% of control cells. The activity of control cells was always higher than 25 000 cpm/well. Mean IC50 values ± standard deviations presented in this table were obtained from at least three independent experiments.

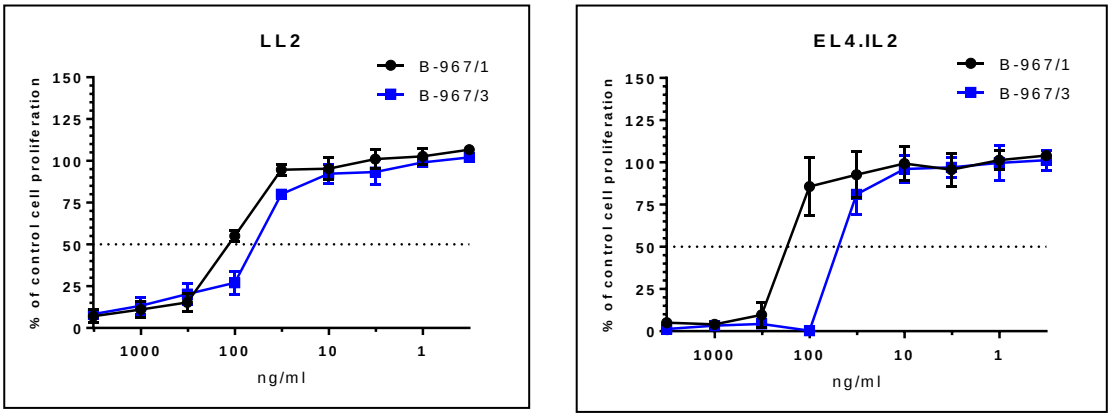

Figure V.14 Representative curves of [^{3}H]-thymidine assay for B-967/1 and B-967/3 in LL2 and EL4.IL2 cell lines. LL2 and EL4.IL2 cells were seeded onto 96-well plates and incubated with a range of concentrations of B-967/1 (black lines) or B-967/3 (blue lines) for 72h under standard culture conditions. [^{3}H]-thymidine was added for the last 6 hours of incubation. Cells were harvested and radioactivity measured. The results are shown as the inhibition of the proliferation of the exposed cells relative to the controls (cells incubated with medium alone). The activity of control cells was always higher than 25 000 cpm/well. Results shown in this figure were obtained from at least three independent experiments.

V.2.6. Assessing the mechanism of B-967/3 toxicity in C57BL/6 mice

We decided to test the effect of i.p. administered B-967/3 on bone marrow function. Thus, we analysed peripheral blood of mice with thiazol orange fluorescent reagent (BD ReticCount; see chapter IV.6) which stains nucleic acids in a population of immature erythrocytes known as reticulocytes [179]. The percentage of reticulocytes in peripheral blood is a convenient marker of erythropoiesis. Erythropoiesis itself, in turn, serves as a readily obtainable marker to evaluate bone marrow integrity. Another way to analyse toxicity of the conjugate was the histology of selected organs (liver, kidney, lung, heart, brain and a sample of femur with bone marrow were collected).

Unexpectedly, all mice from groups treated with B-967/3 in the doses of 125 and 100 mg/kg MBZ eq. rapidly lost weight and died within three days after application before they could be harvested for histological samples, in some cases even before blood collection could be performed (Fig V.15). The mice treated with B-967/3 75 mg/kg MBZ eq. were likewise exhibiting marks of toxicity; the one with the most pronounced signs was sacrificed on D3 after treatment and histological samples of its organs were analyzed.

FACS analysis of the blood samples of mice treated with 75 mg/kg MBZ eq. of B-967/3 and the control groups was performed. Fig V.16, a representative chart from FACS analysis software, shows the percentage of reticulocytes from erythrocytes in physiological conditions in a control sample and conditions of severe bone marrow toxicity in a sample from a 75 mg/kg MBZ eq. B-967/3 treated mouse.

Reticulocyte percentages shown in Figs V.17-19 clearly illustrate that while control mice retained approximately stable levels of reticulocytes before the compensatory increase caused by repeated blood loss took effect, the mice exposed to B-967/3 experienced a marked drop with reticulocytes nearly absent around day 4 before erythropoiesis recovered and reticulocytes again increased to compensate. Fig V.17 shows reticulocyte percentages of B-967/3 treated mice, illustrating clearly the complete inhibition of erythropoiesis. Fig V.18 shows the two respective control groups. Variation between the individual mice within a single control group was comparable with variation between the two groups and thus different blood collection regimens. This could be explained by the fact that though care was taken to minimize blood loss incurred when obtaining the blood samples, the individual mice differed in their tendency to bleed after comparably small incisions. Therefore, the outlying values of extremely high reticulocyte counts seen in some of the mice in Figs V.17–18 could be explained by a proportionally higher increase in erythropoiesis after blood collection resulted in a greater and more prolonged blood loss. These random incidents of profuse

bleeding after incision seem to have even greater importance than the effect of daily collection of small blood samples.

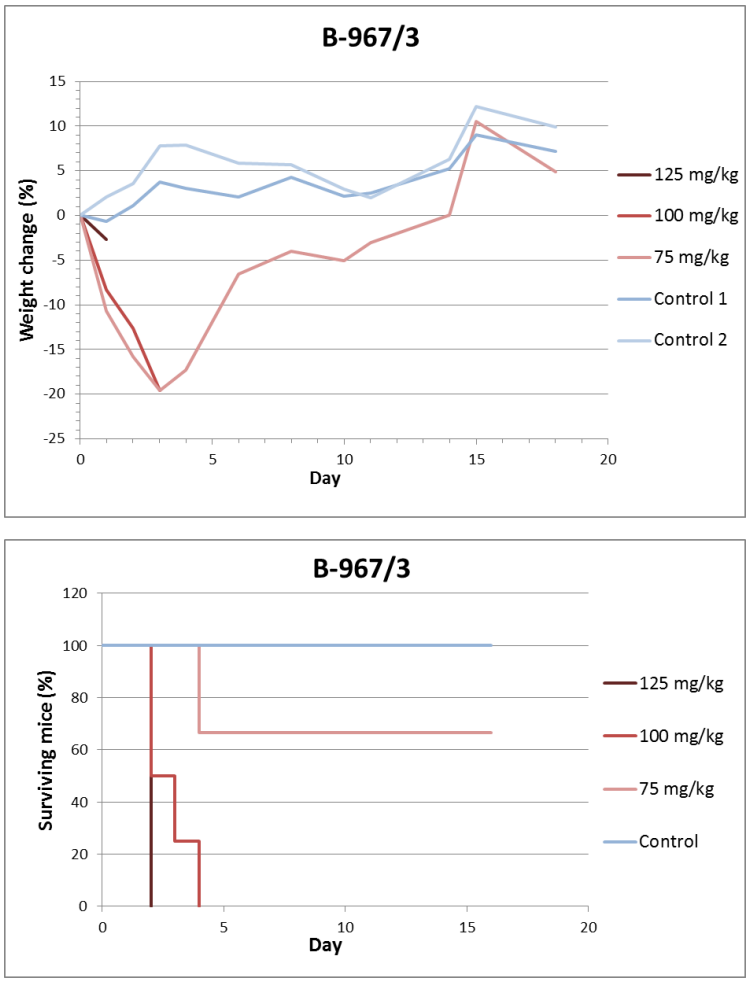

Figure V.15 Reticulocyte percentage determination – weight and survival. C57BL/6 mice (n=3-4) were i.p. administered B-967/3 dissolved in sterile PBS in bolus doses of 75 (light red), 100 (medium red) or 125 (dark red) mg/kg of MBZ eq. on day 0. Control mice (blue) were i.p. treated with an equivalent amount of sterile PBS. Mice were marked with puncture wounds to their earlobes to allow for following individuals over time. They were observed for signs of toxicity and their weight (top, shown in %) and survival (bottom, shown as % of surviving mice) were recorded.
On days 1, 2, 3, 4, 6, 8, 10 and 13, a small amount of blood was collected from an incision on the tail as described in chapter IV.6, stained with thiazol orange and analyzed by flow cytometry for reticulocyte count.

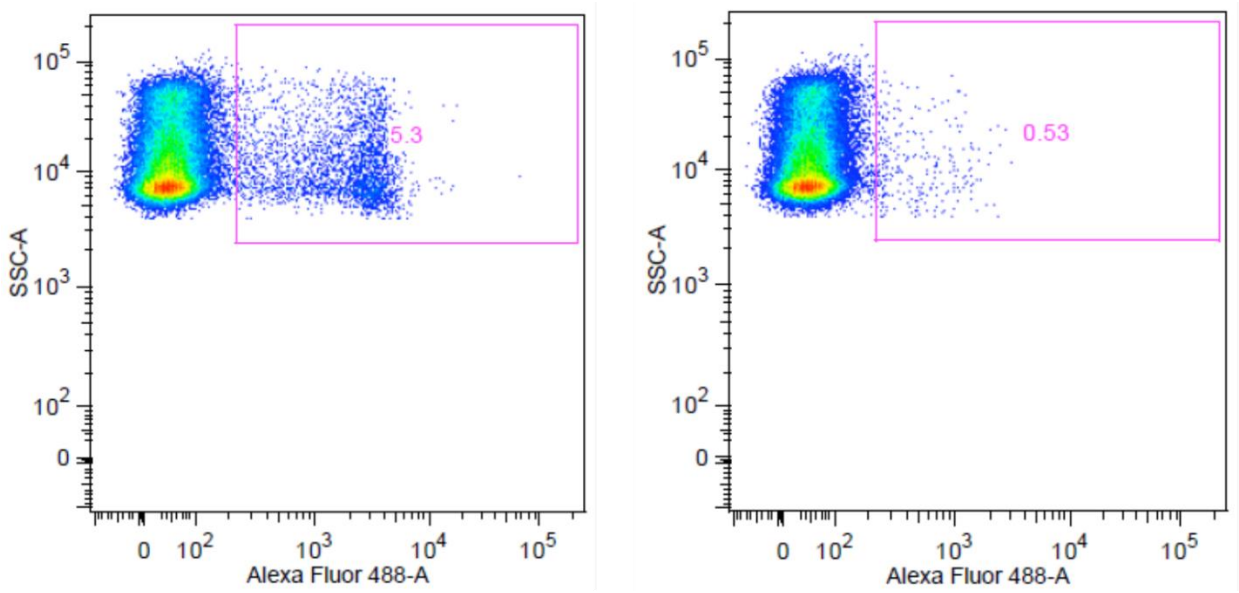

Fig V.16 Reticulocyte count. A representative FACS image of analysis of erythrocytes from blood samples obtained on day 4 from a control mouse (left) and a mouse treated with 75 mg/kg MBZ eq. of B-967/3 (right). Gate shows reticulocytes, with the numbers representing the percent of reticulocytes in erythrocytes. Experimental setup as described in chapter IV.6 and Fig V.15.

Finally, Figs V.19 and V.20 represent histological images taken from mice treated with 75 mg/kg MBZ eq. of B-967/3. No signs of toxicity were found in histological samples of kidney, lung, heart and brain. However, Fig V.19 shows that the femur bone marrow sinuses were markedly hyperemic and almost completely devoid of hematopoietic elements and clusters of blood precursor cells. Combined with the low reticulocyte counts seen in Fig V.17 this suggests a marked toxic effect of parenterally applied B-967/3 on bone marrow and on haematopoiesis.

The histological image of liver from the same mouse (Fig V.20) shows a disperse presence of necrotic/apoptotic elements in the liver tissue, with no signs of immune activation or macrophage response. This finding is most likely a sign of acute liver toxicity of B-967/3.

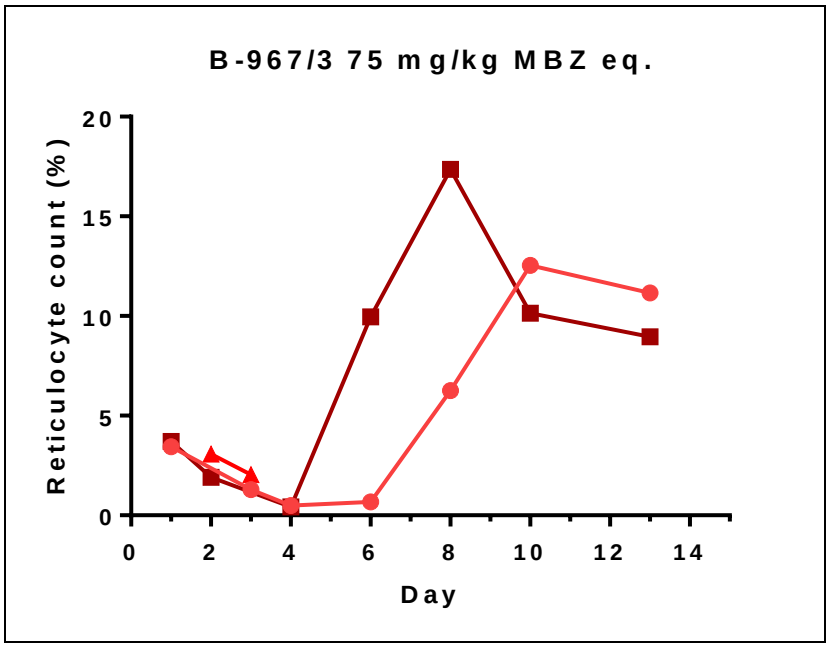

Figure V.17 Reticulocyte percentages in C57BL/6 mice treated with 75 mg/kg MBZ eq. of B-967/3. The percent values of reticulocytes in the erythrocyte population in mice treated as described in chapter IV.6 and Fig V.15. Counts shown were obtained by analysis of FACS data as illustrated in Fig V.16. Representation shows the progression of values in individual mice, tracked via the piercing earlobes and distinguished in the figure as individual data sets.
Note the marked drop in reticulocyte % between days 3-6.

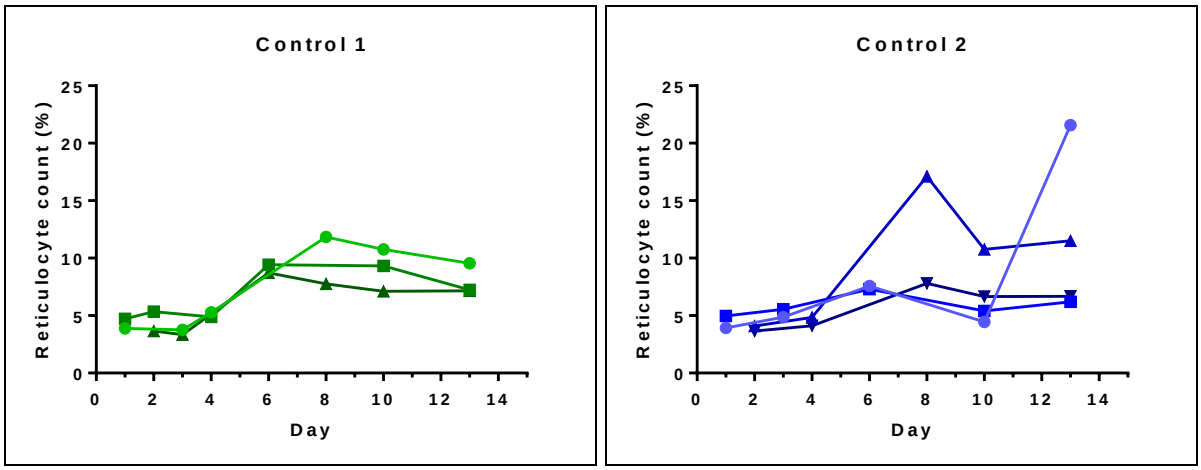

Figure V.18 Reticulocyte percentages in control C57BL/6 mice. The percent values of reticulocytes in the erythrocyte population of mice from the Control 1(left) and Control 2 (right) groups as described in chapter IV.6 and Fig V.15. Counts shown were obtained by analysis of FACS data as illustrated in Fig V.15. Representation shows the progression of values in individual mice, tracked via the piercing earlobes and distinguished in the figure as individual data sets.

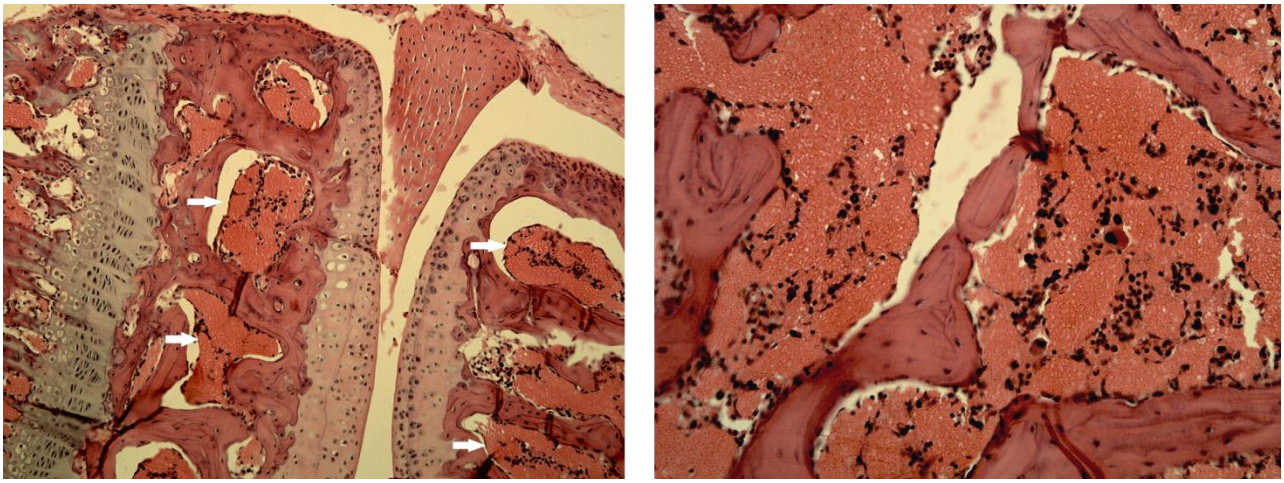

Figure V.20 Histological image of femur bone marrow of a mouse treated with75 mg/kg MBZ eq. of B-967/3. A C57BL/6 mouse treated with 75 mg/kg MBZ eq. of B-967/3 as described earlier was sacrificed and harvested for organs on day 3. Femur bone was gently removed, fixated with 4% formaldehyde, decalcified, prepared for staining and stained with haematoxylin and eosin.
Left: bone marrow sinuses viewed at 10× magnification. Arrows show the hyperemic sinuses devoid of normal hematopoietic elements.
Right: bone marrow sinuses viewed at 20× magnification. Note the absence of hematopoietic clusters.

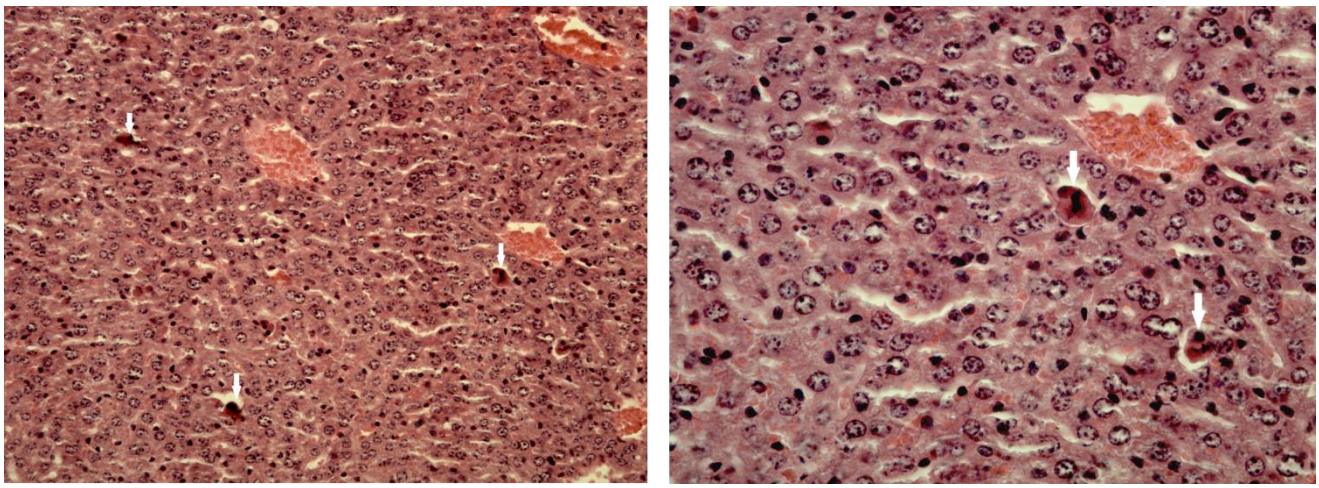

Figure V.21 Histological image of liver of a mouse treated with75 mg/kg MBZ eq. of B-967/3. A C57BL/6 mouse treated with 75 mg/kg MBZ eq. of B-967/3 as described earlier was sacrificed and harvested for organs on day 3. Liver was gently removed, fixated with 4% formaldehyde, prepared for staining and stained with haematoxylin and eosin.
Left: liver parenchyma viewed at 20× magnification. Arrows show dispersedly located necrotic/apoptotic cells.
Right: liver parenchyma viewed at 40× magnification. Arrows show necrotic/apoptotic cells.

V.2.7. Testing B-967/4

At this point, it had been made abundantly clear that the individual batches of B-967 can significantly differ in numerous parameters and that each new batch requires both *in vitro* testing and a separate round of MTD evaluation if it is considered for therapeutic experiments. We therefore tested the new batch B-967/4, starting with *in vitro* characterization in the LL2 and EL4.IL2 cell lines (Fig V.22, Table V.11). The results again showed cytostatic activity *in vitro* comparable to that of MBZ and greater than that of B-967/1 and B-967/2. Fig V.23 and Table V.12 show the representative curves and mean IC50 values for batches B-967/1 – 4 as well as for unconjugated mebendazole. Taken together it seems that while batches 3 and 4 retained the correct molecular weight, their poor solubility and similarity in effectiveness to free MBZ indicate a higher proportion of free drug released from the polymer. This was further supported by the fact that B-967/4 was later proven practically insoluble in concentrations needed for effective *in vivo* experimentation. Testing for the content of free MBZ in B-967/4 in the collaborating laboratory at IMC proved conclusively that these issues were indeed caused by high levels of free MBZ in the sample (19 weight % instead of the usual <0.1 weight %).

Table V.11 Mean IC50 values for B-967/1, B-967/2, B-967/4 and MBZ in LL2 and EL4.IL2 cell lines.*

Cell line	**B-967/1**	**B-967/2**	**B-967/4**	**MBZ**
LL2	134±38	149±38	58±9	67±11
EL4.IL2	138±18	124±3	75±10	60±7

*LL2 and EL4.IL2 cells were seeded onto 96-well plates and incubated with a range of concentrations of B-967/1, B-967/2, B-967/4 or MBZ for 72h. [^{3}H]-thymidine was added for the last 6 hours of incubation. Cells were harvested and radioactivity measured. IC50 values (ng/ml MBZ eq.) were calculated as the concentration of drug which inhibited the incorporation of tracer to 50% of control cells. The activity of control cells was always higher than 25 000 cpm/well. Mean IC50 values ± standard deviations presented in this table were obtained from at least three independent experiments.

Table V.12 Mean IC50 values for B-967/1 – 4 and MBZ in LL2 and EL4.IL2 cell lines.*

Cell line	**B-967/1**	**B-967/2**	**B-967/3**	**B-967/4**	**MBZ**
LL2	134±38	149±38	77±7	58±9	67±11
EL4.IL2	138±18	124±3	57±5	75±10	60±7

*LL2 and EL4.IL2 cells were seeded onto 96-well plates and incubated with a range of concentrations of B-967/1, B-967/2, B-967/3, B-967/4 or MBZ for 72h. [^{3}H]-thymidine was added for the last 6 hours of incubation. Cells were harvested and radioactivity measured. IC50 values (ng/ml MBZ eq.) were calculated as the concentration of drug which inhibited the incorporation of tracer to 50% of control cells. The activity of control cells was always higher than 25 000 cpm/well. Mean IC50 values ± standard deviations presented in this table were obtained from at least three independent experiments.

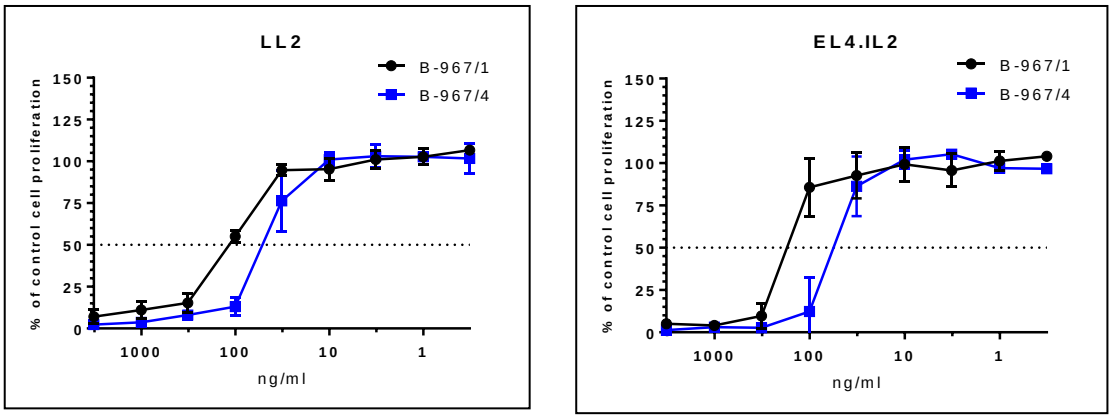

Figure V.22 Representative curves of [^{3}H]-thymidine assay for B-967/1 and B-967/4 in LL2 and EL4.IL2 cell lines. LL2 and EL4.IL2 cells were seeded onto 96-well plates and incubated with a range of concentrations of B-967/1 (black lines) or B-967/4 (blue lines) for 72h under standard culture conditions. [^{3}H]-thymidine was added for the last 6 hours of incubation. Cells were harvested and radioactivity measured. The results are shown as the inhibition of the proliferation of the exposed cells relative to the controls (cells incubated with medium alone). The activity of control cells was always higher than 25 000 cpm/well. Results shown in this figure were obtained from at least three independent experiments.

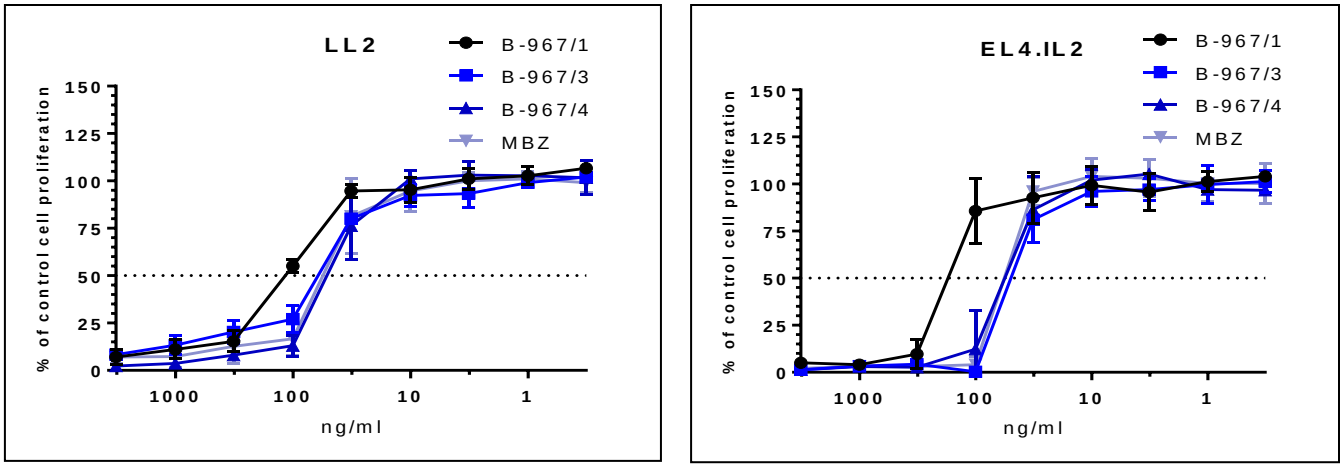

Figure V.23 Representative curves of [^{3}H]-thymidine assay for B-967/1, B-967/3, B-967/4 and MBZ in LL2 and EL4.IL2 cell lines. LL2 and EL4.IL2 cells were seeded onto 96-well plates and incubated with a range of concentrations of B-967/1 (black lines), B-967/3, B-967/4 or MBZ (lines in shades of blue) for 72h under standard culture conditions. [^{3}H]-thymidine was added for the last 6 hours of incubation. Cells were harvested and radioactivity measured. The results are shown as the inhibition of the proliferation of the exposed cells relative to the controls (cells incubated with medium alone). The activity of control cells was always higher than 25 000 cpm/well. Results shown in this figure were obtained from at least three independent experiments.

VI. Discussion

Cancer therapy is a field that has been under continual development over the course of the last century. Ever since the establishment of conventional chemotherapy as the third major pillar in the treatment of malignant cancer, a constant drive for better understanding the underlying principles of cancer biology led the researchers to improve the current protocols, investigate new approaches to rationalize treatment and research new therapeutics. As the therapeutic possibilities started to encounter their limits, strategies to overcome these barriers were investigated and implemented. Because the toxicity and non-specificity of the effect of conventional chemotherapeutics was always the most obvious of the limiting factors, research into ways of more selective and less damaging treatment has been at the forefront of this process since the beginning. This research gave rise to several distinct branches of science, such as clinical oncology – a discipline of modern medicine devoted to devising and administering complex regimens of treatment most often based on combinations of chemotherapeutics – and of course the research into drug delivery systems [105].

Thanks to the establishment of new methods and technologies brought along with the advent of molecular sciences and immunology, a new round of revolutionary changes occurred. The accumulation of great amounts of deeply detailed data [9] made it possible to prepare a new generation of anticancer drugs and drug targeting systems with specificity defined at the molecular level, i.e. molecular target-specific chemotherapeutics and ligand-directed targeted therapy as well as complementary approaches aimed at subverting the various mechanisms and ways in which tumors escape treatment, including MDR inhibitors [104] and antiangiogenic therapeutics [53].

Yet despite this continuous progress, cancer still remains a leading cause of morbidity and mortality in the world, as evidenced by the epidemiological data provided by WHO [182]. Therefore, the drive into cancer research continues with unabated ferocity. The current state of our knowledge suggests that it is research into tumor immunity and immune therapy that holds the greatest promise. Numerous signs show that prognosis of tumor disease often corresponds better to the state of the patient's immune system than to the conventional staging and grading system, which led to a world-wide drive to establish immune score among the prognostic and therapeutic criteria [61]. The previously enigmatic differences among the success rate of therapeutic approaches can be explained through their effect on the tumor immune system, favoring the modalities without immunosuppressive side effects and those

capable of inducing the ICD [41], [42], [80]. Intense research into the complex aspects of immunosuppressive tumor environment and ways to modulate it is being performed.

For all these reasons it is clear that if the immune-based approaches are to reach their full potential, they have a vital need of chemotherapeutic drugs with to support and supplement them, providing the direct anti-tumor effect while remaining immunoprotective and immunostimulatory. New cytostatic drugs are just as needed in this century as in the last. However, the process of researching a novel therapeutic substance from scratch is both time consuming and extremely expensive, with the result often being uncertain. A promising approach of so-called drug repurposing, i.e. searching for promising anti-cancer drugs among therapeutics already established into clinical practice for different indications, has therefore been adopted in the recent past. The first possibility is to make use of the advanced high-throughput and automated methods to screen panels of commercially available drugs for favorable effects such as cytostatic or kinase-inhibiting activity [141]. Second approach lies in exploiting the accessibility of vast amounts of information collected into databases in this so-called ”-omics” era for *in silico* identifying candidate drugs according to parameters which might hint at anticancer effect, e.g. reports of toxicity from the original indication or structural or functional similarities to established cytostatic drugs [140]. This type of research can draw on previously collected data and advance through clinical trials for a new indication easier, faster and cheaper than researching completely new drugs.

Mebendazole, the anthelminthic that was our main focus, was included in the first wave of drugs thus tested. It possessed several characteristics that prompted us to attempt synthesis of an HPMA-copolymer conjugate of MBZ and study its effect in this work.

Firstly, the anticancer effects of MBZ have been described *in vivo* on multiple cell lines representing tumor types of high clinical importance including non-small-cell lung carcinoma, melanoma and colorectal carcinoma [163], [165], [169], [170] as well in two case reports of therapeutic success in humans [156], [157]. The described mechanisms were diverse among the used cell lines and exerted their effect via targeting several hallmark capabilities including anti-angiogenic and pro-apoptotic effects [168], [165]. It would therefore likely be useful for application in combination regimens, as is the common state-of-the-art usage of many anti-angiogenic and anti-apoptotic drugs [53], [137]. HPMA has been described as a useful platform for delivering combinations of drugs ([103], [119], [183]), making it a fine choice of a carrier for MBZ.

Secondly, MBZ is an example of a highly insoluble drug which is exclusively administered perorally in current practice [153]. Although it has been described to enter blood

circulation in sufficient amounts to elicit systemic effect after p.o. administration, it does so to a highly variable extent between individual patients. In addition to the poor ability to penetrate the gut barrier, it also suffers from high first pass effect, i.e. a large percentage of the portion of the drug absorbed from gut is metabolized in liver before it can enter the systemic circulation. It is swiftly bound to plasma proteins in blood, further limiting the therapeutic effect and decreasing its reliability. Conjugates of drugs to HPMA-copolymers have on the other hand been described to be somewhat protected from the binding of plasma proteins and effects of metabolism; furthermore, HPMA is routinely described to improve poor solubility of hydrophobic and insoluble compounds [105]. The possibility of a parenteral application of the resulting conjugate would also eliminate the first pass effect and generally significantly limit the variability in bioavailability. Based on the current state of knowledge, upon conjugating to HPMA, MBZ should also possess lower off-target toxicity and benefit from the EPR effect, improving the anticancer potential.

Lastly, most experiments were done on xenograft models and no data regarding the effect of MBZ on tumor immunity in a syngeneic model have so far been reported. In light of the published results demonstrating the improved capacity of HPMA-bound drugs to induce long-lasting tumor immunity [131], the conjugate could offer some insight into the effect MBZ has on the immune system as well. This was an especially promising option, as unpublished data we have at our disposal suggests that MBZ may at least partially upregulate the markers of ICD on the treated cells.

Based on the abovementioned reasoning, we conducted a round of screening of MBZ along with several novel chemotherapeutic agents (Carfilzomib, Alvespimycin, ABT-737) and DOX as a conventional cytostatic drug with well-described properties as a control. As MBZ performed with efficiency comparable to that of the other screened drugs, we proceeded to further test it in comparison with DOX, for which a large amount of data has been collected both in our laboratory and elsewhere, making it a convenient control. The results we obtained showed that MBZ possessed cytostatic and cytotoxic activity comparable with that of DOX in the model of syngeneic murine cell lines of various tissue and genetic background origins. A highly promising result also was that whereas DOX, a known substrate of Pgp, showed significantly reduced effectiveness in the resistant, Pgp expressing P388/MDR cell line [103], the cytostatic activity of MBZ in P388/MDR did not differ from the sensitive P388 line. This signifies that MBZ may not be a substrate of Pgp, which would provide a significant benefit.

Consequently, two derivatives of MBZ labeled B-956 and B-957 were synthesized at the IMC and tested with the purpose of determining which of the chemical bonds present in

the derivatives would better preserve the favorable biological effect of MBZ observed *in vitro*. The derivative B-956 (*N*-ethoxycarbonyl mebendazole) was thereafter chosen to serve as the basis for the synthesis of a linear HPMA-MBZ conjugate B-967.

Altogether, the *in vitro* results were promising and allowed for the experimentation to proceed into the phase of synthesis and both *in vitro* and *in vivo* testing of the B-967 conjugate. However, it needs to be mentioned that the transition from *in vitro* to *in vivo* testing represents a potential pitfall and that the data obtained from one system do not always correspond well to the other. Matters were further complicated by the fact that B-967 contains MBZ bound via a carbamate linker, which is very specific and was new to our laboratory experience.

The unique and unfavorable properties of this linker, including its low stability under standard laboratory conditions and the rapid kinetics of its release of free MBZ at neutral pH, likely were a major reason of the consequent issues hampered further *in vivo* testing. Therefore, a short sidestep into the underlying chemistry is needed to explain the chemical properties and the rationale behind the use of the carbamate linker. MBZ possesses a specific chemical reactivity strongly differing from simple amines such as DOX. This originates from increased acidity of the heterocyclic NH group and leads to an elevated susceptibility of the corresponding N- derivatives to alkaline hydrolysis. Therefore, it is very difficult to design a linker that would have the desired release kinetics, i.e. exhibit prolonged stability in slightly alkaline media mimicking blood (pH~7.4) but hydrolyze rapidly at a pH of around 5 (such as within the endosomal compartment, the ultimate target of the delivery system). Thus, our effort was preferably focused on development of a linker with satisfactory stability in PBS 7.4 (with half-time > several hours) but maintaining a hydrolytic lability also at the lower pH. Several low-molecular-weight derivatives of MBZ were synthesized in the preliminary stages including amides, sulfonamides, sulfenamides and carbamates and their hydrolytic profile was determined at the IMC. All the above-mentioned model compounds excluding carbamates were either very unstable in the wide range of pH or did not hydrolyze at all. Moreover, there exist supporting literature data indicating usefulness of MBZ carbamates for therapeutic studies [184], [185]. Therefore, the carbamate bond was chosen as a linkage between MBZ and the polymer carrier. Unfortunately, despite being the only feasible alternative, the relatively low stability of this bond in pH~7.4 compared to that of the linkers commonly used in HPMA conjugates of DOX (i.e. GFLG or hydrazone linkers) [129] is far from ideal.

Testing of the B-967/1 batch nonetheless went as expected and MTD was evaluated to be higher than 120 mg/kg in C57BL/6 mice (see Fig V.7). However, due to the high dosing of

MBZ used – rationalized by the extremely low toxicity of the drug observed in clinical practice – the *in vivo* experiments invariably consumed large amounts of the conjugate and required further batches to be synthesized. The next tested batch B-967/2 was used to proceed to therapeutic experiments, however, this was hampered by a very high and unexpected, often lethal toxicity (Figs V.9 &10). It was later discovered that the batch was for some reason faulty and possessed a higher molecular weight of the HPMA molecules than was assumed at the time of testing (150 000 versus the expected ~50 000). Although it's well known that molecular weight of HPMA conjugates is not in itself a cause of toxicity as even much larger conjugates have elicited no adverse effects [186], [187], in this particular case, it may have been indicative of an unplanned chemical or physico-chemical process such as cross-linking between the individual linear molecules of the HPMA copolymer. Such cross-linking could be explained by the hydrophobicity of the MBZ bound to HPMA copolymer side chains. In this regard, it may also be noteworthy to consider the relatively high content (i.e. 10 weight %, see also chapter III.5.2) of MBZ in B-967/2. There are literary reports that higher percent weight of the drug (e.g. DOX as described in [188]) bound in the conjugate may unfavorably influence the anticancer activity and it is plausible that such an effect could be even more pronounced in the case of a highly hydrophobic drug like MBZ, possibly further increasing the risk of a cross-linking of HPMA copolymer chains. Such an explanation would be consistent with the observable increased viscosity of the B-967/2 solution.

The increased viscosity very likely caused the clinical symptoms we observed since they were indicative of embolism by hydrophobic particles, in particular of embolism into the CNS (i.e. trembling, hypothermia and spastic posture and abnormalities of motion suggestive of ataxia similar to that observed in [189]). When the conjugate was applied in dosing low enough as to avoid the toxicity in the BCL1 leukemia model, it unfortunately showed no therapeutic effect at all.

Batch 967/3 again possessed significant toxicity compared to B-967/1, despite having the expected molecular weight of 46 000 (see chapter III.5.2). This at least allowed us to evaluate the mechanisms of said toxicity (see chapter V.2.6) via measuring the percentage of reticulocytes by flow cytometry as a marker of erythropoiesis [179]. We used the reticulocyte count as a measure of myelotoxicity of the conjugate B-967/3 in addition to also searching for signs of acute toxicity via conventional histology. While most organs did not show any pathological findings, there were signs of severe bone marrow aplasia and acute liver toxicity, which is consistent with the reported toxicity of MBZ from literature ([159], [160] and [158], respectively). This finding was noteworthy because in the usual case, conjugation to HPMA

results in a marked decrease in toxicity of the conjugated LMW drug [105], [117], an exact opposite of what was observed in the case of B-967/3. In fact, it seems that improving bioavailability of the drug served to dramatically increase its adverse effects, supporting the notion that the low bioavailability is the chief reason of the low toxicity of MBZ in the first place [154], [155].

It is likely that the high systemic toxicity we observed in the *in vivo* experiments with B-967/2 and B-967/3 was caused or at least compounded by the unfavorable stability of the carbamate linker, which allows free MBZ to be released in blood circulation due to its low stability at pH 7.4. The resulting high toxicity is consistent with at least two accounts of toxicity occurring in Phase I clinical trials of HMW-polymer delivered drugs. A methacryloylglycynamide-bound conjugate of camptotecin [122] and HPMA-bound conjugate of paclitaxel (similarly to our situation a highly insoluble drug bound to HPMA carrier) [123] were reported to cause unexpectedly severe toxicity due to the chemotherapeutic agent being released in blood circulation in significant amounts, very much like in our own case.

The final batch B-967/4 was unfortunately once again faulty, this time because of high weight % content of unconjugated MBZ (19% as opposed to the usual values of < 0.1%), rendering the batch practically insoluble and unusable in any *in vivo* experiments.

Considered all together, the specific and problematic physicochemical properties of MBZ and the carbamate bond which had to be used for conjugation to HPMA resulted in a high variability between the four individual batches of B-967 (see Figs V.7 – 8 and Table V.12) and a highly unfavorable pattern of drug release from the HPMA carrier. In order to be able to effectively continue the *in vivo* testing of HPMA-MBZ conjugates, the exact underlying physical and chemical reasons and processes causing this variability need to be uncovered and circumvented, or else a completely different way of binding MBZ to HPMA needs to be considered, if possible.

I*n vitro* cytostatic activity of MBZ were shown to be comparable to both the established conventional cytostatic chemotherapeutic DOX and several novel molecular target specific drugs (see Fig V.1) and the anticancer activity of MBZ and its derivative compounds were shown for the first time in a panel of several syngeneic murine models (see Fig V.2 – 6). These favorable effects include the potential resistance to the Pgp-mediated efflux (see Fig V.4) and possibly also induction of ICD by MBZ (unpublished data). These properties still make the drug a promising candidate for further testing.

VII. Conclusions

The conclusions of our study are:

5. We tested *in vitro* anticancer effectiveness of mebendazole (MBZ) in panel of murine tumor cell lines.
    a. We compared the cytostatic activity of MBZ with cytostatic activities of carfilzomib, alvespimycin, ABT-737 as well as the established anthracyclin chemotherapeutic doxorubicin (DOX). MBZ showed *in vitro* cytostatic effect comparable to DOX in several different cell lines. Particularly favorable finding was the *in vitro* cytostatic activity in the LL2 cells, generally a very poorly responsive cancer line which showed the same level of sensitivity to MBZ as to DOX.
    b. We compared the cytotoxic activity of MBZ with DOX. MBZ possessed *in vitro* cytotoxic effect comparable to DOX in several different tumor cell lines.
    c. We compared the cytostatic activity of MBZ with DOX in the sensitive P388 and resistant P388/MDR cells lines. Results proved that while DOX was several orders of magnitude less effective in P388/MDR cells than in P388 cells, MBZ showed comparable activity in both cell lines. Thus, unlike DOX, MBZ is not affected by MDR based on the overexpression of Pgp
6. Our collaborating laboratory at the Institute of Macromolecular Chemistry successfully prepared two MBZ derivatives labeled B-956 and B-957 and a conjugate of HPMA copolymer with a derivative of MBZ bound via a carbamate bond. This conjugate was labeled B-967.
    a. We confirmed that both MBZ derivatives retained *in vitro* cytostatic activity comparable to MBZ. B-956 proved to be slightly more effective and offered a bit better solubility than B-957.
    b. We determined that B-956 possesses more favorable properties and thus its chemical structure was used as the basis for modification of MBZ used for the synthesis of HPMA copolymer conjugate B-967. This conjugate possessed remarkably improved solubility in aqueous solutions in comparison to MBZ and enabled parenteral administration of MBZ into mice followed by the release of free MBZ.

7. We tested *in vitro* anticancer effect of two MBZ derivatives B-956 and B-957 as well as conjugate B-967, which was synthesized by binding MBZ to HPMA copolymer backbone using a carbamate bond. Free MBZ is released when B-967 is exposed to *in vitro* or *in vivo* conditions.
    a. B-967 possessed dramatically improved solubility in aqueous environment and slightly reduced *in vitro* cytostatic activity in comparison with free MBZ.
    b. We compared four individual batches of B-967. Unfortunately, there is significant batch to batch variation in terms of *in vitro* cytostatic activity, solubility, viscosity and toxicity *in vivo*.
8. We tested the *in vivo* toxicity of B-967 in C57BL/6 mice and its therapeutic effect in LL2, EL4 and BCL1 murine tumors.
    a. We confirmed the possibility of parenteral application of B-967 and attempted to determine the maximum tolerated dose (MTD) of B-967. Marked variability between the batches of B-967 made the MTD testing inconclusive. MTD of B-967/1 was higher than 120 mg/kg eq. MBZ; MTD for B-967/3 was lower than 100 mg/kg eq. MBZ for bolus application and ~4×25 mg/kg in four consecutive applications over four days. Testing of batches 2 and 4 *in vivo* did not allow reliable determination of MTD.
    b. We tested the therapeutic efficacy of i.v. administered B-967/2 in LL2, EL4 and BCL1 cancer *in vivo*. The high viscosity of the solution of B-967/2 administered to mice led to embolic complications which were lethal when combined with high doses of MBZ. In the model of EL4 tumor, the mice which survived the initial toxicity showed a slight reduction of tumor growth and a prolonging of survival. In BCL1 tumor, no therapeutic effect was achieved, likely due to the low dosing required to avoid the toxicity.
    c. We tested the bone marrow toxicity of B-967/3 by quantifying the percentage of reticulocytes. The results showed a drop in reticulocyte count from day 3 to 6, nearly reaching zero on day 4 followed by a compensatory increase. We also prepared and analyzed histological samples of the following organs from mice parenterally treated with B-967/3. In the kidney, brain, heart and lungs no marks of toxic injury were found. In liver parenchyma, dispersedly located apoptotic/necrotic cells were observed, indicating acute toxic injury to liver. Bone marrow findings were indicative of acute bone marrow toxicity, supporting the data gathered from reticulocyte count assay.

VIII. References

[1] D. Stehelin, H. E. Varmus, J. M. Bishop, and P. K. Vogt, “DNA related to the transforming gene(s) of avian sarcoma viruses is present in normal avian DNA,” *Nature*, vol. 260, no. 5547, pp. 170–173, Mar. 1976.

[2] A. G. Knudson, “Mutation and cancer: statistical study of retinoblastoma,” *Proc. Natl. Acad. Sci. U. S. A.*, vol. 68, no. 4, pp. 820–823, Apr. 1971.

[3] N. Tsuchida, T. Ryder, and E. Ohtsubo, “Nucleotide sequence of the oncogene encoding the p21 transforming protein of Kirsten murine sarcoma virus,” *Science*, vol. 217, no. 4563, pp. 937–939, Sep. 1982.

[4] M. Schwab, K. Alitalo, H. E. Varmus, J. M. Bishop, and D. George, “A cellular oncogene (c-Ki-ras) is amplified, overexpressed, and located within karyotypic abnormalities in mouse adrenocortical tumour cells,” *Nature*, vol. 303, no. 5917, pp. 497–501, Jun. 1983.

[5] S. P. Chellappan, S. Hiebert, M. Mudryj, J. M. Horowitz, and J. R. Nevins, “The E2F transcription factor is a cellular target for the RB protein,” *Cell*, vol. 65, no. 6, pp. 1053–1061, Jun. 1991.

[6] L. V. Crawford, D. C. Pim, E. G. Gurney, P. Goodfellow, and J. Taylor-Papadimitriou, “Detection of a common feature in several human tumor cell lines--a 53,000-dalton protein,” *Proc. Natl. Acad. Sci. U. S. A.*, vol. 78, no. 1, pp. 41–45, Jan. 1981.

[7] I. Berenblum and P. Shubik, “A new, quantitative, approach to the study of the stages of chemical cartinogenesis in the mouse’s skin,” *Br. J. Cancer*, vol. 1, no. 4, pp. 383–391, Dec. 1947.

[8] D. J. Ashley, “The two ‘hit’ and multiple ‘hit’ theories of carcinogenesis,” *Br. J. Cancer*, vol. 23, no. 2, pp. 313–328, Jun. 1969.

[9] D. Hanahan and R. A. Weinberg, “The hallmarks of cancer,” *Cell*, vol. 100, no. 1, pp. 57–70, Jan. 2000.

[10] D. Hanahan and R. A. Weinberg, “Hallmarks of cancer: the next generation,” *Cell*, vol. 144, no. 5, pp. 646–674, Mar. 2011.

[11] D. J. Slamon, G. M. Clark, S. G. Wong, W. J. Levin, A. Ullrich, and W. L. McGuire, “Human breast cancer: correlation of relapse and survival with amplification of the HER-2/neu oncogene,” *Science*, vol. 235, no. 4785, pp. 177–182, Jan. 1987.

[12] K. W. Kinzler and B. Vogelstein, “Lessons from hereditary colorectal cancer,” *Cell*, vol. 87, no. 2, pp. 159–170, Oct. 1996.

[13] L. Hayflick, “THE LIMITED IN VITRO LIFETIME OF HUMAN DIPLOID CELL STRAINS,” *Exp. Cell Res.*, vol. 37, pp. 614–636, Mar. 1965.

[14] S. Srivastava, Z. Q. Zou, K. Pirollo, W. Blattner, and E. H. Chang, “Germ-line transmission of a mutated p53 gene in a cancer-prone family with Li-Fraumeni syndrome,” *Nature*, vol. 348, no. 6303, pp. 747–749, Dec. 1990.

[15] G. Farmer, J. Bargonetti, H. Zhu, P. Friedman, R. Prywes, and C. Prives, “Wild-type p53 activates transcription in vitro,” *Nature*, vol. 358, no. 6381, pp. 83–86, Jul. 1992.

[16] J. D. Oliner, K. W. Kinzler, P. S. Meltzer, D. L. George, and B. Vogelstein, “Amplification of a gene encoding a p53-associated protein in human sarcomas,” *Nature*, vol. 358, no. 6381, pp. 80–83, Jul. 1992.

[17] D. Hanahan and J. Folkman, “Patterns and Emerging Mechanisms of the Angiogenic Switch during Tumorigenesis,” *Cell*, vol. 86, no. 3, pp. 353–364, Aug. 1996.

[18] R. S. Kerbel, “Tumor angiogenesis,” *N. Engl. J. Med.*, vol. 358, no. 19, pp. 2039–2049, May 2008.

[19] M. Burnet, “Cancer; a biological approach. I. The processes of control,” *Br. Med. J.*, vol. 1, no. 5022, pp. 779–786, Apr. 1957.

[20] G. P. Dunn, L. J. Old, and R. D. Schreiber, “The three Es of cancer immunoediting,” *Annu. Rev. Immunol.*, vol. 22, pp. 329–360, 2004.
[21] M. DuPage, C. Mazumdar, L. M. Schmidt, A. F. Cheung, and T. Jacks, “Expression of tumour-specific antigens underlies cancer immunoediting,” *Nature*, vol. 482, no. 7385, pp. 405–409, Feb. 2012.
[22] A. F. Cheung, M. J. P. Dupage, H. K. Dong, J. Chen, and T. Jacks, “Regulated expression of a tumor-associated antigen reveals multiple levels of T-cell tolerance in a mouse model of lung cancer,” *Cancer Res.*, vol. 68, no. 22, pp. 9459–9468, Nov. 2008.
[23] G. Esendagli, K. Bruderek, T. Goldmann, A. Busche, D. Branscheid, E. Vollmer, and S. Brandau, “Malignant and non-malignant lung tissue areas are differentially populated by natural killer cells and regulatory T cells in non-small cell lung cancer,” *Lung Cancer Amst. Neth.*, vol. 59, no. 1, pp. 32–40, Jan. 2008.
[24] K. Murphy, P. Travers, M. Walport, and C. Janeway, *Janeway’s immunobiology*, 7th ed. New York: Garland Science, 2008.
[25] C. Du and Y. Wang, “The immunoregulatory mechanisms of carcinoma for its survival and development,” *J. Exp. Clin. Cancer Res. CR*, vol. 30, p. 12, 2011.
[26] J. O’Connell, M. W. Bennett, G. C. O’Sullivan, D. Roche, J. Kelly, J. K. Collins, and F. Shanahan, “Fas ligand expression in primary colon adenocarcinomas: evidence that the Fas counterattack is a prevalent mechanism of immune evasion in human colon cancer,” *J. Pathol.*, vol. 186, no. 3, pp. 240–246, Nov. 1998.
[27] E. Friedman, L. I. Gold, D. Klimstra, Z. S. Zeng, S. Winawer, and A. Cohen, “High levels of transforming growth factor beta 1 correlate with disease progression in human colon cancer,” *Cancer Epidemiol. Biomark. Prev. Publ. Am. Assoc. Cancer Res. Cosponsored Am. Soc. Prev. Oncol.*, vol. 4, no. 5, pp. 549–554, Aug. 1995.
[28] D. H. Munn and A. L. Mellor, “Indoleamine 2,3-dioxygenase and tumor-induced tolerance,” *J. Clin. Invest.*, vol. 117, no. 5, pp. 1147–1154, May 2007.
[29] A. Witkiewicz, T. K. Williams, J. Cozzitorto, B. Durkan, S. L. Showalter, C. J. Yeo, and J. R. Brody, “Expression of indoleamine 2,3-dioxygenase in metastatic pancreatic ductal adenocarcinoma recruits regulatory T cells to avoid immune detection,” *J. Am. Coll. Surg.*, vol. 206, no. 5, pp. 849–854; discussion 854–856, May 2008.
[30] A. H. Zea, P. C. Rodriguez, M. B. Atkins, C. Hernandez, S. Signoretti, J. Zabaleta, D. McDermott, D. Quiceno, A. Youmans, A. O’Neill, J. Mier, and A. C. Ochoa, “Arginase-producing myeloid suppressor cells in renal cell carcinoma patients: a mechanism of tumor evasion,” *Cancer Res.*, vol. 65, no. 8, pp. 3044–3048, Apr. 2005.
[31] V. Bronte, T. Kasic, G. Gri, K. Gallana, G. Borsellino, I. Marigo, L. Battistini, M. Iafrate, T. Prayer-Galetti, F. Pagano, and A. Viola, “Boosting antitumor responses of T lymphocytes infiltrating human prostate cancers,” *J. Exp. Med.*, vol. 201, no. 8, pp. 1257–1268, Apr. 2005.
[32] N. Hiraoka, K. Onozato, T. Kosuge, and S. Hirohashi, “Prevalence of FOXP3+ regulatory T cells increases during the progression of pancreatic ductal adenocarcinoma and its premalignant lesions,” *Clin. Cancer Res. Off. J. Am. Assoc. Cancer Res.*, vol. 12, no. 18, pp. 5423–5434, Sep. 2006.
[33] R. W. Griffiths, E. Elkord, D. E. Gilham, V. Ramani, N. Clarke, P. L. Stern, and R. E. Hawkins, “Frequency of regulatory T cells in renal cell carcinoma patients and investigation of correlation with survival,” *Cancer Immunol. Immunother. CII*, vol. 56, no. 11, pp. 1743–1753, Nov. 2007.
[34] S. A. Siddiqui, X. Frigola, S. Bonne-Annee, M. Mercader, S. M. Kuntz, A. E. Krambeck, S. Sengupta, H. Dong, J. C. Cheville, C. M. Lohse, C. J. Krco, W. S. Webster, B. C. Leibovich, M. L. Blute, K. L. Knutson, and E. D. Kwon, “Tumor-infiltrating Foxp3-

CD4+CD25+ T cells predict poor survival in renal cell carcinoma," *Clin. Cancer Res. Off. J. Am. Assoc. Cancer Res.*, vol. 13, no. 7, pp. 2075–2081, Apr. 2007.
[35] V. Cortez-Retamozo, M. Etzrodt, A. Newton, P. J. Rauch, A. Chudnovskiy, C. Berger, R. J. H. Ryan, Y. Iwamoto, B. Marinelli, R. Gorbatov, R. Forghani, T. I. Novobrantseva, V. Koteliansky, J.-L. Figueiredo, J. W. Chen, D. G. Anderson, M. Nahrendorf, F. K. Swirski, R. Weissleder, and M. J. Pittet, "Origins of tumor-associated macrophages and neutrophils," *Proc. Natl. Acad. Sci. U. S. A.*, vol. 109, no. 7, pp. 2491–2496, Feb. 2012.
[36] M. Dezfulian, T. Zee, K. B. DeOme, P. B. Blair, and D. W. Weiss, "Role of the mammary tumor virus in the immunogenicity of spontaneous mammary carcinomas of BALB/c mice and in the responsiveness of the hosts," *Cancer Res.*, vol. 28, no. 9, pp. 1759–1772, Sep. 1968.
[37] N. Casares, M. O. Pequignot, A. Tesniere, F. Ghiringhelli, S. Roux, N. Chaput, E. Schmitt, A. Hamai, S. Hervas-Stubbs, M. Obeid, F. Coutant, D. Métivier, E. Pichard, P. Aucouturier, G. Pierron, C. Garrido, L. Zitvogel, and G. Kroemer, "Caspase-dependent immunogenicity of doxorubicin-induced tumor cell death," *J. Exp. Med.*, vol. 202, no. 12, pp. 1691–1701, Dec. 2005.
[38] M. Obeid, A. Tesniere, F. Ghiringhelli, G. M. Fimia, L. Apetoh, J.-L. Perfettini, M. Castedo, G. Mignot, T. Panaretakis, N. Casares, D. Métivier, N. Larochette, P. van Endert, F. Ciccosanti, M. Piacentini, L. Zitvogel, and G. Kroemer, "Calreticulin exposure dictates the immunogenicity of cancer cell death," *Nat. Med.*, vol. 13, no. 1, pp. 54–61, Jan. 2007.
[39] L. Apetoh, F. Ghiringhelli, A. Tesniere, M. Obeid, C. Ortiz, A. Criollo, G. Mignot, M. C. Maiuri, E. Ullrich, P. Saulnier, H. Yang, S. Amigorena, B. Ryffel, F. J. Barrat, P. Saftig, F. Levi, R. Lidereau, C. Nogues, J.-P. Mira, A. Chompret, V. Joulin, F. Clavel-Chapelon, J. Bourhis, F. André, S. Delaloge, T. Tursz, G. Kroemer, and L. Zitvogel, "Toll-like receptor 4-dependent contribution of the immune system to anticancer chemotherapy and radiotherapy," *Nat. Med.*, vol. 13, no. 9, pp. 1050–1059, Sep. 2007.
[40] R. Spisek, A. Charalambous, A. Mazumder, D. H. Vesole, S. Jagannath, and M. V. Dhodapkar, "Bortezomib enhances dendritic cell (DC)-mediated induction of immunity to human myeloma via exposure of cell surface heat shock protein 90 on dying tumor cells: therapeutic implications," *Blood*, vol. 109, no. 11, pp. 4839–4845, Jun. 2007.
[41] J. Fucikova, P. Kralikova, A. Fialova, T. Brtnicky, L. Rob, J. Bartunkova, and R. Spísek, "Human tumor cells killed by anthracyclines induce a tumor-specific immune response," *Cancer Res.*, vol. 71, no. 14, pp. 4821–4833, Jul. 2011.
[42] M. Sirova, M. Kabesova, L. Kovar, T. Etrych, J. Strohalm, K. Ulbrich, and B. Rihova, "HPMA copolymer-bound doxorubicin induces immunogenic tumor cell death," *Curr. Med. Chem.*, vol. 20, no. 38, pp. 4815–4826, 2013.
[43] J. Fucikova, I. Moserova, I. Truxova, I. Hermanova, I. Vancurova, S. Partlova, A. Fialova, L. Sojka, P.-F. Cartron, M. Houska, L. Rob, J. Bartunkova, and R. Spisek, "High hydrostatic pressure induces immunogenic cell death in human tumor cells," *Int. J. Cancer J. Int. Cancer*, vol. 135, no. 5, pp. 1165–1177, Sep. 2014.
[44] M. A. Gimbrone, S. B. Leapman, R. S. Cotran, and J. Folkman, "Tumor dormancy in vivo by prevention of neovascularization," *J. Exp. Med.*, vol. 136, no. 2, pp. 261–276, Aug. 1972.
[45] L. Holmgren, M. S. O'Reilly, and J. Folkman, "Dormancy of micrometastases: balanced proliferation and apoptosis in the presence of angiogenesis suppression," *Nat. Med.*, vol. 1, no. 2, pp. 149–153, Feb. 1995.
[46] J. Folkman, K. Watson, D. Ingber, and D. Hanahan, "Induction of angiogenesis during the transition from hyperplasia to neoplasia," *Nature*, vol. 339, no. 6219, pp. 58–61, May 1989.

[47] D. R. Senger, S. J. Galli, A. M. Dvorak, C. A. Perruzzi, V. S. Harvey, and H. F. Dvorak, “Tumor cells secrete a vascular permeability factor that promotes accumulation of ascites fluid,” *Science*, vol. 219, no. 4587, pp. 983–985, Feb. 1983.
[48] D. R. Senger, C. A. Perruzzi, J. Feder, and H. F. Dvorak, “A highly conserved vascular permeability factor secreted by a variety of human and rodent tumor cell lines,” *Cancer Res.*, vol. 46, no. 11, pp. 5629–5632, Nov. 1986.
[49] T. Veikkola and K. Alitalo, “VEGFs, receptors and angiogenesis,” *Semin. Cancer Biol.*, vol. 9, no. 3, pp. 211–220, Jun. 1999.
[50] K. J. Kim, B. Li, J. Winer, M. Armanini, N. Gillett, H. S. Phillips, and N. Ferrara, “Inhibition of vascular endothelial growth factor-induced angiogenesis suppresses tumour growth in vivo,” *Nature*, vol. 362, no. 6423, pp. 841–844, Apr. 1993.
[51] B. Millauer, L. K. Shawver, K. H. Plate, W. Risau, and A. Ullrich, “Glioblastoma growth inhibited in vivo by a dominant-negative Flk-1 mutant,” *Nature*, vol. 367, no. 6463, pp. 576–579, Feb. 1994.
[52] C. G. Willett, Y. Boucher, E. di Tomaso, D. G. Duda, L. L. Munn, R. T. Tong, D. C. Chung, D. V. Sahani, S. P. Kalva, S. V. Kozin, M. Mino, K. S. Cohen, D. T. Scadden, A. C. Hartford, A. J. Fischman, J. W. Clark, D. P. Ryan, A. X. Zhu, L. S. Blaszkowsky, H. X. Chen, P. C. Shellito, G. Y. Lauwers, and R. K. Jain, “Direct evidence that the VEGF-specific antibody bevacizumab has antivascular effects in human rectal cancer,” *Nat. Med.*, vol. 10, no. 2, pp. 145–147, Feb. 2004.
[53] H. Hurwitz, L. Fehrenbacher, W. Novotny, T. Cartwright, J. Hainsworth, W. Heim, J. Berlin, A. Baron, S. Griffing, E. Holmgren, N. Ferrara, G. Fyfe, B. Rogers, R. Ross, and F. Kabbinavar, “Bevacizumab plus irinotecan, fluorouracil, and leucovorin for metastatic colorectal cancer,” *N. Engl. J. Med.*, vol. 350, no. 23, pp. 2335–2342, Jun. 2004.
[54] S. A. Skinner, P. J. Tutton, and P. E. O’Brien, “Microvascular architecture of experimental colon tumors in the rat,” *Cancer Res.*, vol. 50, no. 8, pp. 2411–2417, Apr. 1990.
[55] K. S. Ho, P. C. Poon, S. C. Owen, and M. S. Shoichet, “Blood vessel hyperpermeability and pathophysiology in human tumour xenograft models of breast cancer: a comparison of ectopic and orthotopic tumours,” *BMC Cancer*, vol. 12, p. 579, 2012.
[56] H. Hashizume, P. Baluk, S. Morikawa, J. W. McLean, G. Thurston, S. Roberge, R. K. Jain, and D. M. McDonald, “Openings between defective endothelial cells explain tumor vessel leakiness,” *Am. J. Pathol.*, vol. 156, no. 4, pp. 1363–1380, Apr. 2000.
[57] T. Konno, H. Maeda, K. Iwai, S. Maki, S. Tashiro, M. Uchida, and Y. Miyauchi, “Selective targeting of anti-cancer drug and simultaneous image enhancement in solid tumors by arterially administered lipid contrast medium,” *Cancer*, vol. 54, no. 11, pp. 2367–2374, Dec. 1984.
[58] Y. Matsumura and H. Maeda, “A new concept for macromolecular therapeutics in cancer chemotherapy: mechanism of tumoritropic accumulation of proteins and the antitumor agent smancs,” *Cancer Res.*, vol. 46, no. 12 Pt 1, pp. 6387–6392, Dec. 1986.
[59] H. Maeda, “Toward a full understanding of the EPR effect in primary and metastatic tumors as well as issues related to its heterogeneity,” *Adv. Drug Deliv. Rev.*, Jan. 2015.
[60] H. Maeda, H. Nakamura, and J. Fang, “The EPR effect for macromolecular drug delivery to solid tumors: Improvement of tumor uptake, lowering of systemic toxicity, and distinct tumor imaging in vivo,” *Adv. Drug Deliv. Rev.*, vol. 65, no. 1, pp. 71–79, Jan. 2013.
[61] J. Galon, F. Pagès, F. M. Marincola, H. K. Angell, M. Thurin, A. Lugli, I. Zlobec, A. Berger, C. Bifulco, G. Botti, F. Tatangelo, C. M. Britten, S. Kreiter, L. Chouchane, P. Delrio, H. Arndt, M. Asslaber, M. Maio, G. V. Masucci, M. Mihm, F. Vidal-Vanaclocha,

J. P. Allison, S. Gnjatic, L. Hakansson, C. Huber, H. Singh-Jasuja, C. Ottensmeier, H. Zwierzina, L. Laghi, F. Grizzi, P. S. Ohashi, P. A. Shaw, B. A. Clarke, B. G. Wouters, Y. Kawakami, S. Hazama, K. Okuno, E. Wang, J. O'Donnell-Tormey, C. Lagorce, G. Pawelec, M. I. Nishimura, R. Hawkins, R. Lapointe, A. Lundqvist, S. N. Khleif, S. Ogino, P. Gibbs, P. Waring, N. Sato, T. Torigoe, K. Itoh, P. S. Patel, S. N. Shukla, R. Palmqvist, I. D. Nagtegaal, Y. Wang, C. D'Arrigo, S. Kopetz, F. A. Sinicrope, G. Trinchieri, T. F. Gajewski, P. A. Ascierto, and B. A. Fox, "Cancer classification using the Immunoscore: a worldwide task force," *J. Transl. Med.*, vol. 10, p. 205, 2012.

[62] J. Galon, F. Pagès, F. M. Marincola, M. Thurin, G. Trinchieri, B. A. Fox, T. F. Gajewski, and P. A. Ascierto, "The immune score as a new possible approach for the classification of cancer," *J. Transl. Med.*, vol. 10, p. 1, 2012.

[63] C. S. D. Roxburgh, J. M. Salmond, P. G. Horgan, K. A. Oien, and D. C. McMillan, "Tumour inflammatory infiltrate predicts survival following curative resection for node-negative colorectal cancer," *Eur. J. Cancer Oxf. Engl. 1990*, vol. 45, no. 12, pp. 2138–2145, Aug. 2009.

[64] R. Forrest, G. J. K. Guthrie, C. Orange, P. G. Horgan, D. C. McMillan, and C. S. D. Roxburgh, "Comparison of visual and automated assessment of tumour inflammatory infiltrates in patients with colorectal cancer," *Eur. J. Cancer Oxf. Engl. 1990*, vol. 50, no. 3, pp. 544–552, Feb. 2014.

[65] K. G. Blume, E. Beutler, K. J. Bross, R. K. Chillar, O. B. Ellington, J. L. Fahey, M. J. Farbstein, S. J. Forman, G. M. Schmidt, E. P. Scott, W. E. Spruce, M. A. Turner, and J. L. Wolf, "Bone-marrow ablation and allogeneic marrow transplantation in acute leukemia," *N. Engl. J. Med.*, vol. 302, no. 19, pp. 1041–1046, May 1980.

[66] W. F. Maguire, M. R. McDevitt, P. M. Smith-Jones, and D. A. Scheinberg, "Efficient 1-step radiolabeling of monoclonal antibodies to high specific activity with 225Ac for α-particle radioimmunotherapy of cancer," *J. Nucl. Med. Off. Publ. Soc. Nucl. Med.*, vol. 55, no. 9, pp. 1492–1498, Sep. 2014.

[67] S. Baldari, F. Ferraù, C. Alafaci, A. Herberg, F. Granata, V. Militano, F. M. Salpietro, F. Trimarchi, and S. Cannavò, "First demonstration of the effectiveness of peptide receptor radionuclide therapy (PRRT) with 111In-DTPA-octreotide in a giant PRL-secreting pituitary adenoma resistant to conventional treatment," *Pituitary*, vol. 15 Suppl 1, pp. S57–60, Dec. 2012.

[68] J. P. Sheehan, C.-P. Yen, C.-C. Lee, and J. S. Loeffler, "Cranial stereotactic radiosurgery: current status of the initial paradigm shifter," *J. Clin. Oncol. Off. J. Am. Soc. Clin. Oncol.*, vol. 32, no. 26, pp. 2836–2846, Sep. 2014.

[69] A. Morales, D. Eidinger, and A. W. Bruce, "Intracavitary Bacillus Calmette-Guerin in the treatment of superficial bladder tumors," *J. Urol.*, vol. 116, no. 2, pp. 180–183, Aug. 1976.

[70] R. J. Sylvester, M. A. Brausi, W. J. Kirkels, W. Hoeltl, F. Calais Da Silva, P. H. Powell, S. Prescott, Z. Kirkali, C. van de Beek, T. Gorlia, T. M. de Reijke, and EORTC Genito-Urinary Tract Cancer Group, "Long-term efficacy results of EORTC genito-urinary group randomized phase 3 study 30911 comparing intravesical instillations of epirubicin, bacillus Calmette-Guérin, and bacillus Calmette-Guérin plus isoniazid in patients with intermediate- and high-risk stage Ta T1 urothelial carcinoma of the bladder," *Eur. Urol.*, vol. 57, no. 5, pp. 766–773, May 2010.

[71] K. Kawai, J. Miyazaki, A. Joraku, H. Nishiyama, and H. Akaza, "Bacillus Calmette-Guerin (BCG) immunotherapy for bladder cancer: current understanding and perspectives on engineered BCG vaccine," *Cancer Sci.*, vol. 104, no. 1, pp. 22–27, Jan. 2013.

[72] J. A. Klapper, S. G. Downey, F. O. Smith, J. C. Yang, M. S. Hughes, U. S. Kammula, R. M. Sherry, R. E. Royal, S. M. Steinberg, and S. Rosenberg, "High-dose interleukin-2

for the treatment of metastatic renal cell carcinoma : a retrospective analysis of response and survival in patients treated in the surgery branch at the National Cancer Institute between 1986 and 2006," *Cancer*, vol. 113, no. 2, pp. 293–301, Jul. 2008.
[73] R. O. Dillman, N. M. Barth, L. A. VanderMolen, K. Mahdavi, and S. E. McClure, "Should high-dose interleukin-2 still be the preferred treatment for patients with metastatic melanoma?," *Cancer Biother. Radiopharm.*, vol. 27, no. 6, pp. 337–343, Aug. 2012.
[74] O. Boyman, C. D. Surh, and J. Sprent, "Potential use of IL-2/anti-IL-2 antibody immune complexes for the treatment of cancer and autoimmune disease," *Expert Opin. Biol. Ther.*, vol. 6, no. 12, pp. 1323–1331, Dec. 2006.
[75] A. Burchert, M. C. Müller, P. Kostrewa, P. Erben, T. Bostel, S. Liebler, R. Hehlmann, A. Neubauer, and A. Hochhaus, "Sustained molecular response with interferon alfa maintenance after induction therapy with imatinib plus interferon alfa in patients with chronic myeloid leukemia," *J. Clin. Oncol. Off. J. Am. Soc. Clin. Oncol.*, vol. 28, no. 8, pp. 1429–1435, Mar. 2010.
[76] R. R. Ricketts, R. M. Hatley, B. J. Corden, H. Sabio, and C. G. Howell, "Interferon-alpha-2a for the treatment of complex hemangiomas of infancy and childhood," *Ann. Surg.*, vol. 219, no. 6, pp. 605–612; discussion 612–614, Jun. 1994.
[77] A. A. Tarhini and J. M. Kirkwood, "Clinical and immunologic basis of interferon therapy in melanoma," *Ann. N. Y. Acad. Sci.*, vol. 1182, pp. 47–57, Dec. 2009.
[78] E. A. Fagan and A. L. Eddleston, "Immunotherapy for cancer: the use of lymphokine activated killer (LAK) cells," *Gut*, vol. 28, no. 2, pp. 113–116, Feb. 1987.
[79] E. Tran, S. Turcotte, A. Gros, P. F. Robbins, Y.-C. Lu, M. E. Dudley, J. R. Wunderlich, R. P. Somerville, K. Hogan, C. S. Hinrichs, M. R. Parkhurst, J. C. Yang, and S. A. Rosenberg, "Cancer immunotherapy based on mutation-specific CD4+ T cells in a patient with epithelial cancer," *Science*, vol. 344, no. 6184, pp. 641–645, May 2014.
[80] I. Adkins, J. Fucikova, A. D. Garg, P. Agostinis, and R. Špíšek, "Physical modalities inducing immunogenic tumor cell death for cancer immunotherapy," *Oncoimmunology*, vol. 3, no. 12, p. e968434, Dec. 2014.
[81] N. Bloy, A. Buqué, F. Aranda, F. Castoldi, A. Eggermont, I. Cremer, C. Sautès-Fridman, J. Fucikova, J. Galon, R. Spisek, E. Tartour, L. Zitvogel, G. Kroemer, and L. Galluzzi, "Trial watch: Naked and vectored DNA-based anticancer vaccines," *Oncoimmunology*, vol. 4, no. 5, p. e1026531, May 2015.
[82] M. A. Cheever and C. S. Higano, "PROVENGE (Sipuleucel-T) in prostate cancer: the first FDA-approved therapeutic cancer vaccine," *Clin. Cancer Res. Off. J. Am. Assoc. Cancer Res.*, vol. 17, no. 11, pp. 3520–3526, Jun. 2011.
[83] B. M. Carreno, V. Magrini, M. Becker-Hapak, S. Kaabinejadian, J. Hundal, A. A. Petti, A. Ly, W.-R. Lie, W. H. Hildebrand, E. R. Mardis, and G. P. Linette, "Cancer immunotherapy. A dendritic cell vaccine increases the breadth and diversity of melanoma neoantigen-specific T cells," *Science*, vol. 348, no. 6236, pp. 803–808, May 2015.
[84] M. Podrazil, R. Horvath, E. Becht, D. Rozkova, P. Bilkova, K. Sochorova, H. Hromadkova, J. Kayserova, K. Vavrova, J. Lastovicka, P. Vrabcova, K. Kubackova, Z. Gasova, L. Jarolim, M. Babjuk, R. Spisek, J. Bartunkova, and J. Fucikova, "Phase I/II clinical trial of dendritic-cell based immunotherapy (DCVAC/PCa) combined with chemotherapy in patients with metastatic, castration-resistant prostate cancer," *Oncotarget*, May 2015.
[85] B. Carnemolla, L. Borsi, E. Balza, P. Castellani, R. Meazza, A. Berndt, S. Ferrini, H. Kosmehl, D. Neri, and L. Zardi, "Enhancement of the antitumor properties of interleukin-2 by its targeted delivery to the tumor blood vessel extracellular matrix," *Blood*, vol. 99, no. 5, pp. 1659–1665, Mar. 2002.

[86] K. Schwager, T. Hemmerle, D. Aebischer, and D. Neri, “The immunocytokine L19-IL2 eradicates cancer when used in combination with CTLA-4 blockade or with L19-TNF,” *J. Invest. Dermatol.*, vol. 133, no. 3, pp. 751–758, Mar. 2013.
[87] T. Wang, R. Somasundaram, and M. Herlyn, “Combination therapy of immunocytokines with ipilimumab: a cure for melanoma?,” *J. Invest. Dermatol.*, vol. 133, no. 3, pp. 595–596, Mar. 2013.
[88] S. D. Scott, “Rituximab: a new therapeutic monoclonal antibody for non-Hodgkin’s lymphoma,” *Cancer Pract.*, vol. 6, no. 3, pp. 195–197, Jun. 1998.
[89] K. Jhaveri, K. Miller, L. Rosen, B. Schneider, L. Chap, A. Hannah, Z. Zhong, W. Ma, C. Hudis, and S. Modi, “A phase I dose-escalation trial of trastuzumab and alvespimycin hydrochloride (KOS-1022; 17 DMAG) in the treatment of advanced solid tumors,” *Clin. Cancer Res. Off. J. Am. Assoc. Cancer Res.*, vol. 18, no. 18, pp. 5090–5098, Sep. 2012.
[90] F. S. Hodi, S. J. O’Day, D. F. McDermott, R. W. Weber, J. A. Sosman, J. B. Haanen, R. Gonzalez, C. Robert, D. Schadendorf, J. C. Hassel, W. Akerley, A. J. M. van den Eertwegh, J. Lutzky, P. Lorigan, J. M. Vaubel, G. P. Linette, D. Hogg, C. H. Ottensmeier, C. Lebbé, C. Peschel, I. Quirt, J. I. Clark, J. D. Wolchok, J. S. Weber, J. Tian, M. J. Yellin, G. M. Nichol, A. Hoos, and W. J. Urba, “Improved survival with ipilimumab in patients with metastatic melanoma,” *N. Engl. J. Med.*, vol. 363, no. 8, pp. 711–723, Aug. 2010.
[91] A. Ito, S. Kondo, K. Tada, and S. Kitano, “Clinical Development of Immune Checkpoint Inhibitors,” *BioMed Res. Int.*, vol. 2015, p. 605478, 2015.
[92] J. L. Miller, “FDA approves antibody-directed cytotoxic agent for acute myeloid leukemia,” *Am. J. Health-Syst. Pharm. AJHP Off. J. Am. Soc. Health-Syst. Pharm.*, vol. 57, no. 13, pp. 1202, 1204, Jul. 2000.
[93] T. E. Witzig, L. I. Gordon, F. Cabanillas, M. S. Czuczman, C. Emmanouilides, R. Joyce, B. L. Pohlman, N. L. Bartlett, G. A. Wiseman, N. Padre, A. J. Grillo-López, P. Multani, and C. A. White, “Randomized controlled trial of yttrium-90-labeled ibritumomab tiuxetan radioimmunotherapy versus rituximab immunotherapy for patients with relapsed or refractory low-grade, follicular, or transformed B-cell non-Hodgkin’s lymphoma,” *J. Clin. Oncol. Off. J. Am. Soc. Clin. Oncol.*, vol. 20, no. 10, pp. 2453–2463, May 2002.
[94] E. A. Lefrak, J. Pitha, S. Rosenheim, and J. A. Gottlieb, “A clinicopathologic analysis of adriamycin cardiotoxicity,” *Cancer*, vol. 32, no. 2, pp. 302–314, Aug. 1973.
[95] K. Chatterjee, J. Zhang, N. Honbo, and J. S. Karliner, “Doxorubicin cardiomyopathy,” *Cardiology*, vol. 115, no. 2, pp. 155–162, 2010.
[96] D. W. McMillin, J. M. Negri, and C. S. Mitsiades, “The role of tumour-stromal interactions in modifying drug response: challenges and opportunities,” *Nat. Rev. Drug Discov.*, vol. 12, no. 3, pp. 217–228, Mar. 2013.
[97] M. M. Gottesman, “How cancer cells evade chemotherapy: sixteenth Richard and Hinda Rosenthal Foundation Award Lecture,” *Cancer Res.*, vol. 53, no. 4, pp. 747–754, Feb. 1993.
[98] M. M. Gottesman, T. Fojo, and S. E. Bates, “Multidrug resistance in cancer: role of ATP-dependent transporters,” *Nat. Rev. Cancer*, vol. 2, no. 1, pp. 48–58, Jan. 2002.
[99] A. L. Davidson, E. Dassa, C. Orelle, and J. Chen, “Structure, function, and evolution of bacterial ATP-binding cassette systems,” *Microbiol. Mol. Biol. Rev. MMBR*, vol. 72, no. 2, pp. 317–364, table of contents, Jun. 2008.
[100] R. L. Juliano and V. Ling, “A surface glycoprotein modulating drug permeability in Chinese hamster ovary cell mutants,” *Biochim. Biophys. Acta*, vol. 455, no. 1, pp. 152–162, Nov. 1976.

[101] C. Sonnenschein, A. M. Soto, A. Rangarajan, and P. Kulkarni, “Competing views on cancer,” *J. Biosci.*, vol. 39, no. 2, pp. 281–302, Apr. 2014.
[102] M. A. Shah and G. K. Schwartz, “The relevance of drug sequence in combination chemotherapy,” *Drug Resist. Updat. Rev. Comment. Antimicrob. Anticancer Chemother.*, vol. 3, no. 6, pp. 335–356, Dec. 2000.
[103] V. Subr, L. Sivák, E. Koziolová, A. Braunová, M. Pechar, J. Strohalm, M. Kabešová, B. Říhová, K. Ulbrich, and M. Kovář, “Synthesis of poly[N-(2-hydroxypropyl)methacrylamide] conjugates of inhibitors of the ABC transporter that overcome multidrug resistance in doxorubicin-resistant P388 cells in vitro,” *Biomacromolecules*, vol. 15, no. 8, pp. 3030–3043, Aug. 2014.
[104] R. Krishna and L. D. Mayer, “Multidrug resistance (MDR) in cancer. Mechanisms, reversal using modulators of MDR and the role of MDR modulators in influencing the pharmacokinetics of anticancer drugs,” *Eur. J. Pharm. Sci. Off. J. Eur. Fed. Pharm. Sci.*, vol. 11, no. 4, pp. 265–283, Oct. 2000.
[105] J. Kopeček, “Polymer-drug conjugates: origins, progress to date and future directions,” *Adv. Drug Deliv. Rev.*, vol. 65, no. 1, pp. 49–59, Jan. 2013.
[106] T. Etrych, T. Mrkvan, B. Říhová, and K. Ulbrich, “Star-shaped immunoglobulin-containing HPMA-based conjugates with doxorubicin for cancer therapy,” *J. Control. Release Off. J. Control. Release Soc.*, vol. 122, no. 1, pp. 31–38, Sep. 2007.
[107] T. Minko, P. Kopecková, V. Pozharov, and J. Kopecek, “HPMA copolymer bound adriamycin overcomes MDR1 gene encoded resistance in a human ovarian carcinoma cell line,” *J. Control. Release Off. J. Control. Release Soc.*, vol. 54, no. 2, pp. 223–233, Jul. 1998.
[108] A. Talevi, M. E. Gantner, and M. E. Ruiz, “Applications of nanosystems to anticancer drug therapy (Part I. Nanogels, nanospheres, nanocapsules),” *Recent Patents Anticancer Drug Discov.*, vol. 9, no. 1, pp. 83–98, Jan. 2014.
[109] M. E. Ruiz, M. E. Gantner, and A. Talevi, “Applications of nanosystems to anticancer drug therapy (Part II. Dendrimers, micelles, lipid-based nanosystems),” *Recent Patents Anticancer Drug Discov.*, vol. 9, no. 1, pp. 99–128, Jan. 2014.
[110] U. Gupta, H. B. Agashe, A. Asthana, and N. K. Jain, “Dendrimers: Novel Polymeric Nanoarchitectures for Solubility Enhancement,” *Biomacromolecules*, vol. 7, no. 3, pp. 649–658, Mar. 2006.
[111] F. Petrelli, K. Borgonovo, and S. Barni, “Targeted delivery for breast cancer therapy: the history of nanoparticle-albumin-bound paclitaxel,” *Expert Opin. Pharmacother.*, vol. 11, no. 8, pp. 1413–1432, Jun. 2010.
[112] A. Abuchowski, J. R. McCoy, N. C. Palczuk, T. van Es, and F. F. Davis, “Effect of covalent attachment of polyethylene glycol on immunogenicity and circulating life of bovine liver catalase,” *J. Biol. Chem.*, vol. 252, no. 11, pp. 3582–3586, Jun. 1977.
[113] J. Kopecek, L. Sprincl, and D. Lïm, “New types of synthetic infusion solutions. I. Investigation of the effect of solutions of some hydrophilic polymers on blood,” *J. Biomed. Mater. Res.*, vol. 7, no. 2, pp. 179–191, Mar. 1973.
[114] B. Říhová, J. Kopeček, K. Ulbrich, and V. Chytrý, “Immunogenicity of N-(2-hydroxypropyl) methacrylamide copolymers,” *Makromol. Chem.*, vol. 9, no. S19851, pp. 13–24, Jan. 1985.
[115] L. Sprincl, J. Exner, O. Stěrba, and J. Kopecek, “New types of synthetic infusion solutions. III. Elimination and retention of poly-[N-(2-hydroxypropyl)methacrylamide] in a test organism,” *J. Biomed. Mater. Res.*, vol. 10, no. 6, pp. 953–963, Nov. 1976.
[116] P. A. Flanagan, R. Duncan, B. Rihova, V. SUbr, and J. Kopecek, “Immunogenicity of Protein-N-(2-Hydroxypropyl)methacrylamide Copolymer Conjugates in A/J and B10 Mice,” *J. Bioact. Compat. Polym.*, vol. 5, no. 2, pp. 151–166, Jan. 1990.

[117] B. Rihova, M. Bilej, V. Vetvicka, K. Ulbrich, J. Strohalm, J. Kopecek, and R. Duncan, "Biocompatibility of N-(2-hydroxypropyl) methacrylamide copolymers containing adriamycin. Immunogenicity, and effect on haematopoietic stem cells in bone marrow in vivo and mouse splenocytes and human peripheral blood lymphocytes in vitro," *Biomaterials*, vol. 10, no. 5, pp. 335–342, Jul. 1989.
[118] P. Chytil, T. Etrych, C. Konák, M. Sírová, T. Mrkvan, J. Boucek, B. Říhová, and K. Ulbrich, "New HPMA copolymer-based drug carriers with covalently bound hydrophobic substituents for solid tumour targeting," *J. Control. Release Off. J. Control. Release Soc.*, vol. 127, no. 2, pp. 121–130, Apr. 2008.
[119] H. Kostková, T. Etrych, B. Říhová, L. Kostka, L. Starovoytová, M. Kovář, and K. Ulbrich, "HPMA copolymer conjugates of DOX and mitomycin C for combination therapy: physicochemical characterization, cytotoxic effects, combination index analysis, and anti-tumor efficacy," *Macromol. Biosci.*, vol. 13, no. 12, pp. 1648–1660, Dec. 2013.
[120] T. Etrych, J. Strohalm, P. Chytil, B. Říhová, and K. Ulbrich, "Novel star HPMA-based polymer conjugates for passive targeting to solid tumors," *J. Drug Target.*, vol. 19, no. 10, pp. 874–889, Dec. 2011.
[121] T. Etrych, L. Kovář, J. Strohalm, P. Chytil, B. Říhová, and K. Ulbrich, "Biodegradable star HPMA polymer-drug conjugates: Biodegradability, distribution and anti-tumor efficacy," *J. Control. Release Off. J. Control. Release Soc.*, vol. 154, no. 3, pp. 241–248, Sep. 2011.
[122] D. Bissett, J. Cassidy, J. S. de Bono, F. Muirhead, M. Main, L. Robson, D. Fraier, M. L. Magnè, C. Pellizzoni, M. G. Porro, R. Spinelli, W. Speed, and C. Twelves, "Phase I and pharmacokinetic (PK) study of MAG-CPT (PNU 166148): a polymeric derivative of camptothecin (CPT)," *Br. J. Cancer*, vol. 91, no. 1, pp. 50–55, Jul. 2004.
[123] J. M. Meerum Terwogt, W. W. ten Bokkel Huinink, J. H. Schellens, M. Schot, I. A. Mandjes, M. G. Zurlo, M. Rocchetti, H. Rosing, F. J. Koopman, and J. H. Beijnen, "Phase I clinical and pharmacokinetic study of PNU166945, a novel water-soluble polymer-conjugated prodrug of paclitaxel," *Anticancer. Drugs*, vol. 12, no. 4, pp. 315–323, Apr. 2001.
[124] B. Říhová, J. Strohalm, O. Hovorka, V. Subr, T. Etrych, P. Chytil, R. Pola, D. Plocová, J. Boucek, and K. Ulbrich, "Doxorubicin release is not a prerequisite for the in vitro cytotoxicity of HPMA-based pharmaceuticals: in vitro effect of extra drug-free GlyPheLeuGly sequences," *J. Control. Release Off. J. Control. Release Soc.*, vol. 127, no. 2, pp. 110–120, Apr. 2008.
[125] J. Kopecek, "Controlled biodegradability of polymers--a key to drug delivery systems," *Biomaterials*, vol. 5, no. 1, pp. 19–25, Jan. 1984.
[126] G. Minotti, P. Menna, E. Salvatorelli, G. Cairo, and L. Gianni, "Anthracyclines: molecular advances and pharmacologic developments in antitumor activity and cardiotoxicity," *Pharmacol. Rev.*, vol. 56, no. 2, pp. 185–229, Jun. 2004.
[127] R. Duncan, L. W. Seymour, K. B. O'Hare, P. A. Flanagan, S. Wedge, I. C. Hume, K. Ulbrich, J. Strohalm, V. Subr, F. Spreafico, M. Grandi, M. Ripamonti, M. Farao, and A. Suarato, "Preclinical evaluation of polymer-bound doxorubicin," *J. Controlled Release*, vol. 19, no. 1–3, pp. 331–346, Mar. 1992.
[128] B. Říhová, J. Strohalm, J. Prausová, K. Kubácková, M. Jelínková, L. Rozprimová, M. Sírová, D. Plocová, T. Etrych, V. Subr, T. Mrkvan, M. Kovár, and K. Ulbrich, "Cytostatic and immunomobilizing activities of polymer-bound drugs: experimental and first clinical data," *J. Control. Release Off. J. Control. Release Soc.*, vol. 91, no. 1–2, pp. 1–16, Aug. 2003.
[129] T. Etrych, P. Chytil, M. Jelínková, B. Říhová, and K. Ulbrich, "Synthesis of HPMA Copolymers Containing Doxorubicin Bound via a Hydrazone Linkage. Effect of Spacer

on Drug Release and in vitro Cytotoxicity," *Macromol. Biosci.*, vol. 2, no. 1, pp. 43–52, Jan. 2002.
[130] T. Etrych, M. Jelínková, B. Říhová, and K. Ulbrich, "New HPMA copolymers containing doxorubicin bound via pH-sensitive linkage: synthesis and preliminary in vitro and in vivo biological properties," *J. Control. Release Off. J. Control. Release Soc.*, vol. 73, no. 1, pp. 89–102, May 2001.
[131] B. Říhová and M. Kovár, "Immunogenicity and immunomodulatory properties of HPMA-based polymers," *Adv. Drug Deliv. Rev.*, vol. 62, no. 2, pp. 184–191, Feb. 2010.
[132] B. J. Druker, F. Guilhot, S. G. O'Brien, I. Gathmann, H. Kantarjian, N. Gattermann, M. W. N. Deininger, R. T. Silver, J. M. Goldman, R. M. Stone, F. Cervantes, A. Hochhaus, B. L. Powell, J. L. Gabrilove, P. Rousselot, J. Reiffers, J. J. Cornelissen, T. Hughes, H. Agis, T. Fischer, G. Verhoef, J. Shepherd, G. Saglio, A. Gratwohl, J. L. Nielsen, J. P. Radich, B. Simonsson, K. Taylor, M. Baccarani, C. So, L. Letvak, R. A. Larson, and IRIS Investigators, "Five-year follow-up of patients receiving imatinib for chronic myeloid leukemia," *N. Engl. J. Med.*, vol. 355, no. 23, pp. 2408–2417, Dec. 2006.
[133] A. M. McCaig, E. Cosimo, M. T. Leach, and A. M. Michie, "Dasatinib inhibits B cell receptor signalling in chronic lymphocytic leukaemia but novel combination approaches are required to overcome additional pro-survival microenvironmental signals," *Br. J. Haematol.*, vol. 153, no. 2, pp. 199–211, Apr. 2011.
[134] M. L. Khan and A. K. Stewart, "Carfilzomib: a novel second-generation proteasome inhibitor," *Future Oncol. Lond. Engl.*, vol. 7, no. 5, pp. 607–612, May 2011.
[135] K. P. Papadopoulos, D. S. Siegel, D. H. Vesole, P. Lee, S. T. Rosen, N. Zojwalla, J. R. Holahan, S. Lee, Z. Wang, and A. Badros, "Phase I study of 30-minute infusion of carfilzomib as single agent or in combination with low-dose dexamethasone in patients with relapsed and/or refractory multiple myeloma," *J. Clin. Oncol. Off. J. Am. Soc. Clin. Oncol.*, vol. 33, no. 7, pp. 732–739, Mar. 2015.
[136] S. Pacey, R. H. Wilson, M. Walton, M. M. Eatock, A. Hardcastle, A. Zetterlund, H.-T. Arkenau, J. Moreno-Farre, U. Banerji, B. Roels, H. Peachey, W. Aherne, J. S. de Bono, F. Raynaud, P. Workman, and I. Judson, "A phase I study of the heat shock protein 90 inhibitor alvespimycin (17-DMAG) given intravenously to patients with advanced solid tumors," *Clin. Cancer Res. Off. J. Am. Assoc. Cancer Res.*, vol. 17, no. 6, pp. 1561–1570, Mar. 2011.
[137] H. Wu, D. S. Schiff, Y. Lin, H. J. R. Neboori, S. Goyal, Z. Feng, and B. G. Haffty, "Ionizing radiation sensitizes breast cancer cells to Bcl-2 inhibitor, ABT-737, through regulating Mcl-1," *Radiat. Res.*, vol. 182, no. 6, pp. 618–625, Dec. 2014.
[138] J. R. Mikhael, C. B. Reeder, E. N. Libby, L. J. Costa, P. L. Bergsagel, F. Buadi, A. Mayo, S. K. Nagi Reddy, K. Gano, A. C. Dueck, and A. K. Stewart, "Phase Ib/II trial of CYKLONE (cyclophosphamide, carfilzomib, thalidomide and dexamethasone) for newly diagnosed myeloma," *Br. J. Haematol.*, vol. 169, no. 2, pp. 219–227, Apr. 2015.
[139] B. McCabe, F. Liberante, and K. I. Mills, "Repurposing medicinal compounds for blood cancer treatment," *Ann. Hematol.*, vol. 94, no. 8, pp. 1267–1276, Aug. 2015.
[140] M. R. Hurle, L. Yang, Q. Xie, D. K. Rajpal, P. Sanseau, and P. Agarwal, "Computational drug repositioning: from data to therapeutics," *Clin. Pharmacol. Ther.*, vol. 93, no. 4, pp. 335–341, Apr. 2013.
[141] P. Nygren, M. Fryknäs, B. Agerup, and R. Larsson, "Repositioning of the anthelmintic drug mebendazole for the treatment for colon cancer," *J. Cancer Res. Clin. Oncol.*, vol. 139, no. 12, pp. 2133–2140, Dec. 2013.
[142] J. Zhang, K. Jiang, L. Lv, H. Wang, Z. Shen, Z. Gao, B. Wang, Y. Yang, Y. Ye, and S. Wang, "Use of genome-wide association studies for cancer research and drug repositioning," *PloS One*, vol. 10, no. 3, p. e0116477, 2015.

[143] A. Eriksson, A. Österroos, S. Hassan, J. Gullbo, L. Rickardson, M. Jarvius, P. Nygren, M. Fryknäs, M. Höglund, and R. Larsson, “Drug screen in patient cells suggests quinacrine to be repositioned for treatment of acute myeloid leukemia,” *Blood Cancer J.*, vol. 5, p. e307, 2015.
[144] D. Micic, G. Cvijovic, V. Trajkovic, L. H. Duntas, and S. Polovina, “Metformin: its emerging role in oncology,” *Horm. Athens Greece*, vol. 10, no. 1, pp. 5–15, Mar. 2011.
[145] A. P. Chavarría, J. C. Swartzwelder, V. M. Villarejos, and R. Zeledón, “Mebendazole, an effective broad-spectrum anthelmintic,” *Am. J. Trop. Med. Hyg.*, vol. 22, no. 5, pp. 592–595, Sep. 1973.
[146] J. K. Grover, V. Vats, G. Uppal, and S. Yadav, “Anthelmintics: a review,” *Trop. Gastroenterol. Off. J. Dig. Dis. Found.*, vol. 22, no. 4, pp. 180–189, Dec. 2001.
[147] J. El-On, “Benzimidazole treatment of cystic echinococcosis,” *Acta Trop.*, vol. 85, no. 2, pp. 243–252, Feb. 2003.
[148] J. S. Keystone, “Drugs Five Years Later: Mebendazole,” *Ann. Intern. Med.*, vol. 91, no. 4, p. 582, Oct. 1979.
[149] P. A. Braithwaite, M. S. Roberts, R. J. Allan, and T. R. Watson, “Clinical pharmacokinetics of high dose mebendazole in patients treated for cystic hydatid disease,” *Eur. J. Clin. Pharmacol.*, vol. 22, no. 2, pp. 161–169, 1982.
[150] M. Legesse, B. Erko, and G. Medhin, “Efficacy of alebendazole and mebendazole in the treatment of Ascaris and Trichuris infections,” *Ethiop. Med. J.*, vol. 40, no. 4, pp. 335–343, Oct. 2002.
[151] R. Larocque, M. Casapia, E. Gotuzzo, J. D. MacLean, J. C. Soto, E. Rahme, and T. W. Gyorkos, “A double-blind randomized controlled trial of antenatal mebendazole to reduce low birthweight in a hookworm-endemic area of Peru,” *Trop. Med. Int. Health TM IH*, vol. 11, no. 10, pp. 1485–1495, Oct. 2006.
[152] N. R. de Silva, J. L. Sirisena, D. P. Gunasekera, M. M. Ismail, and H. J. de Silva, “Effect of mebendazole therapy during pregnancy on birth outcome,” *Lancet Lond. Engl.*, vol. 353, no. 9159, pp. 1145–1149, Apr. 1999.
[153] A. . Dayan, “Albendazole, mebendazole and praziquantel. Review of non-clinical toxicity and pharmacokinetics,” *Acta Trop.*, vol. 86, no. 2–3, pp. 141–159, May 2003.
[154] J. F. Wilson, M. Davidson, and R. L. Rausch, “A clinical trial of mebendazole in the treatment of alveolar hydatid disease,” *Am. Rev. Respir. Dis.*, vol. 118, no. 4, pp. 747–757, Oct. 1978.
[155] G. Edwards and A. M. Breckenridge, “Clinical pharmacokinetics of anthelmintic drugs,” *Clin. Pharmacokinet.*, vol. 15, no. 2, pp. 67–93, Aug. 1988.
[156] I. Y. Dobrosotskaya, G. D. Hammer, D. E. Schteingart, K. E. Maturen, and F. P. Worden, “Mebendazole monotherapy and long-term disease control in metastatic adrenocortical carcinoma,” *Endocr. Pract. Off. J. Am. Coll. Endocrinol. Am. Assoc. Clin. Endocrinol.*, vol. 17, no. 3, pp. e59–62, Jun. 2011.
[157] P. Nygren and R. Larsson, “Drug repositioning from bench to bedside: tumour remission by the antihelmintic drug mebendazole in refractory metastatic colon cancer,” *Acta Oncol. Stockh. Swed.*, vol. 53, no. 3, pp. 427–428, Mar. 2014.
[158] A. Bekhti and J. Pirotte, “Hepatotoxicity of mebendazole. Relationship with serum concentrations of the drug,” *Gastroentérologie Clin. Biol.*, vol. 11, no. 10, pp. 701–703, Oct. 1987.
[159] P. A. Braithwaite, R. J. Thomas, and R. C. Thompson, “Hydatid disease: the alveolar variety in Australia. A case report with comment on the toxicity of mebendazole,” *Aust. N. Z. J. Surg.*, vol. 55, no. 5, pp. 519–523, Oct. 1985.

[160] R. Speare, L. F. Skerratt, L. Berger, and P. M. Johnson, "Toxic effects of mebendazole at high dose on the haematology of red-legged pademelons (Thylogale stigmatica)," *Aust. Vet. J.*, vol. 82, no. 5, pp. 300–303, May 2004.
[161] P. Köhler and R. Bachmann, "Intestinal tubulin as possible target for the chemotherapeutic action of mebendazole in parasitic nematodes," *Mol. Biochem. Parasitol.*, vol. 4, no. 5–6, pp. 325–336, Dec. 1981.
[162] G. J. Russell, J. H. Gill, and E. Lacey, "Binding of [3H]benzimidazole carbamates to mammalian brain tubulin and the mechanism of selective toxicity of the benzimidazole anthelmintics," *Biochem. Pharmacol.*, vol. 43, no. 5, pp. 1095–1100, Mar. 1992.
[163] T. Mukhopadhyay, J. Sasaki, R. Ramesh, and J. A. Roth, "Mebendazole elicits a potent antitumor effect on human cancer cell lines both in vitro and in vivo," *Clin. Cancer Res. Off. J. Am. Assoc. Cancer Res.*, vol. 8, no. 9, pp. 2963–2969, Sep. 2002.
[164] J. Sasaki, R. Ramesh, S. Chada, Y. Gomyo, J. A. Roth, and T. Mukhopadhyay, "The anthelmintic drug mebendazole induces mitotic arrest and apoptosis by depolymerizing tubulin in non-small cell lung cancer cells," *Mol. Cancer Ther.*, vol. 1, no. 13, pp. 1201–1209, Nov. 2002.
[165] N. Doudican, A. Rodriguez, I. Osman, and S. J. Orlow, "Mebendazole Induces Apoptosis via Bcl-2 Inactivation in Chemoresistant Melanoma Cells," *Mol. Cancer Res.*, vol. 6, no. 8, pp. 1308–1315, Aug. 2008.
[166] N. A. Doudican, S. A. Byron, P. M. Pollock, and S. J. Orlow, "XIAP downregulation accompanies mebendazole growth inhibition in melanoma xenografts," *Anticancer. Drugs*, vol. 24, no. 2, pp. 181–188, Feb. 2013.
[167] C. P. Coyne, T. Jones, and R. Bear, "Gemcitabine-(C4-amide)-[anti-HER2/neu] Anti-Neoplastic Cytotoxicity in Dual Combination with Mebendazole against Chemotherapeutic-Resistant Mammary Adenocarcinoma," *J. Clin. Exp. Oncol.*, vol. 2, no. 2, 2013.
[168] R.-Y. Bai, V. Staedtke, C. M. Rudin, F. Bunz, and G. J. Riggins, "Effective treatment of diverse medulloblastoma models with mebendazole and its impact on tumor angiogenesis," *Neuro-Oncol.*, vol. 17, no. 4, pp. 545–554, Apr. 2015.
[169] R.-Y. Bai, V. Staedtke, C. M. Aprhys, G. L. Gallia, and G. J. Riggins, "Antiparasitic mebendazole shows survival benefit in 2 preclinical models of glioblastoma multiforme," *Neuro-Oncol.*, vol. 13, no. 9, pp. 974–982, Sep. 2011.
[170] P. Nygren, M. Fryknäs, B. Agerup, and R. Larsson, "Repositioning of the anthelmintic drug mebendazole for the treatment for colon cancer," *J. Cancer Res. Clin. Oncol.*, vol. 139, no. 12, pp. 2133–2140, Dec. 2013.
[171] P. A. Spagnuolo, J. Hu, R. Hurren, X. Wang, M. Gronda, M. A. Sukhai, A. Di Meo, J. Boss, I. Ashali, R. Beheshti Zavareh, N. Fine, C. D. Simpson, S. Sharmeen, R. Rottapel, and A. D. Schimmer, "The antihelmintic flubendazole inhibits microtubule function through a mechanism distinct from Vinca alkaloids and displays preclinical activity in leukemia and myeloma," *Blood*, vol. 115, no. 23, pp. 4824–4833, Jun. 2010.
[172] A. R. Larsen, R.-Y. Bai, J. H. Chung, A. Borodovsky, C. M. Rudin, G. J. Riggins, and F. Bunz, "Repurposing the antihelmintic mebendazole as a hedgehog inhibitor," *Mol. Cancer Ther.*, vol. 14, no. 1, pp. 3–13, Jan. 2015.
[173] J. S. Bertram and P. Janik, "Establishment of a cloned line of Lewis Lung Carcinoma cells adapted to cell culture," *Cancer Lett.*, vol. 11, no. 1, pp. 63–73, Nov. 1980.
[174] P. A. Gorer, "Studies in antibody response of mice to tumour inoculation," *Br. J. Cancer*, vol. 4, no. 4, pp. 372–379, Dec. 1950.
[175] J. J. Farrar, J. Fuller-Farrar, P. L. Simon, M. L. Hilfiker, B. M. Stadler, and W. L. Farrar, "Thymoma production of T cell growth factor (Interleukin 2)," *J. Immunol. Baltim. Md 1950*, vol. 125, no. 6, pp. 2555–2558, Dec. 1980.

[176] I. J. Fidler, “Biological behavior of malignant melanoma cells correlated to their survival in vivo,” *Cancer Res.*, vol. 35, no. 1, pp. 218–224, Jan. 1975.
[177] M. Wang, V. Bronte, P. W. Chen, L. Gritz, D. Panicali, S. A. Rosenberg, and N. P. Restifo, “Active immunotherapy of cancer with a nonreplicating recombinant fowlpox virus encoding a model tumor-associated antigen,” *J. Immunol. Baltim. Md 1950*, vol. 154, no. 9, pp. 4685–4692, May 1995.
[178] S. Strober, E. S. Gronowicz, M. R. Knapp, S. Slavin, E. S. Vitetta, R. A. Warnke, B. Kotzin, and J. Schröder, “Immunobiology of a spontaneous murine B cell leukemia (BCL1),” *Immunol. Rev.*, vol. 48, pp. 169–195, 1979.
[179] H. J. Tanke, P. H. van Vianen, F. M. Emiliani, I. Neuteboom, N. de Vogel, A. D. Tates, E. A. de Bruijn, and A. T. van Oosterom, “Changes in erythropoiesis due to radiation or chemotherapy as studied by flow cytometric determination of peripheral blood reticulocytes,” *Histochemistry*, vol. 84, no. 4–6, pp. 544–548, 1986.
[180] D. J. Ferguson, S. F. Lee, and P. A. Gordon, “Evaluation of reticulocyte counts by flow cytometry in a routine laboratory,” *Am. J. Hematol.*, vol. 33, no. 1, pp. 13–17, Jan. 1990.
[181] J. J. Shiah, Y. Sun, C. M. Peterson, and J. Kopecek, “Biodistribution of free and N-(2-hydroxypropyl)methacrylamide copolymer-bound mesochlorin e(6) and adriamycin in nude mice bearing human ovarian carcinoma OVCAR-3 xenografts,” *J. Control. Release Off. J. Control. Release Soc.*, vol. 61, no. 1–2, pp. 145–157, Aug. 1999.
[182] “Global Health Observatory Data Repository,” *WHO*. [Online]. Available: http://apps.who.int/gho/data/node.main.A864. [Accessed: 12-Aug-2015].
[183] H. Krakovicová, T. Etrych, and K. Ulbrich, “HPMA-based polymer conjugates with drug combination,” *Eur. J. Pharm. Sci. Off. J. Eur. Fed. Pharm. Sci.*, vol. 37, no. 3–4, pp. 405–412, Jun. 2009.
[184] L. S. Nielsen, “Improved peroral bioavailability of mebendazole in rabbits by administration of various N-alkoxycarbonyl derivatives of mebendazole,” *Int. J. Pharm.*, vol. 104, no. 2, pp. 175–179, Apr. 1994.
[185] L. S. Nielsen, F. Sløk, and H. Bundgaard, “N-Alkoxycarbonyl prodrugs of mebendazole with increased water solubility,” *Int. J. Pharm.*, vol. 102, no. 1–3, pp. 231–239, Feb. 1994.
[186] B. Rihova, “Clinical experience with anthracycline antibiotics-HPMA copolymer-human immunoglobulin conjugates,” *Adv. Drug Deliv. Rev.*, vol. 61, no. 13, pp. 1149–1158, Nov. 2009.
[187] M. Sirova, J. Strohalm, V. Subr, D. Plocova, P. Rossmann, T. Mrkvan, K. Ulbrich, and B. Rihova, “Treatment with HPMA copolymer-based doxorubicin conjugate containing human immunoglobulin induces long-lasting systemic anti-tumour immunity in mice,” *Cancer Immunol. Immunother. CII*, vol. 56, no. 1, pp. 35–47, Jan. 2007.
[188] M. Sirova, T. Mrkvan, T. Etrych, P. Chytil, P. Rossmann, M. Ibrahimova, L. Kovar, K. Ulbrich, and B. Rihova, “Preclinical evaluation of linear HPMA-doxorubicin conjugates with pH-sensitive drug release: efficacy, safety, and immunomodulating activity in murine model,” *Pharm. Res.*, vol. 27, no. 1, pp. 200–208, Jan. 2010.
[189] Y. Miyoshi, Y. Yoshioka, K. Suzuki, T. Miyazaki, M. Koura, K. Saigoh, N. Kajimura, Y. Monobe, S. Kusunoki, J. Matsuda, M. Watanabe, and N. Hayasaka, “A new mouse allele of glutamate receptor delta 2 with cerebellar atrophy and progressive ataxia,” *PloS One*, vol. 9, no. 9, p. e107867, 2014.